The role of PI3K and NADPH oxidases in vasculogenesis/angiogenesis of mouse embryonic stem cells

Dissertation
zur Erlangung des akademischen Grades
doctor rerum naturalium
(Dr. rer. nat.)

vorgelegt dem Rat der Medizinischen Fakultät
der Friedrich-Schiller-Universität Jena

von Mohamed Mohamed Bekhite ELsaied (PhD)

geboren am 04. Oktober 1970 in Alexandria, Ägypten

Gutachter

1- **Prof. Dr. rer. nat. Maria Wartenberg** (FSU, Jena)

2- **PD Dr. rer. nat. Jörg Müller** (FSU, Jena)

3- **PD Dr. med. Yaser Abdallah** (Justus-Liebig-University, Gießen)

Tag der öffentlichen Verteidigung: 07 April 2015

CONTENTS

LIST OF FIGURES

LIST OF ABBREVIATIONS

A

A	Arteriole
Akt inhibitor	1L6-Hydroxymethyl-chiro-inositol-2-(R)-2-O- methyl-3-O-octadecyl-*sn*-glycerocarbonate
ampR	Ampicillin resistance gene for bacterial selection
Ang-1	Angiopoietin-1
Ang-2	Angiopoietin-2
APS	Ammonium persulphate
2-APT	Acetylphenothiazine

B

bFGF	Basic fibroblast growth factor
BIM-1	Bisindolylmaleimide-I
BMC	Bone-marrow-derived angiogenic cells
BSA	Bovine serum albumine

C

CGR8	Murine embryonic stem cell line
CK2	Casein kinase 2
CMFDA	5-Chloromethylfluorescein diacetate
Compound 15e	3-(4-Morpholinothieno[3,2-d]pyrimidin-2-yl)phenol
Cppt	Central polypurine tract

D

DAPI	4 ',6-diamidino-2-phenylindole
DHE	Dihydroethidium
DIA	Differentiation inhibiting activity
DMEM	Dulbecco's modified eagle's medium
DMSO	Dimethyl sulfoxide
DNA	Deoxyribonucleic acid
DNase I	Deoxyribonuclease I
dNTP	Deoxynucleotide
DPI	Diphenyleneiodonium
DTT	Dithiotreitol
DU 145	Human prostate carcinoma cell line

E

E. coli	*Escherichia coli*
E1	Bath solution
ECACC	European Collection of Cell Cultures
EDTA	Ethylene diamine tetraacetic acid
EGFR	Epidermal growth factor receptor
Erk1/2	Extracellular signal-regulated protein kinases 1 and 2
ES	Embryonic stem

F

f1 ori	f1 origin of replication
FACS	Fluorescence activated cell sorting
FAD	Flavin adenine dinucleotide
FBS	Fetal bovine serum
FCM	Flow Cytometry
FGF	Fibroblast growth factor
Flk-1	Fetal liver kinase-1
Flt-1	fms-related tyrosine kinase-1

G

GAPDH	Glyceraldehyde-3-phosphate dehydrogenase
GFAP	Glial fibrillary acidic protein
GMEM	Glasgow minimum essential medium
GPCRs	G protein-coupled receptor

H

h	Hour
H_2DCF-DA	2`,7`- dichlorodihydrofluorescein diacetate
H_2O_2	Hydrogen peroxide
HEK	Human Embryonic Kidney
HEPES	2-(4-(2-Hydroxyethyl)- 1-piperazinyl)-ethansulfon acid
HGF	Hepatocyte growth factor
HIV	Human immunodeficiency virus
hPGK	Human phosphoglycerate kinase eukaryotic promoter
HRP	Horseradish peroxidise

I

ICM	Inner cell mass
IF	Immunofluorescence
IGF-I	Insulin-like growth factor-I
IgG	Immunoglobulin G
IK-buffer	Cell dissociation buffer

J

JNK	c-Jun N-terminal kinase

K

kDa	Kilodaltons

L

LB-Broth base	Luria Bertani Broth Base
LIF	Leukemia inhibitory factor
LPS	Lipopolysaccharide
LSM	Laser scanning microscope
5' LTR	5' long terminal repeat

M

MACS	Magnetic-activated cell sorting
MAPK	Mitogen activated protein kinase
M-MLV	Moloney Murine Leukemia Virus
mRNA	Messenger RNA
mTOR	Mammalian target of rapamycin

N

NADPH	Nicotinamide adenine dinucleotide phosphate
NADPH oxidase	NOX
NaOH	Sodium hydroxide
NEAA	Non-essential amino acids

O

O_2^-	Superoxide

P

PBS	phosphate-buffered saline
PBS-T	PBS-Tween/ PBS-Triton
PCT	Pericytes
PDGF-A	Platelet derived growth factor-A
PDGFR	platelet-derived growth factor receptor
PE	Phycoerythrin
PECAM-1	Platelet endothelial cell adhesion molecule
PEI	Polyethylenimine
PFA	Paraformaldehyde
PI3K	Phosphoinositide 3 kinase
PKB	Protein kinase B
PKC	Protein kinase C
PlGF	Placental growth factor
PLK	Polo-like kinase
Polybrene	1,5-dimethyl-1,5-diazaundecamethylene polymethobromide
Psi	RNA packaging signal
PtdIns(3,4,5)P3	Phosphatidylinositol-3,4,5-trisphosphate
PtdIns(4,5)P2	Phosphatidylinositol-4,5-bisphosphate
pUC ori	pUC origin of replication
puroR	Puromycin resistance gene for mammalian selection

R

Rac1	Ras-related C3 botulinum toxin substrate 1
Rac1 inhibitor	N6-[2-[[4-(Diethylamino)-1-methylbutyl]amino]-6-methyl-4-pyrimidinyl]-2-methyl-4,6-quinolinediamine trihydrochloride
Rev	Regulator of expression of virion proteins
RNA	Ribonucleic acid
RNase A	Ribonuclease A
ROS	Reactive oxygen species
RRE	Rev response element

S

S1P	Sphingosine-1-phosphate
SAPK	Stress-activated protein kinase

SD	Standard deviation
SDS-PAGE	Sodium dodecyl sulphate-polyacrylamide gel electrophoresis
shRNA	Short hairpin RNA
SIN/LTR	3' self inactivating long terminal repeat
SMC	Smooth muscle cells
SV40	Simian vacuolating virus 40

T

Taurine	2-aminoethanesulfonic acid
TBE	Tris-borate-EDTA
TBST	Tris-buffered saline with 0.1% Tween
TEMED	*N*,*N*,*N*′,*N*′-tetramethyl-ethane-1,2-diamine
TGF	Transforming growth factor
Tris	Tris (hidroxymethyl) aminomethan
Tween 20	Polyoxyethylensorbitanmonolaurat

V

V	Venule
VAS2870	3-benzyl-7-(benzoxazolyl) thio-1,2,3-triazolo(4,5-d)pyrimidine
VE-Cadherin	Vascular endothelial-Cadherin
VEGF	Vascular endothelial growth factor

SUMMARY

The mechanism of vascular formation has been the subject of intensive research for many years, but still the mechanisms of vascular stimulation and inhibition remain a major topic of investigation. The impact of reactive oxygen species (ROS) and Phosphoinositide 3 kinase (PI3K) in vascular differentiating of embryonic stem (ES) cells is largely unknown. Here we show that silencing PI3K catalytic subunit p110α and NOX1 using short hairpin RNA (shRNA) or inhibition of Rac1 significantly abolished the superoxide (O_2^-) production stimulated by vascular endothelial growth factor (VEGF) in mouse ES cells and in ES cell-derived Flk-1^+ vascular progenitor cells. Moreover, silencing p110α or inhibition the Rac1 arrested vascular development at initial stages of vasculogenesis in embryoid bodies as indicated by PECAM-1 positive areas and branching points even under VEGF treatment. In sorted Flk-1 positive ES cells tube-like structure formation on matrigel and cell migration in the scratch migration assay were totally impaired in absence of p110α, whereas silencing NOX1 in ES cells caused a significant reduction in the PECAM-1 positive area, branching points, cell migration and tube length upon VEGF treatment. However, vascular differentiation markers were still produced in shRNA VEGF treated NOX1 knock down ES cells. Interestingly, silencing p110α but not NOX1 significantly inhibited the activation of Rac1 and RhoA, which led to abrogation of VEGF-induced lamellipodia structure formation. In addition, MAP kinase p44/42 phosphorylation was blocked by the PI3K inhibitor wortmannin and the p110α inhibitor compouned15e. In contrast, the NOX1 inhibitor 2-APT did not prevent VEGF-induced MAP kinase p44/42 phosphorylation. The efficiency of silencing the p110α catalytic subunit of PI3K and NOX1 to inhibit angiogenesis/vasculogenesis were investigated for their capacity to inhibit tumor-induced angiogenesis in confrontation cultures consisting of embryoid bodies and multicellular DU-145 prostate tumor spheroids. Interestingly, we found that silencing p110α can strongly inhibited the vascularization of multicellular tumor spheroids in confrontation cultures. These findings provide direct evidence that the activity of p110α in endothelial cells is essential in vasculogenesis/angiogenesis and suggest that p110α and their downstream signalling cascade may represent promising therapeutic targets for the treatment of numerous human diseases that involve aberrant neovascularization.

ZUSAMMENFASSUNG

Die Vaskulogenese ist seit vielen Jahren Gegenstand intensiver Forschung, dennoch sind noch immer die Mechanismen der Gefäßstimulation und Hemmung ein wichtiges Thema der Forschung. Insbesondere die Einflüsse reaktiver Sauerstoffspezies (ROS) sowie der Phosphoinositide 3 kinase (PI3K) in Bezug auf die Gefäßdifferenzierung embryonaler Stammzellen (ES-Zellen), ist noch weitgehend unbekannt. In dieser Arbeit wird gezeigt, dass ein mittels spezifischer shRNA durchgeführtes „silencing" der katalytischen Untereinheit p110α der PI3-Kinase sowie von NOX1 ebenso wie eine Hemmung von Rac1 zu einer Reduktion der Superoxid Produktion bei durch vascular endothelial growth factor (VEGF) stimulierten murinen ES Zellen sowie bei ES-Zell abgeleiteten Flk-1^+ vaskulären Progenitorzellen führt.

Darüber hinaus führte ein „silencing" der katalytischen p110α Untereinheit ebenso wie eine Inhibition von Rac1 zu einem Arrest der Gefäßerntwicklung in einem frühen Stadium der Vaskulogense in murinen Embroid Bodies. Dieses ließ sich anhand durchgeführter quantitativer PECAM-1 Immunfluoreszenzen sowie anhand der Analyse von endothelialen Verzweigungspunkten belegen. Der Effekt war selbst insbesondere unter einer zusätzlichen VEGF Stimulation nachweisbar.

Ergänzend zu diesen Ergebnissen zeigte sich bei der Analyse von aufgereinigten Flk-1-positiven ES-Zellen, bei denen mittels shRNA Technik die katalytische Untereinheit p110α der PI3-Kinase sowie NOX1 nicht translatiert wurden, dass insbesondere die dreidimensionale Verzweigung der Endothelzellen auf einer Matrigel-Oberfläche sowie die Zellmigration in einem Migrationsassay zu einer signifikanten Verringerung der PECAM-1-positiven Bereiche, der Verzweigungspunkte sowie der Zellmigration führten. Dieser Effekt war insbesondere bei einer zusätzlichen VEGF Behandlung nachweisbar.

Trotz des shRNA silencing von NOX1 ließen sich bei additiver VEGF-Stimulation in den untersuchten ES-Zellen auch noch weiterhin typische endotheliale Differenzierungsmarker nachweisen. Interessanterweise führte jedoch ein silencing der katalytischen Untereinheit p110α der PI3-Kinase mittels shRNA, jedoch nicht von NOX1, zu einer signifikanten Aktivierung von Rac1 und RhoA, was konsekutiv zu einer Inhibition der VEGF-induzierten Bildung von Lamellipodien führte.

Weiterhin konnte gezeigt werden, dass eine Posphorylierung der MAP Kinase p44/42 durch den PI3K Inhibitor Wortmannin und den p110α Inhibitor com-

pound15e erreicht wurde. Im Gegensatz dazu konnte der NOX1-Inhibitor 2-APT die VEGF-induzierte Phosphorylierung der MAP Kinase p44/42 nicht verhindern. Ergänzend wurde die Effizienz des shRNA-siliencing der katalytischen Untereinheit p110α der PI3K und der NOX1 anhand von Konfrontationskulturen zwischen EBs und multizellulären Tumorzellsphäroiden der Prostatakarzinomzellinie DU145, welche eine Tumor induzierte Angiogenese simulieren, evaluiert.

Interessanterweise fanden wir, dass ein silencing der katalytischen Untereinheit p110α zu einer starken Inhibition der Gefäßbildung in den Konfrontationskulturen zwischen EBs und multizellulären Tumorsphäroiden führte. Diese Daten belegen, dass die katalytische Untereinheit p110α in Endothelzellen für eine reibungslose Vasculogenese/Angiogenese ist. Weiterhin legen die erhobenen Daten nahe, das eine potentielle pharmakologische Inhibition der katalytischen Untereinheit p110α zu einem potentiellen Ansatzpunkt bei der Behandlung zahlreicher Krankheiten, welche eine übermäßige Neovaskularisation bzw. eine Tumorangiogenese begünstigen, sinnvoll erscheint.

1. INTRODUCTION

The vasculature is the first functional organ to develop during embryonic development for supply of metabolic substrate (Ribatti 2006). Hemangioblasts (primitive angiogenic cells) differentiate into endothelial cells that begin to form rudimentary tubes or vessels (Fig. 1.1) and into hematopoietic stem cells that embed in the wall of these developing vessels (de Bruijn et al. 2002, Fischer et al. 2006, Risau 1997). The mechanism of vascular formation has been the subject of intensive research for many years (Folkman 1971, McAuslan and Gole 1980, Patan 2000, Tammela et al. 2008), but still the mechanisms of vascular stimulation and inhibition remain a major topic of investigation (Muramatsu et al. 2013, Tammela et al. 2008). Numerous publications have been shown that vascular endothelial growth factor (VEGF) plays a pivotal role (Carmeliet et al. 1996, Ferrara et al. 1996) in differentiation and proliferation of endothelial cells (vasculogenesis) (Pardanaud and Dieterlen-Lievre 1999) and blood vessel sprouting and branching (angiogenesis) (Risau 1995) (Fig. 1.1). In addition, the VEGF receptors, VEGFR1 (fms-related tyrosine kinase-1, Flt-1) and VEGFR2 (fetal liver kinase-1, Flk-1/KDR), are also crucial for the development of the vascular endothelial cell lineage and for the formation of early capillary networks (Fong et al. 1995, Millauer et al. 1993). VEGF has been shown to activate several downstream signaling pathways. For example, following VEGF treatment Flk-1 (Kroll and Waltenberger 1997), phosphoinositide 3-kinase (PI3K) (Guo et al. 1995), protein kinase C (PKC) (Xia et al. 1996), Akt (Gerber et al. 1998) and extracellular-signal-regulated kinase-1/2 (Erk1/2) (Colavitti et al. 2002) were activated. However, the cellular signaling pathways and the molecular players involved in the vasculogenesis/angiogenesis processes have not yet been fully identified (Adams and Alitalo 2007, Welti et al. 2013). By interaction with Flk-1 VEGF regulates endothelial cell development, via activation of class IA PI3K (Bekhite et al. 2011, Bos 1995, Gerber et al. 1998). The role of PI3Kα in vascular development was demonstrated PI3Kα knockout mice, which resulted in impaired migration of endothelial cells and subsequent loss of angiogenic activity (Bi et al. 1999, Graupera et al. 2008). This study provides an avenue for better understanding of the effect of VEGF on blood vessels formation to treat many pathological blood vessel conditions (Boheler et al. 2002, Guan et al. 1999).

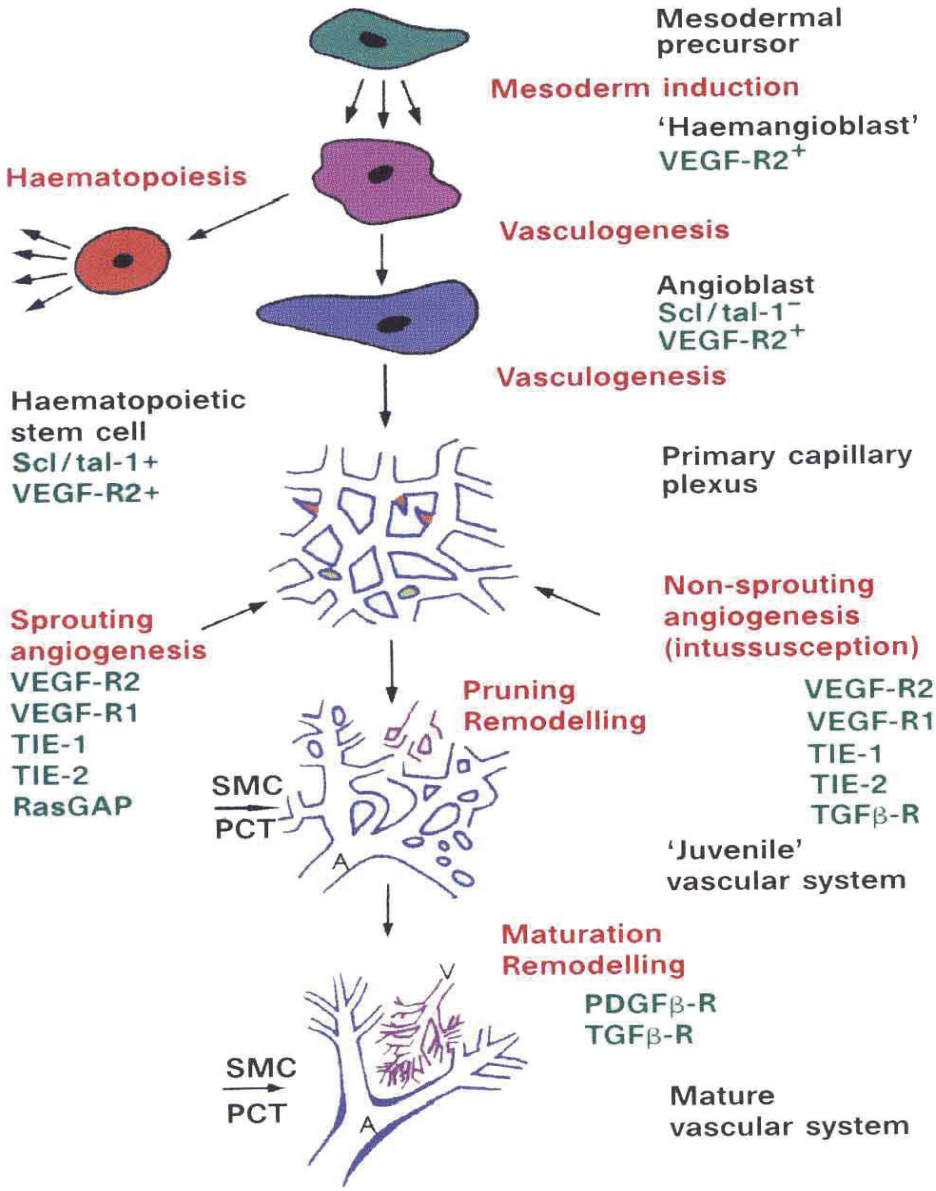

Figure 1.1: Mechanisms of angiogenesis and vasculogenesis**.** The processes (red labels), molecules (green labels) and appearances (black labels) involved in vascular development. Red tips in the primary capillary plexus represent sprouts, yellow circles represent splitting pillars. Remodelling and maturation is dependent on the tissue and organ context. A, arteriole, V, venule, SMC, smooth muscle cells, PCT, pericytes. (Risau, 1997), used with permission.

1.1 Phosphoinositide 3-kinase (PI3K)

Previous publications have shown that PI3K proteins are a key regulatory protein that is involved in a wide variety of cellular processes, including cell growth, endothelial proliferation, migration, differentiation, survival and intracellular trafficking. (Gerber et al. 1998, Graupera et al. 2008, Jiang et al. 2000). The emerging links between PI3Ks and many human diseases, including inflammation, cardiovascular disease and cancer, have made them the focus of intense study. The increased activity of

PI3K signaling can be the result of gene mutations, amplification and protein over-expression (Steelman et al. 2011). The first generation of PI3K inhibitors, in particular the fungal metabolite wortmannin and the flavone-based compound LY294002 have been extensively used for more than two decades to analyse PI3K driven pathways (Vlahos et al. 1994, Wymann et al. 1996). However, these molecules are poorly selective, inhibiting not only the lipid PI3K, but also other members of the PI3K superfamily. For example, kinase profiling has shown that wortmannin and LY294002 potently inhibit the mammalian target of rapamycin (mTOR) and unrelated enzymes, such as casein kinase 2 (CK2), myosin light chain kinase (MLCK) and polo-like kinase (PLK). Furthermore, both agents are known to suffer from problematic pharmaceutical properties, particularly in relation to stability and pharmacokinetics (Davies et al. 2000, Knight et al. 2004, Liu et al. 2005). Consequently, some of the phenotypes that were originally attributed to class I PI3K, using these inhibitors, could also be due to the inhibition of other related pathways. Concomitantly, some of the phenotypes observed in gene-modified mice that lack the entire PI3K protein (gene deletion, knockout mice), as opposed to mice that only lack PI3K enzyme activity (site-directed kinase-inactive mutant, knock-in mice), could also be caused by the loss of protein functions that are independent of class I PI3K enzymatic activity (Clayton et al. 2002, Okkenhaug et al. 2002). It is therefore advisable to combine genetic and pharmacological strategies for the analysis of PI3K-mediated signalling cascades.

1.1.1 PI3K structure

PI3Ks are evolutionary conserved from yeast to high mammals and are classified based on their lipid specificity, molecular structure, cellular regulation and *in vivo* substrate specificities into class I, II and III PI3Ks (Vanhaesebroeck et al. 1997). The most important enzymes related to vascular differentiation are class I enzymes, which are further divided into class IA (PI3Kα, β, δ) and class IB (PI3Kγ) enzymes (Marone et al. 2008, Morello et al. 2009). All four class I PI3Ks are heterodimers composed of a catalytic subunit with a molecular weight of 110 kDa and a tightly associated regulatory subunit that controls activation and subcellular localization (Stephens et al. 1991, Whitman et al. 1988). All catalytic subunits of the depicted kinases share a core catalytic domain (PI3Kc), which contains the ATP-binding site (Fig. 1.2). At their N-terminus, the catalytic domains of PI3K class I have a regulatory subunit binding domain (p85B binds p85/55/50 regulatory subunits, pRegB

binds p101 and p84/87^{PIKAP} proteins), followed by a Ras-binding domain (RasB), a C2 domain (protein kinase C homology domain 2) and a PI3K accessory (helical) domain (PI3Ka). The 110 kDa catalytic subunit of PI3Kγ, the only class IB PI3K isoform described so far, associates with one of two regulatory subunits, p101 and p84 (also known as p87PIKAP), that are distinct from any of the p85 subunits. PI3Kγ contains interaction sites for βγ subunits of trimeric G proteins in the pRegB and the PI3Kc domains (Fig. 1.2). The regulatory subunits of class IA PI3Ks contain a P (proline-rich region), two SH2 (Src-homology 2) domains, as well as an iSH2 region, which interacts with the catalytic subunit. p85α and p85β have at the N-terminus an additional SH3 (Src-homology 3) and BH (BCR homology) domain. The structure of p101 and p84/87^{PIKAP} is not well explored (Fig. 1.2). The N-terminus is required for association with PI3Kγ, and Gβγ interaction is mediated by the C-terminal part of these adaptors (Marone et al. 2008, Stephens et al. 1994).

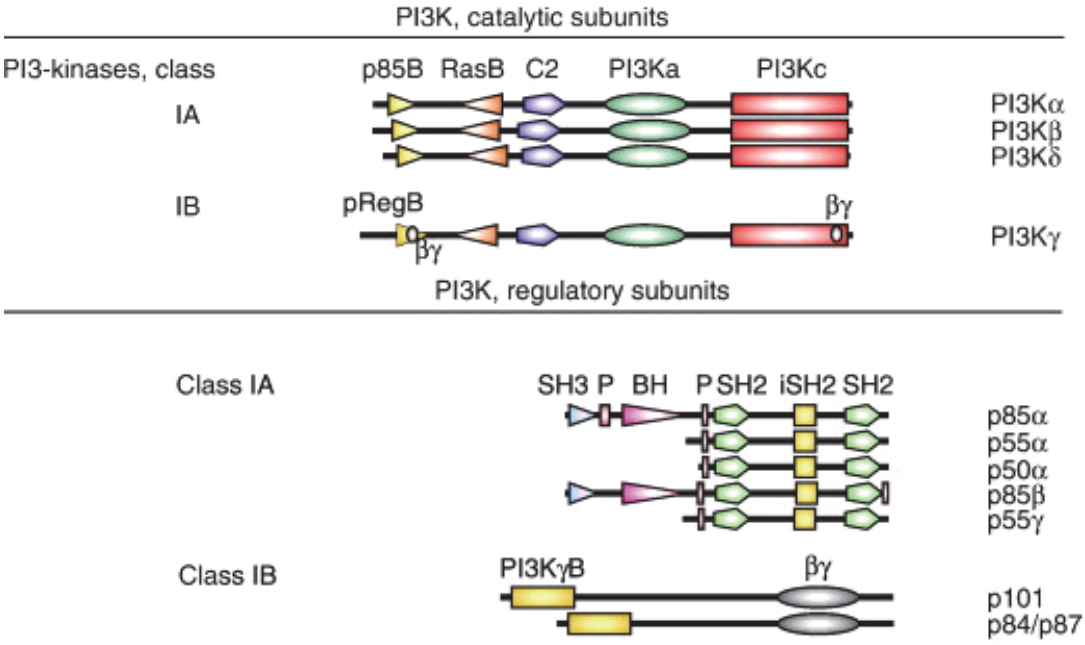

Figure 1.2: Domain structure of PI3K class I. From Marone *et al* (2008), used with permission.

1.1.2 PI3K activation

Class IA PI3Ks are mainly present in cytoplasm without stimulation, where p85 subunit forms dimer with p110 and prevents it from degradation. Activation of PI3K by ligands involves its translocation to the plasma membrane so as to gain access to lipid substrates. Heterodimeric PI3Kα, PI3Kβ, and PI3Kδ complexes are activated

downstream of growth factors, cytokine receptors and their substrates, whereas PI3Kγ activation is triggered downstream of G protein-coupled receptors (GPCRs). Binding of growth factors to their cognate receptor leads to receptor dimerisation and auto-phosphorylation of multiple tyrosines. This act as docking sites for the SH2 domains present in the PI3K regulatory subunits p85, p55, and p50 (Fig. 1.3). This translocates the catalytic PI3K subunit to the plasma membrane to initiate the phosphorylation of phosphatidylinositol-4,5-bisphosphate (PtdIns(4,5)P_2) giving rise to the second messenger phosphatidylinositol-3,4,5-trisphosphate (PtdIns(3,4,5)P_3) (Koyasu 2003, Marone et al. 2008). PtdIns(3,4,5)P_3 then recruits proteins with a pleckstrin homology (PH) domain and amplifies the growth factor signaling cascade (Fig. 1.3). In the case of PI3Kγ, binding of chemokines to GPCRs induces the dissociation of heterotrimeric G-proteins. Free $G_{\beta\gamma}$ subunits interact with PI3Kγ and the adaptor proteins p101 and p84/87, usually triggering transient, high amplitude signals of PtdIns(3,4,5)P_3 (Wymann et al. 2003).

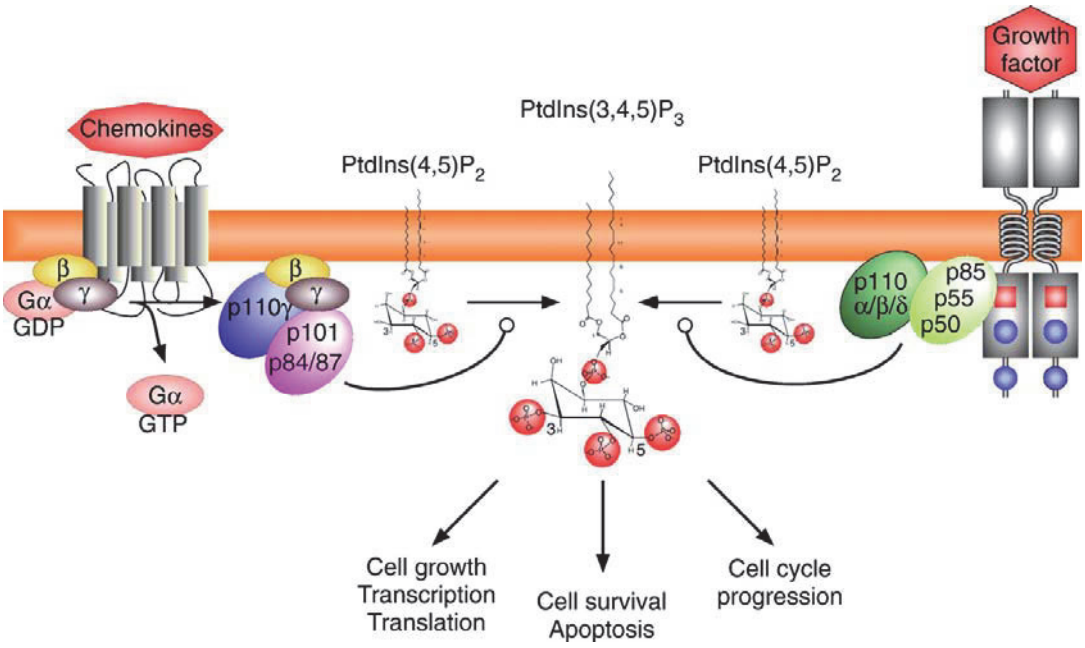

Figure 1.3: Simplified activation scheme of class I PI3Ks. (Marone *et al.*, 2008), used with permission.

1.1.3 PI3K-Akt signaling pathway

The most important link between PI3K and its downstream targets is Akt also known as protein kinase B (PKB) (Sui et al. 2008). The PI3K- Akt pathway is highly conserved, and its activation is tightly controlled via PtdIns(3,4,5)P_3. PI3K-Akt signaling pathway has been implicated in mediating the intracellular effects of several endothe-

lial cell stimuli including angiopoietin-1 (Ang-1), angiopoietin-2 (Ang-2) (Brindle et al. 2006, Papapetropoulos et al. 2000), insulin-like growth factor-I (IGF-I) (Michell et al. 1999), sphingosine-1-phosphate (S1P) (Igarashi and Michel 2001, Morales-Ruiz et al. 2001) and hepatocyte growth factor (HGF) (Nakagami et al. 2001), indicating the pivotal role of this signaling pathway in controlling endothelial cell survival, adhesion and migration, which are important processes in angiogenesis.

1.2 The reactive oxygen species

Increased oxidative stress plays a central role in the pathogenesis of vascular disease (Heistad 2006, Madamanchi et al. 2005, Violi et al. 2005). However, moderate levels of reactive oxygen species (ROS), such as superoxide anions (O_2^-) and hydrogen peroxide (H_2O_2), produced in response to the activation of various cell surface receptors and serve as intracellular signals to mediate various biological responses such as cell migration, proliferation, gene expression and angiogenesis (Caliceti et al. 2014, Oshikawa et al. 2012, Ushio-Fukai and Urao 2009). Furthermore, many studies have revealed that a major source of ROS is generated from nicotinamide adenine dinucleotide phosphate **(**NADPH**)** oxidase **(**NOX**),** which play an important role in Flk-1 signaling and angiogenic responses in endothelial cells (Ushio-Fukai 2007, Ushio-Fukai and Urao 2009). Although the role of ROS in angiogenesis has been reported (Maulik 2002, Sauer et al. 2005, Sauer and Wartenberg 2005), the upstream signaling events stimulating ROS production by VEGF-PI3Ks are still not well characterized (Chatterjee et al. 2012, Chen et al. 2006, Kennedy and DeLeo 2008).

NADPH oxidases are comprised of membrane proteins (i.e. the catalytic flavin–heme protein), NOX, of which five isoforms exist (NOX1–5), and the non-catalytic 22 kDa binding protein, $p22^{phox}$. Catalytic NOX subunits include an N-terminal domain composed of 6 transmembrane helices, numbered I though VI. Four histidine residues in helices III and V coordinate 2 heme (Fig. 1.4). The iron in haems is capable of undergoing reduction and re-oxidation, thereby functioning as an electron carrier. The two haems together provide a channel for electrons to pass across the membrane. A cytosolic C-terminal dehydrogenase domain includes an flavin adenine dinucleotide (FAD) cofactor and NADPH substrate binding site. Both NOX1 and NOX2 form a complex with $p22^{phox}$, which includes 2 transmembrane domains and a C-terminal proline-rich region (PRR) (Lassegue and Clempus 2003, Lassegue et al. 2012). Other components of the NADPH oxidase can include a cytosolic organizer ($p47^{phox}$ or

Noxo1), an activator ($p67^{phox}$ or Noxa1) and $p40^{phox}$ (only with $p67^{phox}$) (Lassegue et al. 2012, Opitz et al. 2007). On activation, electrons are transferred from NADPH to flavin adenine dinucleotide (FAD) and across the membrane, via heme irons, to molecular oxygen, thus producing superoxide anion (O_2^-), which can be dismutated into hydrogen peroxide (H_2O_2) as indicated in Figure 1.4 (Lassegue et al. 2012). However, NOX4 and NOX5 may be independent of cytosolic subunits and constitutively active (Bedard and Krause 2007, Lambeth et al. 2007, Opitz et al. 2007). NOX4 also forms a complex with $p22^{phox}$. Whereas NOX5 is composed of a catalytic subunit plus an amino-terminal calcium-binding domain with 4 EF-hands (Bedard and Krause 2007, Lassegue et al. 2012) (Fig. 1.4).

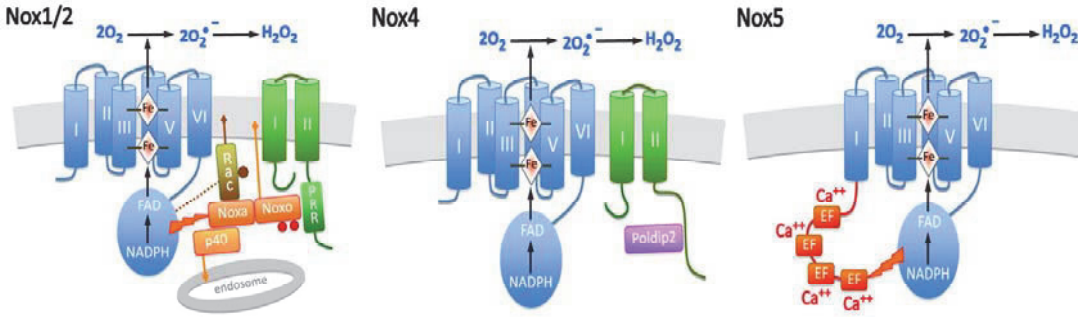

Figure 1.4: Subunits composition and activation of NOX enzymes. Both NOX1 and NOX2 (blue) form a complex with $p22^{phox}$ (green). A cytosolic complex, is composed of an organizer (Noxo1 or $p47^{phox}$), an activator (Noxa1 or $p67^{phox}$) and $p40^{phox}$ (only with $p67^{phox}$). The organizer, stimulated by phosphorylation (red dots) in the case of $p47^{phox}$, binds the proline-rich region of $p22^{phox}$ and membrane lipids. Likewise, $p40^{phox}$ binds lipids in endosomal membranes. Rac, activated by GTP (brown dot), binds membrane, NOX and NOX activators which trigger FAD reduction. Nox4 (blue) also forms a complex with $p22^{phox}$. Its activity, constitutive in the absence of cytosolic subunits, can be increased by binding of polymerase delta interacting protein 2 (Poldip2) to the cytosolic C-terminal of $p22^{phox}$. NOX5 is composed of a catalytic subunit similar to the other oxidases (blue), plus an amino-terminal calcium-binding domain (red) with 4 EF-hands. Binding of cytosolic calcium to the EF hands triggers NOX5 activation. (Lassègue *et al.,* 2012), used with permission.

A previous study has demonstrated that ras-related C3 botulinum toxin substrate 1 (Rac1) activity corresponds with angiogenesis in hepatocellular carcinoma (Lee et al. 2006). Moreover, it has been found that PI3K regulates the cell migration through activation the Rac1 (Williams et al. 2000, Xu et al. 2012). Also, Rac1 has been found to bind to NOX1 and NOX2 and activate NADPH oxidase (Lambeth 2007). Other studies have shown that Rac1 is involved in the control of angiogenesis by inducing ROS production (Diebold et al. 2009, Li et al. 2010, Tobar et al. 2008). Thus, it is

worthwhile to explore whether PI3K and Rac1 signaling pathways are involved in VEGF-induced ROS production in vasculogenesis/angiogenesis of ES cells.

1.3 Embryonic stem cells

The first murine embryonic stem (ES) cell lines were successfully derived directly from inner cell mass (ICM) of pre-implantation embryos at the blastocyst stage in 1981 (Evans and Kaufman 1981). The abilities of ES cells to self-renew indefinitely and to differentiate in all the three germ layers make these ES cells very attractive tool to investigate molecular mechanisms and genes involved in mammalian development (Rathjen et al. 1998). ES cells can be maintained in their pluripotent state if cultured in the presence of leukemia inhibitory factor (LIF) or cultured on feeder layers, which inhibit their differentiation. When LIF is removed, ES cells spontaneously differentiate *in vitro* and form embryo-like aggregates, called the embryoid bodies (Fig. 1.5), which can give rise to any cell type in the body including hematopoietic cells, neuronal cells, cardiomyocytes and muscle cells, epithelial cells, and cells of the endothelial lineage see figure 1.5 (Rathjen et al. 1998, Wobus and Boheler 2005).

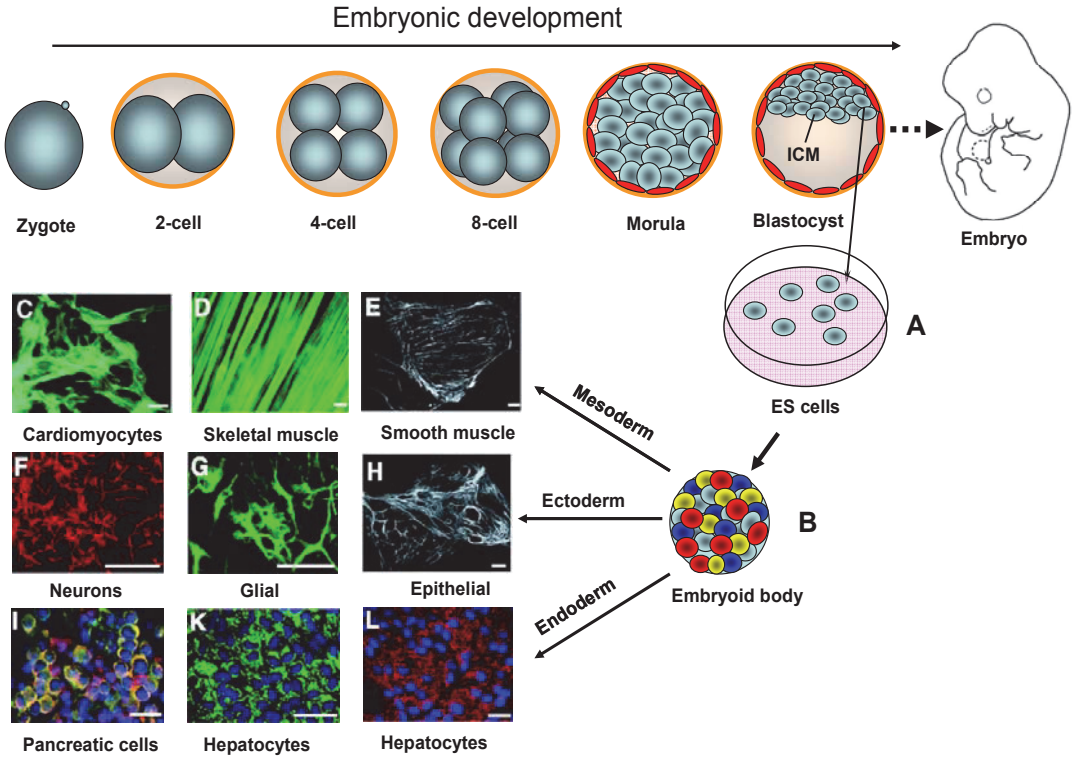

Fig. 1.5: In vitro differentiation of ES cells. ES cells isolated from inner cell mass (ICM) of pre-implantation embryos at the blastocyst stage. Undifferentiated mouse ES cells (A) develop *in vitro* via three-dimensional aggregates (embryoid body, B) into differentiated cell

types of all three primary germ layers. Shown are differentiated cell types labeled by tissue-specific antibodies (in parentheses). C: cardiomyocytes (titin Z-band epitope). (D), skeletal muscle (titin Z-band epitope). (E), smooth muscle (smooth muscle α-actin). (F), neuronal (βIII tubulin). (G), glial (glial fibrillary acidic protein, GFAP). (H), epithelial cells (cytokeratin 8). (I), pancreatic endocrine cells [insulin (red), C-peptide (green), insulin and C-peptide colabeling (yellow)]. (K) and (L), hepatocytes (K, albumin, L, α1-antitrypsin). (modified from Wobus and Boheler, 2005).

1.4 Differentiation of pluripotent ES cells into endothelial cell

The abilities of ES cells to differentiate into endothelial cell and vascular structure formation provide a powerful *in vitro* model system to study the molecular mechanisms of earliest stages of vascular formation (Vittet et al. 1996). Moreover, the expression of various endothelial cell markers in the ES cells derived embryoid bodies was found to follow the sequence of events occurring *in vivo* (Kabrun et al. 1997, Redick and Bautch 1999). Interestingly, vascular progenitor cells in 4-day-old embryoid bodies express the Flk-1 one of the early marker for endothelial lineage (Keller 2005). Furthermore, the isolated Flk-1 positive cells from the ES cells were able to differentiate *in vitro* and also *in vivo* into vascular endothelial cells (Yamashita et al. 2000). We previously established purification system for $Flk1^+$ cells from ES cells and showed that $Flk1^+$ cells give rise to endothelial cells *in vitro* (Bekhite et al., 2011). Therefore it is possible to track the transition from early differentiation to mature vascular cells, distinguishing them from other cell lineages. The ES model system has the advantage to be devoid of interference with host responses. Moreover, it may constitute an alternative to animal experimentation, which suffers from ethical constraints. Moreover, the ES system allows the study of both vasculogenesis and angiogenesis, which is a unique property conferring superiority to all other *in vitro* angiogenesis models. In addition, the differentiation of genetically modified ES cells analyses are also excellent alternatives and substitutes to *in vivo* studies to analyze the consequences of vascular development (Wobus and Boheler 2005). Moreover, this model responding to both positive and negative modulators of angiogenesis can be exploited for the identification of novel signaling molecules (Feraud et al. 2001).Due to increasing the number of new antiangiogenic agents, each of them representing promising tools in therapy, this model can be useful to quickly identify their effects on vascular differentiation (Feraud et al. 2001).

1.5 Tumors and antiangiogenic therapies

More than a century ago, early pioneering researchers observed that dense vascular networks often accompanied human tumors (Ide et al. 1939). In 1971, Judah Folkman, who became known as the “father of tumor angiogenesis,” first emphasized the importance of tumor vascularity for tumor growth (Folkman 1971). This observation led to the development of antiangiogenic therapy by Folkman and colleagues (Folkman 1971, Folkman et al. 1971), which is based on the assumption that inhibition of tumor-induced angiogenesis would deprive the growing tumor of nutrients and oxygen supplied by the host circulation and, consequently, would retard or even abolish tumor growth. In a similar manner as in embryogenesis, most tumor masses grow avascular, until an equilibrium between proliferation and apoptosis is reached, and thus can persist in this dormant encapsulated state (Leite de Oliveira et al. 2011). The gradient in oxygen, pH, nutrients and the absence of sufficient detoxicfication then results in growth arrest (Awwad et al. 1986). Many tumors produce growth factors that stimulate angiogenesis, other tumors somehow induce surrounding normal cells to synthesize and secrete such factors as presented in figure 1.6. The resulting new blood vessels “feed” growing tumors with oxygen and nutrients, allowing the cancer cells to invade nearby tissue, to move throughout the body and to form new colonies of cancer cells, called metastases (Ferrara and Kerbel 2005). The "angiogenic switch" that initiates this process depends on a net balance of positive and negative angiogenic factors secreted by tumor (Keyhani et al. 2001). The VEGF family of ligands and receptors are potent inducers of angiogenesis. In most circumstances, the increased production of VEGF begins when tumors grow into certain size and tumor cells within the tissue undergo hypoxia (Roskoski 2007). The use of VEGF blockers to prevent this process is the most established of the anti-angiogenic modalities (Ferrara and Kerbel 2005, Kim et al. 1993). However, several studies have shown that VEGF blockade damages not only tumor vessels but also healthy vessels and results in severe problems such as hemorrhagic and thrombotic events (Ratner 2004, Verheul and Pinedo 2007).

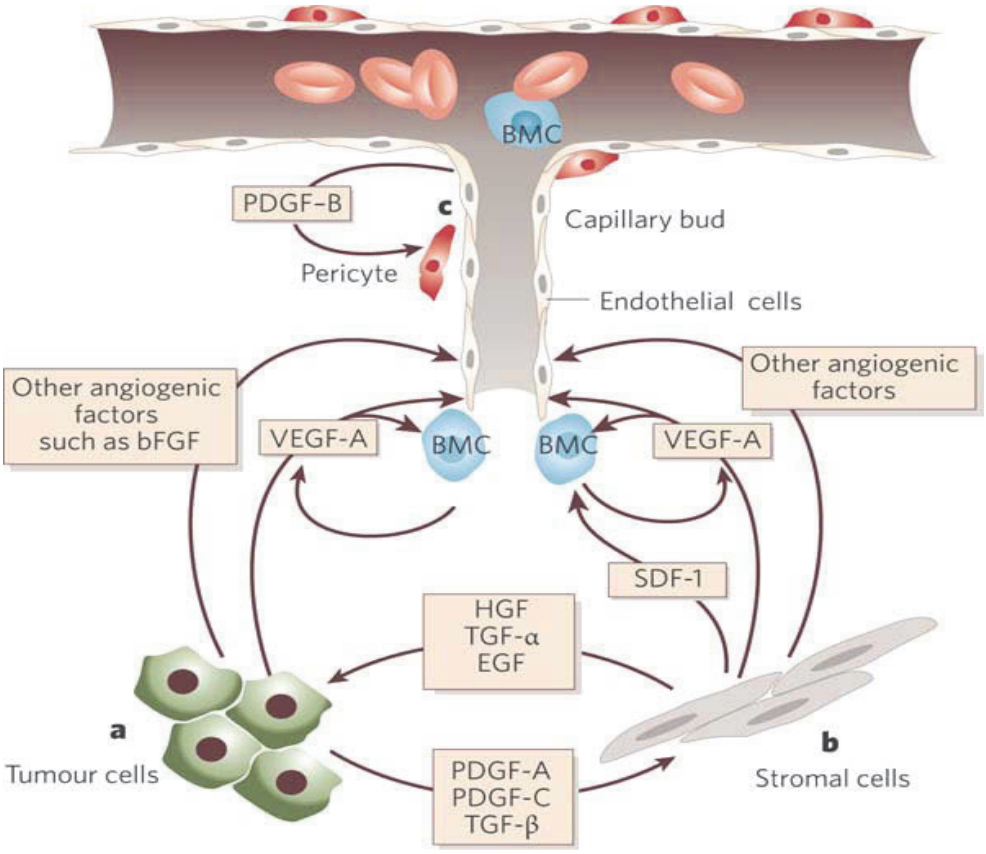

Figure 1.6: Tumor produce growth factors that stimulate angiogenesis for delivery of oxygen and nutrients required for their growth and metastasis. (a), tumour cells produce VEGF-A and other angiogenic factors such as basic fibroblast growth factor (bFGF), angiopoietins, interleukin-8, placental growth factor (PlGF) and VEGF-C. These stimulate resident endothelial cells to proliferate and migrate. (b), an additional source of angiogenic factors is the stroma. This is a heterogeneous compartment, comprising fibroblastic, inflammatory and immune cells. Recent studies indicate that tumour-associated fibroblasts produce chemokines such as stromal cell-derived factor-1 (SDF-1), which may recruit bone-marrow-derived angiogenic cells (BMC). Tumour cells may also release stromal cell-recruitment factors, such as platelet-derived growth factor-A (PDGF-A), PDGF-C or transforming growth factor (TGF). A well-established function of tumour-associated fibroblasts is the production of growth/survival factor for tumour cells such as epidermal growth factor receptor (EGFR) ligands, hepatocyte growth factor (HGF) and heregulin. (c), endothelial cells produce PDGF-B, which promotes recruitment of pericytes in the microvasculature after activation of platelet-derived growth factor receptors (PDGFR). HGF, hepatocyte growth factor. (Ferrara and Kerbel, 2005), used with permission.

1.5.1 Confrontation culture of ES cells with multicellular tumor spheroids

Multicellular tumor spheroids are three-dimensional cell systems for avascular micrometastases or avascular microregions of solid tumors (Mueller-Klieser 1997). Multicellular aggregates are more useful than two-dimensional monolayer cultures from an experimental perspective, because preservation of the three-dimensional

structure is important for cell-to-cell and cell-to-matrix interactions. These spheroids have been applied in various studies, including study tumor-induced angiogenesis, i.e., the invasion of endothelial host-derived cells into a tumor tissue (Wartenberg et al. 2001). Using confrontation culture consists of embryoied bodies and multicellular tumor spheroids from human prostate carcinoma cell line (DU-145), tumor-induced angiogenesis were studied in NOX1 isoform and PI3Kα knockdown embryoid bodies derived from ES cells.

2. AIM OF THE STUDY

The aim of the study is to investigate the role of class IA PI3Kα-NADPH oxidases signaling pathways and their downstream effectors that mediate VEGF-induced angiogenesis/vasculogenesis of mouse embryonic stem (ES) cells. Thus the aims were:

1. To determine the expression pattern of class IA PI3K catalytic subunits p110α, Flk-1 and the vascular differentiation indicted by CD31 (PECAM-1) as well as intracellular ROS production in the embryoid bodies derived from the ES cells.
2. To determine whether ROS is necessary for VEGF-PI3K signaling regulated vasculogenesis/angiogenesis.
3. To determine whether the ROS production from NADPH oxidases is depend on PI3K activation.
4. To study the role of PI3Kα-NADPH oxidases for vasculogenesis/angiogenesis and cell migration using ES cells stably producing shRNA targeting PI3Kα or NADPH oxidases.
5. To assessment the efficiency of inhibition the NOX isoform and PI3Kα on tumor-induced angiogenesis using the confrontation cultures consisting of embryoid bodies and multicellular DU-145 prostate tumor spheroids.

This study may provide an avenue for better understanding of the effect of VEGF on blood vessels formation to treat many pathological blood vessel conditions.

3. MATERIAL AND METHODS

3.1 Materials

3.1.1 Equipments

Equipment	Company
Agar gel electrophoresis	Biometra GmbH, Göttingen, Germany
AMAXA Nucleofector	Loanza Cologne GmbH, Germany
Analytical balance BP 221S	Sartorius AG, Göttingen, Germany
ApoTome	Carl Zeiss AG, Jena, Germany
Autoclave	MELAG oHG, Berlin, Germany
Cellspin stirrer system	Integra Biosciences GmbH, Fernwald, Germany
Cell scrapers	Greiner Bio-One GmbH, Frickenhausen, Germany
Centrifuge	Hettich GmbH & Co. KG, Tuttlingen, Germany
Clean bench HERAsafe	Heraeus Instruments GmbH, Hanau, Germany
CO_2-incubator HERAsafe	Heraeus Instruments GmbH, Hanau, Germany
Counting cell chamber	Paul Marienfeld GmbH & Co. KG, Germany
FACSCalibur	Becton Dickinson GmbH, Heidelberg, Germany
Hot plate	Labotect, Rosdorf, Germany
Laboratory centrifuge	Eppendorf AG, Hamburg, Germany
LAS-3000 imager	Fujifilm, Tokyo, Japan
LSM 510	Carl Zeiss AG, Jena, Germany
Light-optical microscope TELAVAL 31	Carl Zeiss AG, Jena, Germany
MACS Separator	Miltenyi GmbH, Bergisch Gladbach, Germany
Magnetic plate stirrer	IKA-Werke GmbH & Co. KG, Staufen, Germany
Mastercycler gradient	Eppendorf AG, Hamburg, Germany
Microplate reader infinite m200	Tecan Group, Switzerland
Mini-PROTEAN 3 Multi-Casting Chamber	BioRad GmbH, Dreieich, Germany
Mini-PROTEAN 3 glass plates	BioRad GmbH, Dreieich, Germany
Mini-PROTEAN 3 spacer plates	BioRad GmbH, Dreieich, Germany
Nanodrop	Peqlab Biotechnologie GmbH, Erlangen, Germany
pH-meter inoLAB	WTW GmbH, Weilheim, Germany
Photometer	Eppendorf AG, Hamburg, Germany
Pipettor	Integra Biosciences GmbH, Fernwald, Germany
PowerPac™ 300 Power Supply	BioRad GmbH, Dreieich, Germany
Shaker TH15	Edmund Bühler GmbH, Germany
Spinner flask cellspin	Integra Biosciences GmbH, Fernwald, Germany
Syngene G:Box	VWR International GmbH, Darmstadt, Germany

Thermal cycler UNO II	Biometria GmbH, Göttingen, Germany
Water bath Grant SUB36	VWR International GmbH, Darmstadt, Germany
Vortex-Genie 2	VWR International GmbH, Darmstadt, Germany

3.1.2 Software

Software	Company
AxioVision	Carl Zeiss AG, Jena, Germany
Image Reader LAS-3000	Fujifilm, Tokyo, Japan
CellQuest Pro	Becton Dickinson GmbH, Heidelberg
EndNote	Thomson Reuters, San Francisco, USA
GraphPad Instat 3	GraphPad Software, San Diego, USA
LSM Image Examiner Software	Carl Zeiss AG, Jena, Germany
LSM 510 software	Carl Zeiss AG, Jena, Germany
SigmaPlot 12.0	Systat Software, München, Germany
Syngene GeneTools image analysis program	Syngene, Maryland, USA

3.1.3 Chemicals and reagents

Name	Producer
Acetone	Carl Roth GmbH & Co.KG, Karlsruhe Germany
Acrylamide-bisacrylamide (40%)	Merck KGaA, Darmstadt, Germany
Agarose	SERVA GmbH, Heidelberg , Germany
APS	Merck KGaA, Darmstadt, Germany
Aprotinin	Merck KGaA, Darmstadt, Germany
Bromophenol blue	Sigma-Aldrich GmbH, Taufkirchen, Germany
BSA	Sigma-Aldrich GmbH, Taufkirchen, Germany
Calcium chloride	Sigma-Aldrich GmbH, Taufkirchen, Germany
Carbamide, urea (≥99.5%)	Carl Roth GmbH & Co.KG, Karlsruhe Germany
Celltracker CMFDA	Invitrogen GmbH, Karlsruhe, Germany
Collagenase type II	PAA GmbH, Coelbe, Germany
DHE	Invitrogen GmbH, Karlsruhe, Germany
DMSO	Sigma-Aldrich GmbH, Taufkirchen, Germany
DTT	Invitrogen GmbH, Karlsruhe, Germany
Dulbecco's PBS	PAA GmbH, Coelbe, Germany
ECL™ Western blotting detection reagents	Amersham GmbH, Freiburg, Germany
Ethanol (≥99.8%)	Merck KGaA, Darmstadt, Germany
EDTA	Sigma-Aldrich GmbH, Taufkirchen, Germany
Gelatine	Sigma-Aldrich GmbH, Taufkirchen, Germany
Glucose	Sigma-Aldrich GmbH, Taufkirchen, Germany
Glycine	Sigma-Aldrich GmbH, Taufkirchen, Germany

HEPES	Sigma-Aldrich GmbH, Taufkirchen, Germany
H_2DCF-DA	Invitrogen GmbH, Karlsruhe, Germany
LB-Agar, powder (Lennox L agar)	Invitrogen GmbH, Karlsruhe, Germany
Leupeptin hydrochloride	Sigma-Aldrich GmbH, Taufkirchen, Germany
Magnesium chloride	Sigma-Aldrich GmbH, Taufkirchen, Germany
Magnesium sulphate	Sigma-Aldrich GmbH, Taufkirchen, Germany
Methanol (>99%)	Carl Roth GmbH & Co.KG, Karlsruhe Germany
Milk powder, blotting grade	Carl Roth GmbH & Co.KG, Karlsruhe Germany
Pepstatin A, 100,000 units/mg	Sigma-Aldrich GmbH, Taufkirchen, Germany
PFA	Carl Roth GmbH & Co.KG, Karlsruhe Germany
Phenylmethylsulfonyl fluoride	Sigma-Aldrich GmbH, Taufkirchen, Germany
Phosphatase inhibitor Cocktail 3	Sigma-Aldrich GmbH, Taufkirchen, Germany
Potassium chloride	Carl Roth GmbH & Co.KG, Karlsruhe Germany
Sigmacote	Sigma-Aldrich GmbH, Taufkirchen, Germany
Sodium chloride	Carl Roth GmbH & Co.KG, Karlsruhe Germany
SDS(≥99.0%)	Sigma-Aldrich GmbH, Taufkirchen, Germany
Sodium hydrogen phosphate	Sigma-Aldrich GmbH, Taufkirchen, Germany
Sodium hydroxide	Carl Roth GmbH & Co.KG, Karlsruhe Germany
Sodium pyruvate	Biochrom AG, Berlin, Germany
Sodium vanadate (≥90%)	Sigma-Aldrich GmbH, Taufkirchen, Germany
Taurine	Sigma-Aldrich GmbH, Taufkirchen, Germany
TEMED	Merck KGaA, Darmstadt, Germany
Tris base (≥99.8%)	Sigma-Aldrich GmbH, Taufkirchen, Germany
Triton® X-100	Sigma-Aldrich GmbH, Taufkirchen, Germany
Tween 20	Carl Roth GmbH & Co.KG, Karlsruhe Germany

3.1.4 Antibodies

3.1.4.1 Primary antibodies

Antigen	Origin	Dilution	Producer
Polyclonal GAPDH	Rabbit	1:1000	Abcam
Phosphor-RhoA (Ser188)	Rabbit	1:1000	Abcam
Polyclonal RhoA	Rabbit	1:1000	Cell Signaling Technology
Rac1/2/3	Rabbit	1:1000	Cell Signaling Technology
Phosphor-Rac1(Ser71)	Rabbit	1:1000	Cell Signaling Technology
Phospho-p44/42 MAPK (Erk1/2) (Thr202/Tyr204)	Rabbit	1:1000	Cell Signaling Technology
Phospho-p38 MAPK (Thr180 /Tyr182)	Rabbit	1:1000	Cell Signaling Technology
Phospho-SAPK/JNK (Thr183 /Tyr185)	Rabbit	1:1000	Cell Signaling Technology
Phospho-Akt (Ser473)	Rabbit	1:1000	Cell Signaling Technology
Polyclonal Akt,	Rabbit	1:1000	Cell Signaling Technology

Polyclonal p44/42 MAPK (Erk1/2)	Rabbit	1:1000	Cell Signaling Technology
Polyclonal p38 MAPK	Rabbit	1:1000	Cell Signaling Technology
Polyclonal SAPK/JNK	Rabbit	1:1000	Cell Signaling Technology
Monoclonal anti-PECAM-1	Rat	1:100	Chemicon
Polyclonal anti-NOX1	Goat	1:1000	Santa Cruz Biotechnology
Polyclonal anti-NOX2/gp91phox	Rabbit	1:1000	Abcam
Polyclonal ani-PI 3-kinase p110α	Goat	1:500	Santa Cruz Biotechnology
Polyclonal ani-PI 3-kinase p110β	Rabbit	1:500	Santa Cruz Biotechnology
Polyclonal ani-PI 3-kinase p110δ	Mouse	1:500	Santa Cruz Biotechnology
PE-conjugated anti-mouse Flk-1	Rat	1:10	BD Pharmingen
Phalloidin-Alexa Fluor® 488	*A.phalloides*	1:100	Invitrogen

3.1.4.2 Secondary antibodies

Name	Dilution	Producer
Anti-PE MicroBeads (isotype: mouse IgG1)	1:10	Miltenyi Biotec
Goat anti-rat IgG, Cy5 conjugate	1:100	Chemicon
Goat anti-mouse IgG-HRP	1:1000	Santa Cruz Biotechnology
Goat anti-rabbit IgG-HRP	1:1000	Santa Cruz Biotechnology
Rabbit anti-goat IgG-HRP	1:1000	Santa Cruz Biotechnology

3.1.5 Inhibitors

Product name	Producer
Akt inhibitor	Calbiochem GmbH, Bad Soden, Germany
Apocynin	Sigma-Aldrich GmbH, Taufkirchen, Germany
2-APT	Calbiochem GmbH, Bad Soden, Germany
Compound 15e	Alexis®Biochemicals GmbH, Lörrach, Germany
DPI	Sigma-Aldrich GmbH, Taufkirchen, Germany
Rotenone	Calbiochem GmbH, Bad Soden, Germany
Rac1 inhibitor	Calbiochem GmbH, Bad Soden, Germany
VAS2870	Calbiochem GmbH, Bad Soden, Germany
Wortmannin	Sigma-Aldrich GmbH, Taufkirchen, Germany

3.1.6 RT-PCR materiales

Product name	Producer
DTT 0.1 M	Invitrogen GmbH, Karlsruhe, Germany

Desoxyribonucleae I, Amp Grade 1 U/µl	Invitrogen GmbH, Karlsruhe, Germany
DNase I reaction buffer 10x	Invitrogen GmbH, Karlsruhe, Germany
dNTP Mix, 10 mM, PCR Grade	Invitrogen GmbH, Karlsruhe, Germany
EDTA 25 mM	Invitrogen GmbH, Karlsruhe, Germany
Ethidium bromide 2	Carl Roth GmbH & Co.KG, Karlsruhe Germany
First-strand buffer 5x	Invitrogen GmbH, Karlsruhe, Germany
HyperLadder™ IV DNA Ladder	Invitrogen GmbH, Karlsruhe, Germany
M-MLV reverse transcriptase 200 U/µl	Invitrogen GmbH, Karlsruhe, Germany
QIAshredder	Qiagen GmbH, Hildesheim, Germany
Random primer oligonucleotides	Invitrogen GmbH, Karlsruhe, Germany
Red load taq master 5x	Jena Bioscience, Jena, Germany
TBE buffer 10x Ultra Pure™	Invitrogen GmbH, Karlsruhe, Germany

3.1.6.1 List of primers used in this study for RT-PCR

Primer		Primer sequence
NOX1	Sense	5'-CTG CTC ATT TTG CAA CCG TA-3'
	Antisense	5'-AGA AG CGA GAG ATC CAT CCA-3
NOX2	Sense	5'-ACT GCG GAG AGT TTG GAA GA-3'
	Antisense	5'-GGT GAT GAC CAC CTT TTG CT-3
NOX3	Sense	5'-GAT GGC ACC TGG ACA GTA CAT-3'
	Antisense	5'- TCT CCT GAG GCT CTG ATG TGT-3'
NOX4	Sense	5'-GAT CAC AGA AGG TCC CTA GCA-3'
	Antisense	5'-GTT GAG GGC ATT CAC CAA GT-3'
PI3K p110α	Sense	5'-ACT GTT CAG AGA GGC CAG GA-3'
	Antisense	5'-CGG TTG CCT ACT GGT TCA AT-3'
PI3k p110β	Sense	5'-AGC TGG TCT TCG TTT CCT GA-3'
	Antisense	5'-TCC ACC ACG ACT TGA CAC AT-3'
PI3k p110δ	Sense	5'-CTG ACC CCT CAT CTG ACC AT-3'
	Antisense	5'-TCG TCA GCA TTC ACT TTT CG-3'
Polymerase II	Sense	5'-GAC AAA ACT GGC TCC TCT GC-3'
	Antisense	5'-GCT TGC CCT CTA CAT TCT GC-3'

3.1.7 shRNA materials

Product name	Producer
Ampicillin	Sigma-Aldrich GmbH, Taufkirchen, Germany
EndoFree Plasmid Maxi Kit	Qiagen GmbH, Hildesheim, Germany
PEI	Sigma-Aldrich GmbH, Taufkirchen, Germany
MISSION® Lentiviral Packaging Mix	Sigma-Aldrich GmbH, Taufkirchen, Germany
MISSION® non-Target shRNA	Sigma-Aldrich GmbH, Taufkirchen, Germany

control vector	
MISSION® p110α shRNA	Sigma-Aldrich GmbH, Taufkirchen, Germany
MISSION® NOX1 shRNA	Sigma-Aldrich GmbH, Taufkirchen, Germany
MISSION® NOX2 shRNA	Sigma-Aldrich GmbH, Taufkirchen, Germany
pLKO.1-puro derivative plasmids	Sigma-Aldrich GmbH, Taufkirchen, Germany
Penicillin/Steptomycin	Biochrom AG, Berlin, Germany
Polybrene	Sigma-Aldrich GmbH, Taufkirchen, Germany
Puromycin	Sigma-Aldrich GmbH, Taufkirchen, Germany
Syringe filter holders (0.2 µm)	Sartorius AG, Göttingen, Germany

3.1.7.1 Hairpin sequence

Clone ID	Hairpin Sequence (forward-loop-reverse)
	p110α MISSION® shRNA
NM_008839.1-2719s1c1	5'-gcaacctttatcttgggaatt-**ctcgag**-aattcccaagataaaggttgc-3'
	NOX1 MISSION® shRNA
NM_172203.1-882s1c1	5'-cgtgattaccaaggttgtcat-**ctcgag**-atgacaaccttggtaatcacg-3'
	NOX2 MISSION® shRNA
NM_007807.2-1153s1c1	5'-gcctggaaactacctaagata-**ctcgag**-tatcttaggtagtttccaggc- 3'

3.1.8 Consumables materials

Product name	Producer
Cellstar tissue culture flasks	Greiner Bio-One GmbH, Frickenhausen, Germany
Cellstar® Falcon tubes (15 ml, 50 ml)	Greiner Bio-One GmbH, Frickenhausen, Germany
Centrifuge tubes	Sarstedt AG & Co, Nümbrecht Germany
Cover slip	Menzel GmbH & Co KG, Braunschweig, Germany
Cryogenic storage vial	Fisher Scientific, Schwerte, Germany
Disinfectant descosept AF	Dr. Schumacher GmbH, Malsfeld, Germany
Disposable pipette	Greiner Bio-One GmbH, Frickenhausen, Germany
Disposable syringes Omnifix® 50 ml	Braun Melsungen AG, Melsungen, Germany
Microscope slide	Menzel GmbH & Co KG, Braunschweig, Germany
Microcentrifuge tubes	Sarstedt AG & Co, Nümbrecht Germany
MS Columns	Miltenyi GmbH, Bergisch Gladbach
Petri dish (adherent and not adherent)	Greiner Bio-One GmbH, Frickenhausen, Germany
Pipette tips	Nerbe pluc GmbH, Winsen, Germany
Polypropylene tube, sterile 15/50 ml	Greiner Bio-One GmbH, Frickenhausen, Germany
Precision plus protein standard 10-250 kDa	BioRad GmbH, Dreieich, Germany
Pre-Separation-Filter	Miltenyi GmbH, Bergisch Gladbach
Protran nitrocellulose	Whatman GmbH, Dassel, Germany

membrane	
Serological pipettes	Greiner Bio-One GmbH, Frickenhausen, Germany
Stericup	Millipore GmbH, Schwalbach, Germany
Sterile filter (0.2 µm)	Sartorius AG, Göttingen, Germany
6/12/24/96-well cell culture plate	Greiner Bio-one GmbH, Frickenhausen

3.1.9 Buffers

Buffer	Components
Cell dissociation buffer (IK-buffer)	120 mM $NaCl_2$, 5.4 mM KCl, 5 $MgSO_4$, 5 mM Na pyruvate, 1 mM $MgCl_2$, 20 mM Glucose , 20 taurine and 10 mM HEPES
E1 buffer	135 mM NaCl, 5.4 mM KCl, 1 mM $MgCl_2$, 10mM glucose, 10 mM HEPES, 1.8 mM $CaCl_2$, pH 7.5
FACS buffer	PBS 1x, 2% FBS
Lysis buffer	20 mM Tris-HCl pH 7.5, 1% Triton X-100, 1 mM EDTA, 1 mM phenylmethylsulfonyl fluoride, 1 mM DTT, 10 µg/ml aprotinin, 5 µg/ml pepstatin A, 25 µg/ml leupeptin, 1 mM sodium vanadate, 10 µl/ml Phosphatase Inhibitor cocktail 3
MACS buffer	0,5 mM FBS, 2 mM EDTA in PBS
PBS 1x	137 mM NaCl, 2.7 mM KCl, 10 mM Na_2HPO_4, 1.76 mM K_2HPO_4, pH 7.4
PBS-Triton 1%	1% Triton X-100 in 1x PBS
PBS-Tween 0.1%	1x PBS, 0.1% Tween 20
PFA 4% buffer	4% PFA in 1x PBS
Resolving gel	40% acrylamide, 1.5 M Tris-HCl (pH 8.8), 10% SDS, dH_2O, 10% APS, TEMED
5x SDS-PAGE electrophoresis buffer	25 mM Tris-base, 200 mM glycine, 0.1% SDS
SDS-PAGE loading buffer	0.5 M Tris (pH 6.8), 10% SDS, 99% glycerol, DTT, carbamide/ urea, bromophenol blue
Stacking gel 4%	40% acrylamide, 0.5 Tris-HCl (pH 6.8), 10% SDS, dH_2O, 10% APS, TEMED
Stripping buffer	20 ml SDS 10%,12.5 ml 0.5 MTris-HCl pH 6.8, 0.8 ß-mercaptoethanol, 67.5 dH_2O
Transfer buffer	25 mM Tris base, 192 mM glycine, 20% methanol
1.5 M Tris-HCl, pH 8.8	54.5 g Tris base, pH to 8.8, 300 ml dH_2O.
0.5 M Tris-HCl, pH 6.8	12.1 g Tris base, pH to 6.8, 200 ml dH_2O.
1x TBS	50 mM Tris-Cl, 150 mMNaCl, pH 7.5

3.1.10 Cell culture media

3.1.10.1 Basic components and supplements

Product name	Producer
Basal Iscove	Biochrom AG, Berlin, Germany
DMEM	Invitrogen GmbH, Karlsruhe, Germany
FBS	Sigma-Aldrich GmbH, München, Germany
Ham's F-10	Biochrom AG, Berlin, Germany
GMEM	Sigma-Aldrich GmbH, Taufkirchen, Germany
LIF	Millipore GmbH, Schwalbach, Germany
LB-Broth base	Invitrogen GmbH, Karlsruhe, Germany
L-glutamine	Biochrom AG, Berlin, Germany
β-mercaptoethanol	Sigma-Aldrich GmbH, München
NEAA	Biochrom AG, Berlin, Germany
Sodium pyruvate	Biochrom AG, Berlin, Germany
Trypsin-EDTA (0.25%), phenol red	Invitrogen GmbH, Karlsruhe, Germany

3.1.10.2 Composition of cell culture media

Medium	Components
CGR8-Culture medium	25 ml GMEM 2,5 ml heat-inactived FBS 12,5 µl ß-mercaptoethanol (70.4 µl ß-mercaptoethanol in 10 ml PBS sterile) 250 µl L-glutamine 250 µl LIF, (103 U/ml LIF)
CGR8-Differentiation medium	500 ml Basal Iscove Medium w/o L-glutamin 100 ml heat-inactived FBS 0,5 ml ß-mercaptoethanol (70.4 µl ß-mercaptoethanol in 10 ml PBS sterile) 6,25 ml L-glutamine 6,25 ml NEAA
CGR8-Freezing medium	45 ml CGR8 differentiation medium 5 ml DMSO
HEK293T-Culture medium	500 ml DMEM 50 ml heat-inactived FBS 5 ml L-glutamine 5 ml NEAA 2,5 ml Penicillin/Steptomycin
DU-145 -Culture medium	500 ml Ham's F-10 medium 50 ml heat-inactived FBS 5 ml L-glutamine 5 ml β-mercaptoethanol (140 µl ß-

	mercaptoethanol in 200 ml PBS sterile) 5 ml NEAA 2.5 ml Penicillin/Steptomycin
E. coli.-Culture medium (LB-Medium)	1 liter dH_2O 20 g LB Broth Base (Lennox L Broth Base) Ampicillin (100µg/ml)

3.1.11 Cell lines

3.1.11.1 CGR8 ES cell line (ECACC, Salisbury, UK)

CGR8 ES cell line was established from the inner cell mass of a 3.5 day male pre-implanted mouse embryo (*Mus musculus*, strain 129). These pluripotent cells were retained the ability to participate in normal embryonic development. Differentiation of CGR8 cell was inhibited by the leukaemia inhibiting factor (LIF) which is identical to pleiotropic cytokine differentiation inhibiting activity (DIA)(Nichols et al. 1990, Robertson et al. 1993).

3.1.11.2 DU-145 cell line was a kind gift of Dr. J. Carlsson (Uppsala, Sweden)

DU-145 cell line was established from the tumor tissue removed from the metastatic central nervous system lesion of a 69-year-old man with prostate carcinoma (Stone et al. 1978). The cells are epithelial, grow in isolated islands on plastic Petri dishes, and form embryoied bodies in spinner flask culture (Wartenberg et al. 1998b).

3.1.11.3 HEK293T cell line (German Collection of Microorganisms and Cell Cultures (DSMZ)

Human Embryonic Kidney (HEK) 293T cells were originally derived from human embryonic kidney (HEK) of healthy aborted fetus. Then HEK 293 cells were generated in the early 70s by transformation of cultures of normal HEK cells with DNA from human adenovirus type 5 (Graham et al. 1977, Graham and van der Eb 1973). The HEK293T cell line was derived from HEK 293 cell line by inserted the gene for T-antigen of Simian Virus 40 (SV40) (Naldini et al. 1996).

3.1.12 Bacteria

Strain	Genotype	Source
E.coli DH5α	F^-, φ80d*lacZ*ΔM15, Δ(*lacZYA-argF*)U169, *deoR*, *recA*1, *endA*1, *hsdR*17(rk^-, mk^+), *phoA*, *supE*44, λ^-, *thi*-1, *gyrA*96, *relA*1	Sigma-Aldrich

3.2 Methods

3.2.1 ES cells and embryoid body culture

The pluripotent ES cell line CGR8 was obtained from European Collection of Cell Cultures (ECACC, UK). The CGR8 cell line was cultured on gelatine-coated cell culture flask (0.1% gelatine in distilled water) in GMEM plus LIF in a humidified environment containing 5% CO_2 at 37°C. ES cells were routinely passaged every 2 days. Cells were covered with 2 ml of trypsin-EDTA solution, then returned to 37°C incubator for 1-2 minutes or until cells were uniformly dispersed into single cells. 9 ml of ES cells medium were added to inactivate the Trypsin. At day 0 of differentiation, adherent cells were enzymatically dissociated using trypsin-EDTA. To generate the embryoid bodies, a total of 1×10^7 cells were seeded in 250 ml siliconized (sigmacot, Sigma-Aldrich) spinner flasks containing 125 ml CGR8-differentiation medium. After 24 hrs, 125 ml medium was added to give a final volume of 250 ml. The spinner flask medium was stirred at 22.5 r.p.m. using a cell-spin stirrer system and 125 ml cell culture medium were exchanged every day as previously described (Wartenberg et al. 1998a). The spinner flask culture technique proved to be efficient, especially for the differentiation of cells of the endothelial and the cardiac lineage. Over 50% of the embryoid bodies manifested into beating cardiomyocytes on day 8, and 100% embryoid bodies showed proper development of vascular-like structures within the embryoid bodies (Wartenberg et al. 1998a). At day four of spinner flask cultivation, embryoid bodies were removed from the spinner flask and placed in non-adherent bacteriological petri dishes for incubation with the various substances.

3.2.2 Thawing and freezing of CGR8 cells

Since DMSO can induce the differentiation of ES cells. Cells must be thawed late in the thawing day and the medium must be changed the following morning to minimize the effects of residual DMSO. Cells were thawed quickly in 37°C water bath. Afterwards they were diluted into prewarmed ES cell medium 10 ml and gently mixed. After centrifugation medium above the pellet was removed and cells were resuspended in 6 ml of prewarmed GMEM medium plus LIF and plated into a gelatine-coated culture flask at 37°C in a humidified 5% CO_2 incubator.

For freezing the CGR8 cells, the cells were trypsinized and resuspended in complete medium and gently centrifuged (800 rpm, 4 min). The medium above the pellet was removed and upto 1×10^7 cells/ml were re-suspended in 3 ml CGR8 freezing me-

dium. Cells were aliquoted into three Cryo-vials. The vials were frozen at -80°C overnight then transferred to liquid nitrogen for long-term storage.

3.2.3 Culture technique of multicellular spheroids

The human prostate cancer cell line DU-145 was grown routinely in 5% CO2, humidified air at 37˚C with DU-145-Culture medium. Cell monolayers were enzymatically dissociated with trypsin-EDTA and seeded in siliconized 250 ml spinner flasks with 250 ml of Ham's F-10 complete medium using a Cell-spin stirrer system as described previously (Wartenberg et al. 2001). Cell culture medium was partially (100 ml) changed every day.

3.2.4 Cultivation of HEK293T

The Human Embryonic Kidney (HEK293T) cell line is for use in facilitating optimal lentivirus production. The HEK293T cell line is an HEK 293 derived cell line that expresses the SV40 large T-antigen (Naldini et al. 1996). T-antigen can also bind to several proteins which inhibit cell cycle. So the cell is forced entering into more number of cell cycle (Bednarz et al. 2000). This adds on to increase the amplification of the transfected plasmid thus increasing the efficiency of transfection, higher vector production and higher transduction efficiency. HEK293T cells were cultured in a complete DMEM medium at 37ºC with 5% CO2.

3.2.5 pLKO.1-puro vector description and features

Features of the pLKO.1-puro vector allow for transient or stable transfection of the shRNA as well as production of lentiviral particles (Stewart et al. 2003). Stable gene silencing is selected using the puromycin selectable marker while self-inactivating replication incompetent viral particles can be produced in packaging cells (HEK293T) by co-transfection with compatible packaging plasmids (Zufferey et al. 1998, Zufferey et al. 1997). Lentiviral based particles permit efficient infection and integration of the specific shRNA construct into differentiated and non-dividing cells and provides long-term knockdown. The length of the pLKO.1-puro plasmid is 7,086 bp, as indicated in the vector map below (Fig. 2.1). Without an shRNA insert, pLKO.1-puro vector has a length of 7,052 bp.

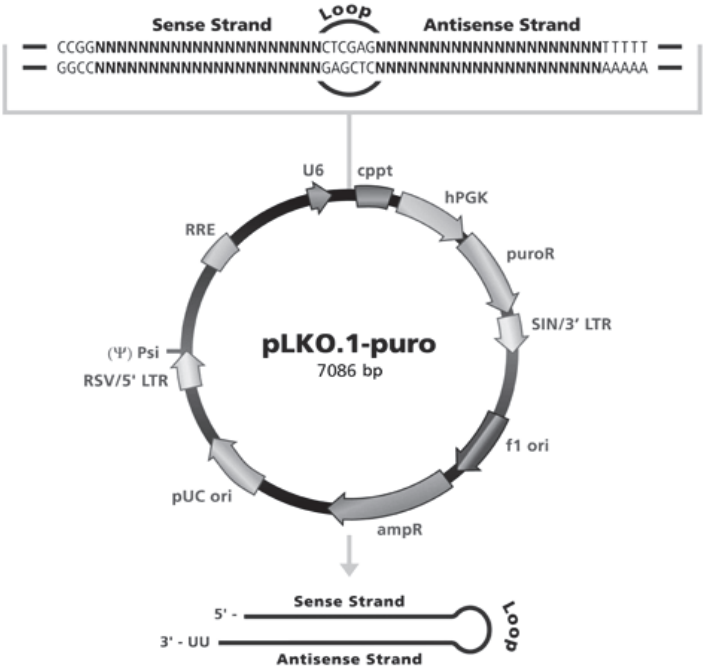

Figure 3.1: Map of pLKO.1 containing an shRNA insert. Abbreviations: Cppt, Central polypurine tract: hPGK, Human phosphoglycerate kinase eukaryotic promoter, puroR, Puromycin resistance gene for mammalian selection, SIN/LTR, 3' self inactivating long terminal repeat, f1 ori, f1 origin of replication, ampR, Ampicillin resistance gene for bacterial selection, pUC ori, pUC origin of replication, 5' LTR, 5' long terminal repeat, Psi, RNA packaging signal, RRE, Rev response element (http://www.sigmaaldrich.com/RNAi).

3.2.6 Competent cells and plasmids transformation

The *Escherichia coli (E.Coli)* strains DH5α was used for propagation of plasmid constructs. Bacterial cells *E.Coli* DH5α were grown in Luria-Bertani (LB) Broth Base or on LB-Agar supplemented with ampicillin antibiotics according to the method previously described by Hanahan 1983 (Hanahan 1983). For each transformation, 2 µl of DNA was added to 100 µl of *E.Coli* competent cells in electroporation cuvette and incubated on ice for 20 minutes, followed by electroporation using AMAXA Nucleofector system. The cells were allowed to recover in 1 ml LB-Medium and then incubated for 1h at 37°C. 50 µl of bacterial culture were plated on LB-Agar plate containing ampicillin antibiotics (50 µg/ml) and incubated at 37°C overnight to select the transformants. *E. coli* cells containing the recombinant plasmids were inoculated into 10 ml of LB- Medium containing 50 µg/ml ampicillin at 37°C 8 h in a shaker. Then 0.5 ml of each cultures were transferred to 250 ml of fresh LB-Medium containing 50 µg/ml ampicillin and were grown at 37 ºC overnight in a shaker.

3.2.7 Isolation of plasmid DNA from *E. coli*

Large-scale plasmid DNA isolation was carried out using EndoFree Plasmid Maxi Kit (Qiagen) as per the manufacturer's protocol (Qiagen). Cells were harvested by centrifugation (5000*g* for 1 h at 4 ºC) and re-suspended in solution P1 (50 mM Tris-Cl, pH 8.0, 10 mM EDTA, 100 ug/mL RNase A) with gentle vortexing and then lysed with solution P2 (200 mM NaOH, 1% SDS), SDS breaks apart the lipid membranes and solubilizes cellular proteins, NaOH denatures DNA (both plasmid and genomic). After 5 min solution P3 (3.0 M potassium acetate, pH 4.8) was then added with strongly mix to neutralize the acidic pH. The supernatant containing plasmid DNA was filtered by QIAfilter Cartidge into a clean tube and incubated 30 min on ice with endotoxin removal (ER) buffer to prevent lipopolysacharide (LPS) molecules from binding to the resin in the QIAGEN-tips. For plasmid DNA binding the mixture was transferred into QIAGEN-tip and allowed it to enter the resin by gravity flow. Then all the contaminants in the plasmid preparations were removed by washing three times with buffer QC (1.0 M NaCl, 50 mM MOPS, pH 7.0, 15% isopropanol) by allowed the buffer to move through the QIAGEN-tip by gravity flow. For eluting DNA buffer QN (1.25M NaCl, 50mM Tris-Cl, pH 8.5, 15% isopropanol) was added to the column and allowed to drain by gravity flow in a endotoxin-free or pyrogen-free tube. Cold isopropanol was added to the eluting DNA then was centrifuged at 15000*g* for 30 min at 4 ºC. The supernatant was discarded and the pellet was rinsed with cold 70% ethanol and centrifuged at 15000*g* for 10 min. Then, the pellet was dried for 5-10 min and dissolved in a suitable volume of endotoxin-free Buffer TE (10 mM Tris-Cl, pH 8.0, 1 mM EDTA).

3.2.8 The shRNA mediated down regulation of p110α and NOX

In order to study the function of particular proteins stable small hairpin RNA (shRNA)-mediated down-regulation of gene expression has been proven to be a powerful tool. pLKO.1-puro (Sigma-Aldrich) derivative plasmids encoding shRNA sequence targeting murine PI3K p110α catalytic subunit, murine NOX1 and NOX2 or a non-targeting control shRNA were separately introduced into CGR8 ES cells by lentiviral particles, which showed advantage to infect the proliferating and quiescent cells compared to other delivery system (Manjila et al. 2013). Ecotropic lentiviral particles were generated using Human Embryonic Kidney (HEK293T) based packaging cells. In order to obtain high viral titers Phoenix packaging cell was cultured to

70% confluency at 37°C. 100% confluence should be prevented. For a 10 cm dish, lentiviral vector plasmid (10 µg) were cotransfected with plasmids encoding the HIV-Rev (5 µg), HIV-MDL (10 µg) and the ecotropic envelope (2 µg) in the presence of PEI (70 µg). Supernatants were harvested after 24 h and 48 h and filtrated through 0.25 µm filters (Schambach et al. 2006). The viral particles were stored at 4°C for several days and for long-term at -80°C. Lentiviral particles were added to CGR8 ES cells which were plated in a well of a 6-well plate with polybrene (8 µg/ml) to enhances efficiency of virus infection, centrifuged at 400 *g* in a cell culture centrifuge for 1 h and replaced with fresh medium on the following day. A total of three (24 + 36 + 48 hrs) infection rounds were carried out. On the following day the cells were selected with 2 µg/ml puromycin for 10-14 days. Down regulation of PI3K p110 catalytic subunit p110α, NOX1 and NOX2 was analysed by RT-PCR and western blot (Bartsch et al. 2011, Bekhite et al. 2011, Milosevic et al. 2010).

3.2.9 Magnetic cell separation (MACS) and flow cytometry (FCM) analysis

Embryoid bodies were generated and cultivated as described above. 4-day-old embryoid bodies were dissociated by incubation with collagenase type II (2 mg/ml) dissolved in cell dissociation buffer (IK-buffer) at 37°C for 5-10 minutes. For cell separation MACS separation columns were used. The separation procedure was carried out using a PE-conjugated rat anti-mouse Flk-1 antibody (dilution 1:10). For labelling anti-PE MicroBeads (Miltenyi Biotec) was used. Cells from the positive selected fraction were plated and incubated at 37°C and 5% CO_2 for starting the respective co-incubation experiments. Purity analysis was carried out using a FACSCalibur with a scanning wave length of 488 nm (PE-labelled cells) and a detection wave length of 575 nm.

3.2.10 Treatment with inhibitors

To investigate the role of the PI3K in vascular differentiation, embryoid bodies derived from ES cells were incubated in the presence or absence of VEGF-165 (500 pM) (Sigma-Aldrich) with pan PI3K inhibitor wortmannin (1 µM), or with the p110α inhibitor of catalytic subunit compound 15e (0.5 µM) (Bekhite et al. 2011, Hayakawa et al. 2006). We also used DPI (10 µM) or VAS2870 (50 µM) the pan inhibitors for NADPH, the novel NOX1 inhibitor 2-APT (0,5 µM), apocynin (100

μM), the respiratory chain complex I inhibitor rotenone (2.5 μM), Rac1 inhibitor (50 μM) and Akt inhibitor (50 μM) as shown in the results section.

3.2.11 Immunofluorescence staining and quantitative analysis

Blood vessels like structures in embryoid bodies were identified by immunolabeling platelet endothelial cell adhesion molecule (PECAM-1, CD31). Embryoid bodies were fixed in methanol-acetone (7:3) for 1 h at -20°C and were subsequently permeabilized for 10 min with phosphate-buffered saline (PBS) supplemented with 1% Triton X-100 (PBST). Fluorescence recordings were performed using a confocal laser scanning microscope (LSM 510) connected to an inverted microscope (Axiovert 135). Quantitative IF was analysed as previously described (Sauer et al. 2005) using an Axiovision software tool. Briefly, images (512 x 512 pixels) were acquired from PECAM-1-stained embryoid bodies corrected for background fluorescence using the extended depth of focus algorithm of the confocal setup. Generally 4 full frame images separated by a distance of 8 μm in the *z*-direction were recorded that included the information of the capillary area and spatial organization in a tissue slice 32 μm thick. From the acquired images an overlay image of the vascular structures in the scanned tissue slice was generated. By use of the image analysis facilities of the confocal setup the antigen-positive vascular areas within the three-dimensional projection of vascular structures were identified in the embryoid bodies.

To investigate the changes in actin structures during the migration process, we used cytoskeleton staining by phalloidin-Alexa Fluor® 488. Flk-1^+ cells were grown on cover glass in 24-wells up to semi confluence and stimulated with VEGF (500 pM) or media alone for 30 min. Then the cells were fixed with 4% paraformaldehyde for 1h on ice, and stained with phalloidin- Alexa Fluor 488 for 30 min at room temperature in dark and analyzed by LSM. Nuclei were stained with 4 ',6-diamidino-2-phenylindole (DAPI) before covering the slides. DAPI is binds selectively to DNA and thus colours the content of the nucleus of the cell. Results are bright blue fluorescence nuclei (excitation maximum at 340 nm, emission maximum at 488 nm), which is helpful for finding the best focus during microscope scanning.

3.2.12 Measurement of ROS

Intracellular ROS levels were measured using the fluorescent dye 2`,7`- dichlorodihydrofluorescein diacetate (H_2DCF-DA), which is a nonpolar compound that is con-

verted into a nonfluorescent polar derivative 2`,7`- dichlorodihydrofluorescein (H_2DCF) by intracellular esterase. H_2DCF is membrane impermeable and is rapidly oxidized to the highly fluorescent 2`,7`-dichlorofluorescein (DCF) in the presence of intracellular ROS. For the experiments, embryoid bodies were incubated in serum-free medium and 20 µM H_2DCF-DA was added. After 20 min, intracellular DCF fluorescence was evaluated by the LSM 510 (Milosevic et al. 2010).

3.2.13 Measurement of intracellular superoxide

Intracellular generation of superoxide (O_2^-) was estimated using the superoxide indicator dihydroethidium (DHE), which can be used specifically for measuring intracellular O_2^-. Cytosolic DHE exhibits blue fluorescence. However, once this probe is oxidized to ethidium it intercalates into chromosomal DNA, staining its nucleus with brightly red fluorescence. Washed ES cells were pre-incubated with 10 µM DHE for 20 min at 37°C in darkness and then rinsed with E1-buffer to remove excess dye. For fluorescence excitation, the 488-nm band of the argon ion laser of the LSM 510 (Zeiss) was used. Emission was recorded using a longpass LP515-nm filter set.

3.2.14 RNA isolation and reverse transcription-polymerase chain reaction (RT-PCR)

Total RNA isolation from ES cells was performed using the RNeasy Mini Kit (Qiagen) according to the manufacturer's recommended procedures followed by genomic DNA digestion using DNaseI (Invitrogen). cDNA was synthesized from 2 µg total RNA using a Superscript II reverse transcriptase (Invitrogen) according to manufacturer's instructions using random primer. The RT product was diluted 1:10 and PCR was performed using the primers (Sigma) indicated in material with 40 cycles performed at 58°C annealing temperature. Gel images and visualising bands were performed by GenSnap from SynGene (VWR) using a 1% agarose gel (SERVA).

3.2.15 Western blot assay

ES cells were washed in ice cold PBS and subsequently lysed in lysis buffer for 30 min on ice. Samples were centrifuged at 13.000 *g* for 10 min to pellet the debris. After determination of protein concentrations using the method of Bradford, 40 µg of protein per sample was heated to 95°C for 10 min with SDS-PAGE loading buffer and separated in SDS polyacrylamide gels and transferred to nitrocellulose mem-

branes in transfer buffer at 20 V over 10 h. Membranes were blocked with 10% (wt/volume) dry fat-free milk powder in Tris-buffered saline with 0.1% Tween (TBST) for 3 h at 4˚C. Incubation with primary antibodies was performed at 4 °C overnight. Subsequently, membranes were washed with 0.1% TBST. For secondary antibody reaction, membranes were incubated with the adequate horseradish peroxidase (HRP) conjugated secondary antibodies (Santa Cruz) for 60 min at room temperature. Corresponding bands were visualised using the ECL detection kit (Amersham). Chemiluminescence signals were quantified using a charge coupled device (CCD) camera-based chemiluminescence detection system (LAS 3000).

3.2.16 Angiogenesis assay

Matrigel (BD Biosciences) was added to 96-well plates on ice and allowed to polymerize for 1 h at 37°C. The isolated Flk-1^+ cells from 4-days-old embryoid bodies incubated in CGR8 medium for one day were harvested after trypsin-EDTA treatment, resuspended in CGR8 medium in the presence or absence of VEGF, plated onto the Matrigel at a density of 10000 cells/well. Matrigel cultures were incubated at 37°C and photographed after 16 hours.

3.2.17 Scratch migration assay

To assess whether p110α and NOX1 play a role in cell migration of Flk-1^+ cells, a scratch cell migration assay was performed in 12-well tissue culture plates coated with 0.1% gelatine for a minimum of 2 h at 37°C. Upon reaching 80-90 % confluence, the Flk-1^+ cells were scratched using a pipette tip and cell debris was removed. Cells were cultured for 6 h, to allow for cell migration in the presence or absence of VEGF. Each treatment was performed in triplicate wells, and the mean distance of migrating cells in each well was measured from five randomly chosen fields under light microscopy at 0 h and 6 h (Bhattacharya et al. 2009).

3.2.18 Long-term labelling of multicellular tumor spheroids

To discriminate tumor spheroids grown in confrontation culture from embryoid bodies, tumor spheroids were labeled with the long-term cell tracker dye 5-chloromethylfluorescein diacetate (CMFDA) (Invitrogen). In brief, tumor spheroids were incubated for 1 h in F10 cell culture medium that contained 10 µm CMFDA (stock solution 10 mm, dissolved in DMSO). Subsequently, spheroids were washed

and incubated for a further 24 hours in bacteriologic Petri dishes. Stable CMF fluorescence was observed for more than 5 days of tumor spheroid culture (Wartenberg et al. 2003). Fluorescence excitation was performed by the 488-nm line of an argon-ion laser of the confocal setup. Emission was recorded using a longpass LP515-nm filter set.

3.2.19 Generation of confrontation cultures

Confrontation cultures are tissues generated by culturing three-dimensional tumor spheroids and embryoid bodies in close contact. After few days the tumor spheroid is vascularised by the embryoid body through tumor-induced angiogenesis (Wartenberg et al. 2003). For the generation of confrontation cultures, multicellular tumor spheroids and embryoid bodies were removed from spinner flasks. To discriminate tumor spheroids grown in confrontation culture from embryoid bodies, tumor spheroids were labelled with CMFDA as described previously. One embryoid body (6-days-old) and one tumor spheroid (20-days-old) were inoculated in a 35 µl drop of mixed culture medium (50 % DU145 medium, 50 % CGR8 medium) placed onto the lid of a 10 cm Petri dish. The lid was turned around and placed on the Petri dish, which was filled with 15 ml of sterile PBS. Within 48 hours, embryoid bodies and tumor spheroids closely attached within the hanging drops and were subsequently transferred to 10-cm bacteriologic Petri dishes filled with 10 ml of CGR8 medium. PE-CAM-1 and CMFDA fluorescence recordings were performed by LSM 510 (Carl Zeiss, Germany).

3.2.20 Statistical analysis

Data were expressed as mean values ± SD with *n* denoting the number of 3 experiments unless otherwise indicated. In each experiment at least 15 embryoid bodies were analyzed. GraphPad InStat-3 software (GraphPad Software Inc., San Diego, USA) was applied for One-way ANOVA or *t-test* of unpaired data. Data are expressed as fold or percentage of expression relative to control values. Differences were considered statistically significant at a p value of <0.05. The graphical representation of a p value<0.05 is indicated by an asterisk (*).

4. RESULTS

4.1 Class IA PI3Ks catalytic subunit p110α, Flk-1 and PECAM-1 production during ES cell differentiation

To investigate the differentiation dependent appearance of the class IA PI3K p110α catalytic subunit in embryoid bodies during vascular differentiation, the protein level of p110α, Flk-1and PECAM-1 was examined using western blot analysis. This analysis was performed from day 2 to day 10 of embryoid body culture (Fig. 4.1A). Interestingly, we found that embryoid bodies significantly produce p110α and Flk-1 before day 4 of culture. Moreover, the highest increase of p110α occurs at day 4 of ES cell differentiation in parallel to Flk-1, which is a marker of cardiovascular progenitor cells (Choi et al. 1998), the production level of Flk-1 declined during subsequent days, while p110α remained constant till day 7 (Fig. 4.1A). Furthermore, a significant increase of PECAM-1 production was observed in a time frame between day 6 and day 10 of culture (Fig. 4.1A). Moreover, the level of endogenous ROS was up-regulated from day 4 of culture and remained elevated till day 6 (Fig. 4.1B). Therefore it can be concluded that a significant synchronicity of endothelial cell commitment with the appearance of class IA PI3K catalytic subunit p110α and ROS occurred during ES cell differentiation. Thus it is reasonable to assume that p110α and ROS play a role during the vascular differentiation of ES cells.

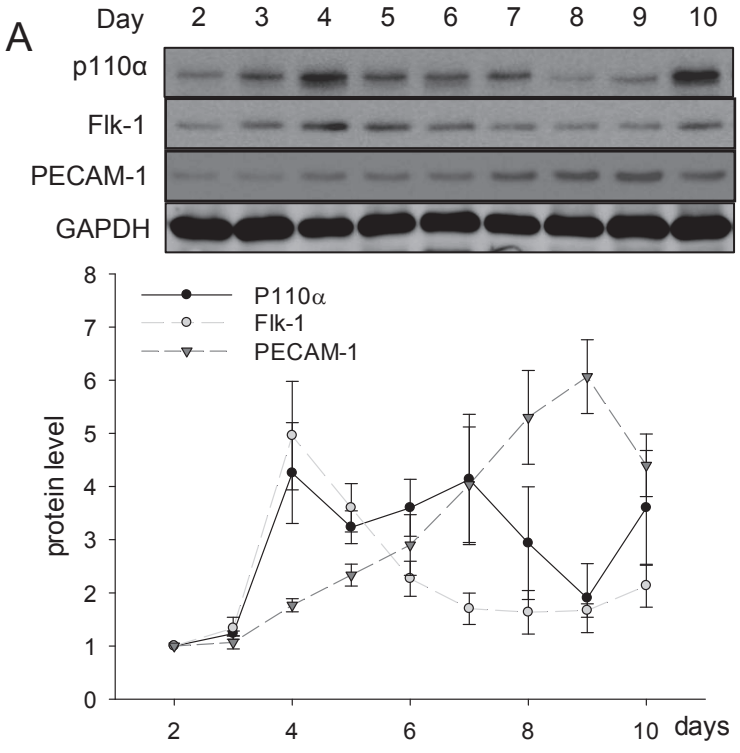

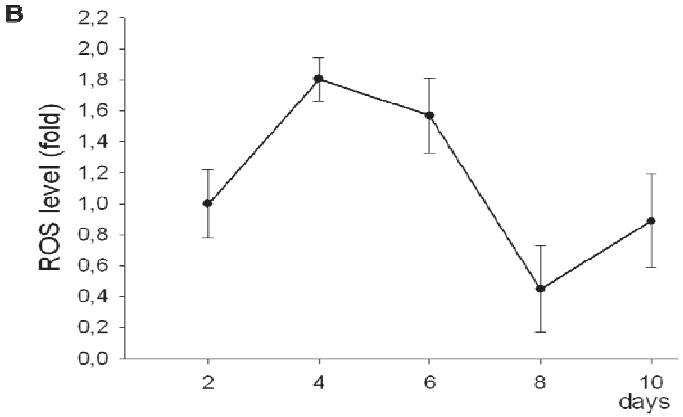

Figure 4.1: Production of class IA PI3K catalytic subunit p110α and ROS during vascular differentiation. (A), western blot analysis of catalytic subunit p110α, Flk-1 and PECAM-1. Whole cell lysates were blotted at indicated time points. GAPDH was used as an internal standard. The blots shown are representative for at least 3 experiments with consistent results. Graphs under the blots shows mean values (+/- standard deviation). (B), endogenous ROS generation during ES cell differentiation. ROS production was analysed using image analysis facilities of the LSM 510. Results are based on three independent experiments.

4.2 Silencing of PI3Ks class IA p110 catalytic subunits and NOX using shRNA technology

To obtain stable down regulation or inhibition of p110α, NOX1 and NOX2 we used stable short hairpin RNA (shRNA) targeting PI3K catalytic subunit p110α, NOX1 and NOX2. For these experiments undifferentiated CGR8 cells were transduced with the respective shRNA which was introduced in the pLKO.1 vector. The level of inhibition of p110α subunit (Fig. 4.2A), NOX1 (Fig. 4.2B) and NOX2 (Fig. 4.2C) were analysed by western blot in 5-day-old embryoid bodies (Fig. 4.2A-C). The shRNA cells significantly reduced p110α, NOX1 and NOX2 protein production compared to shRNA control (pLKO.1) cells (Fig. 4.2A-C). Interestingly, no interfere was showed with other non interesting target (Fig. 4.2A-C).

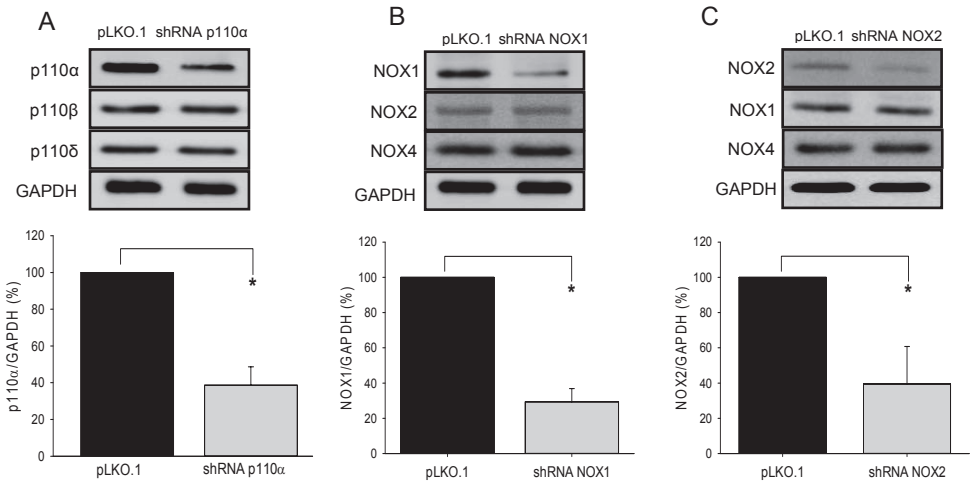

Figure 4.2: Analysis of proteins production for gene-inactivated embryoid bodies. The blots shown are representative for at least 3 experiments with consistent results. Graphs under the blots shows mean values (+/- standard deviation) of 3 independent experiments. GAPDH was used as an internal standard. (A), embryoid bodies showed specific and significant inhibition of the phosphoinositide 3-kinase (PI3K) catalytic subunit p110α using short hairpin RNA (shRNA) without interfering the production of p110β and p110δ. (B), embryoid bodies showed specific and significant inhibition of the NOX1 using shRNA without interfering the production of NOX2 and NOX4. (C), embryoid bodies showed specific and significant inhibition of the NOX2 using shRNA without interfering the production of NOX1 and NOX4. $*P < 0.05$, statistically significant as indicated, n. s. not significant.

4.3 Flk-1$^+$ cells derived from differentiated ES cells produce NOX isoforms and PI3Ks class IA p110 catalytic subunits

To examine whether members of the NADPH oxidase family are produced in vascular progenitor cells, Flk-1$^+$ cells were isolated from 4-day-old embryoid bodies by magnetic cell sorting (MACS). Flow cytometry (FCM) analysis for Flk-1$^+$ cell after sorting resulted in a purity of approximately 95.7% Flk-1$^+$ cells (Fig. 4.3A). Moreover, the relative mRNA and protein production level of NOX isoforms was examined using RT-PCR and western blot analysis (Fig. 4.3D-F). Results from mRNA (Fig. 4.3B,C) and western blot (Fig. 4.3D,F) analysis showed that Flk-1$^+$ cells mainly produced NOX1 and NOX4 (Fig. 4.3B-F), whereas NOX2 was scarcely produced in Flk-1$^+$ cells (Fig. 4.3B,E). In contrast, NOX3 was not produced in Flk-1$^+$ cells isolated from 4-day-old embryoid bodies (Fig. 4.3C). Furthermore, the production of PI3K class IA p110 catalytic subunits in the Flk-1$^+$ cells was analysed. The results showed that PI3K class IA p110 catalytic subunits (p110α, β and δ) were significantly produced in Flk-1$^+$ cells (Fig. 4.3G). These findings indicate that the catalytic subunits are produced in parallel to the first steps of vascular differentiation in ES cells.

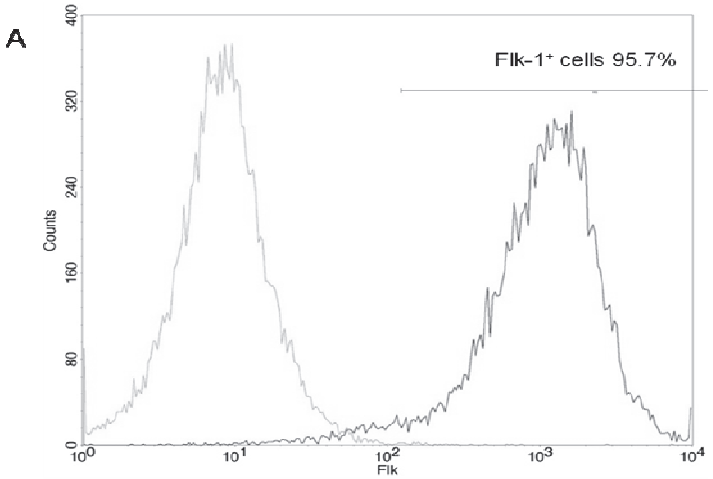

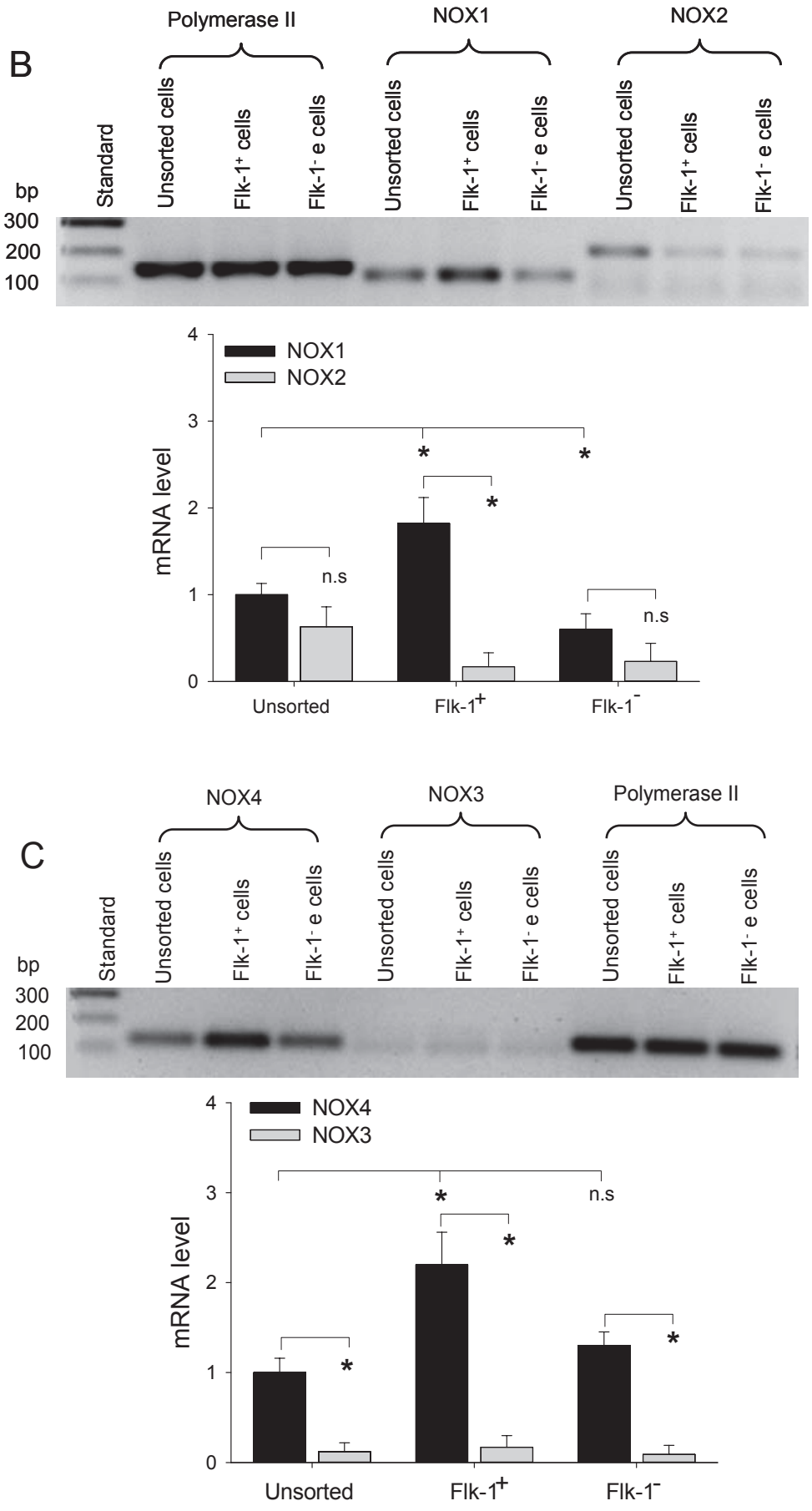
B
Polymerase II
NOX1
NOX2
Standard
Unsorted cells
Flk-1+ cells
Flk-1- e cells
bp
300
200
100
NOX1
NOX2
mRNA level
n.s
Unsorted
Flk-1+
Flk-1-
C
NOX4
NOX3
Polymerase II
NOX4
NOX3
n.s

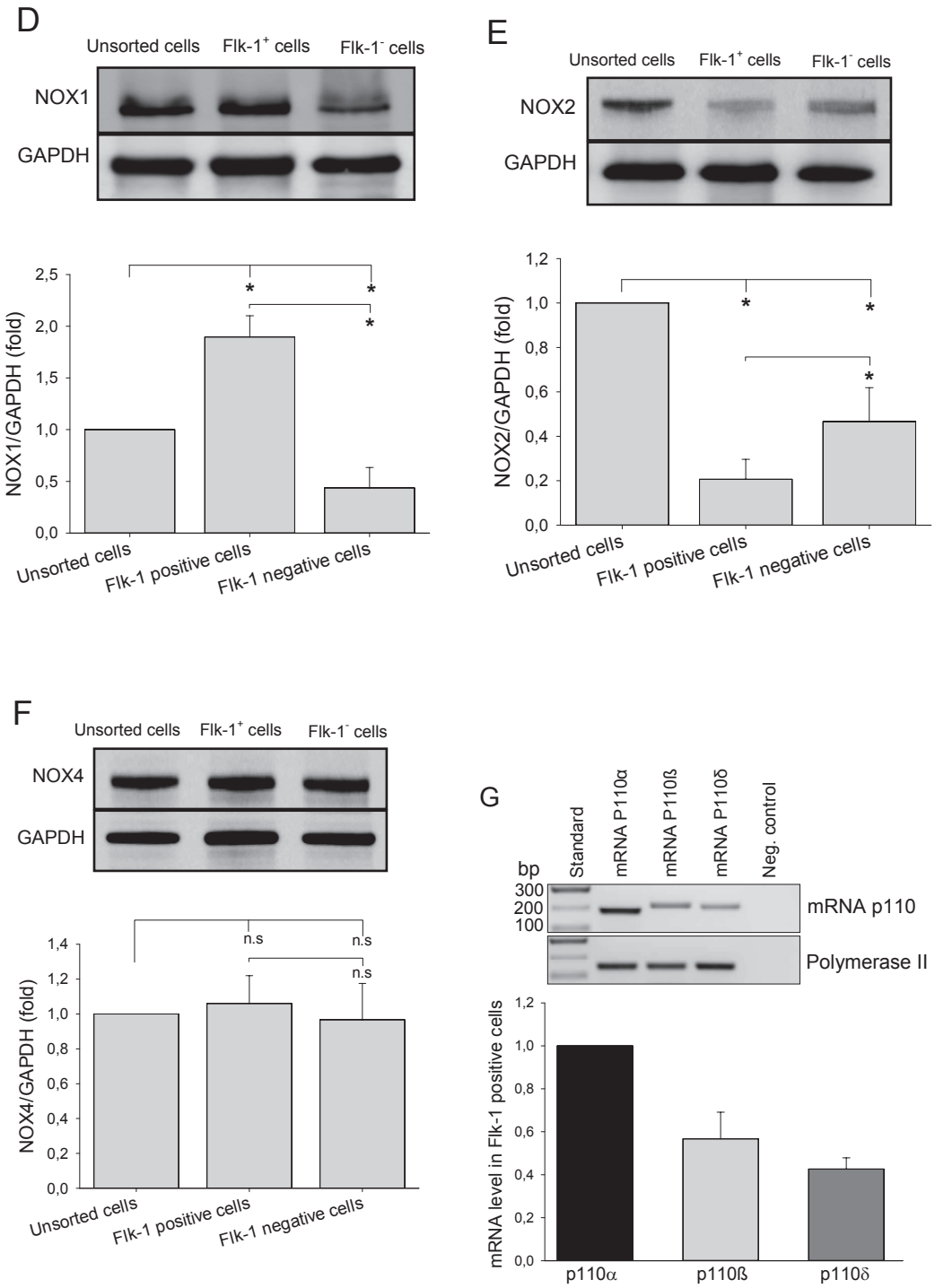

Figure 4.3: Purity of vascular progenitor cells isolated from embryoid bodies and expression of NOX and p110 in ES cells. Flk-1 positive cells were MACS sorted from 4-day-old embryoid bodies. (A), Flk1 cells were labelled using PE-conjugated rat anti-mouse Flk-1 antibody and processed by FCM. Cells of 4-day-old embryoid bodies were MACS sorted and analysed for mRNA levels using RT-PCR. mRNA of NOX1 and NOX2 (B), NOX3 and NOX4 (C) of 4-day-old sorted Flk1 positive, negative and unsorted cells was amplified using RT-PCR and processed by DNA agarose gel electrophoresis. Polymerase II was used as internal standard. Representative gels for at least 3 repeated experiments are demonstrated. Graphs under the blot show mean values (+/- standard deviation) of 3 independent experiments. Specific mRNA level was calculated in relation to Polymerase II. GAPDH was used as an internal standard for western blot analysis of NOX1 (D), NOX2 (E) and NOX4 (F). The blots shown are representative for at least 3 experiments with consistent results. Graphs

under the blots shows mean values (+/- standard deviation). (G), mRNA of the class IA PI3K catalytic subunit (p110α, β, δ). *P < 0.05, statistically significant as indicated, n. s. not significant.

4.4 VEGF induces ROS production mediated by NADPH oxidases

It has been shown that ROS such as hydrogen peroxide (H_2O_2) and superoxide (O_2^-) are created as a result of normal cellular signaling and metabolism (Becker 2004). Interestingly, our previous report demonstrated a link between ROS and vascular differentiation (Bekhite et al. 2010). According to the working hypothesis of the present study VEGF may stimulate vasculogenesis/angiogenesis in the ES cell derived embryoid bodies by stimulating ROS production through PI3K. Using H_2DCF as a fluorescent ROS indicator it was demonstrated that VEGF (500 pM) significantly increased ROS generation in 4-day-old embryoid bodies (Fig. 4.4A,B). However, no increase in ROS was observed when embryoid bodies were incubated with NADPH oxidase inhibitors DPI (10 μM) or VAS2870 (50 μM) as well as with apocynin (100 μM) (Fig. 4.4A,B). In contrast, co-incubation the embryoid bodies with rotenone (10 μM), a mitochondrial inhibitor, could not abolish the effect of VEGF on ROS generation, thus suggesting a distinct source of ROS from NADPH oxidase (see Fig. 4.4A,B). Furthermore, inhibition the ROS generation by apocynin suggests an impact of the NOX1 and NOX2 in the ROS production in the ES cells (Fig. 4.4A,B).

To investigate the involvement of class IA PI3Kα, NOX1 and NOX2 in VEGF stimulated ROS generation in ES cells, we treated 5-day-old shRNA p110α, shRNA NOX1 and shRNA NOX2 embryoid bodies with VEGF. In shRNA p110α and shRNA NOX1 embryoid bodies VEGF treatment failed to increase ROS whereas ROS generation was not affected in shRNA NOX2 embryoid bodies (Fig. 4.4C,D). Thus our data indicate that p110α and NOX1 but not NOX2 are involved in ROS production in ES cell derived embryoid bodies during VEGF treatment (Fig. 4.4C,D).

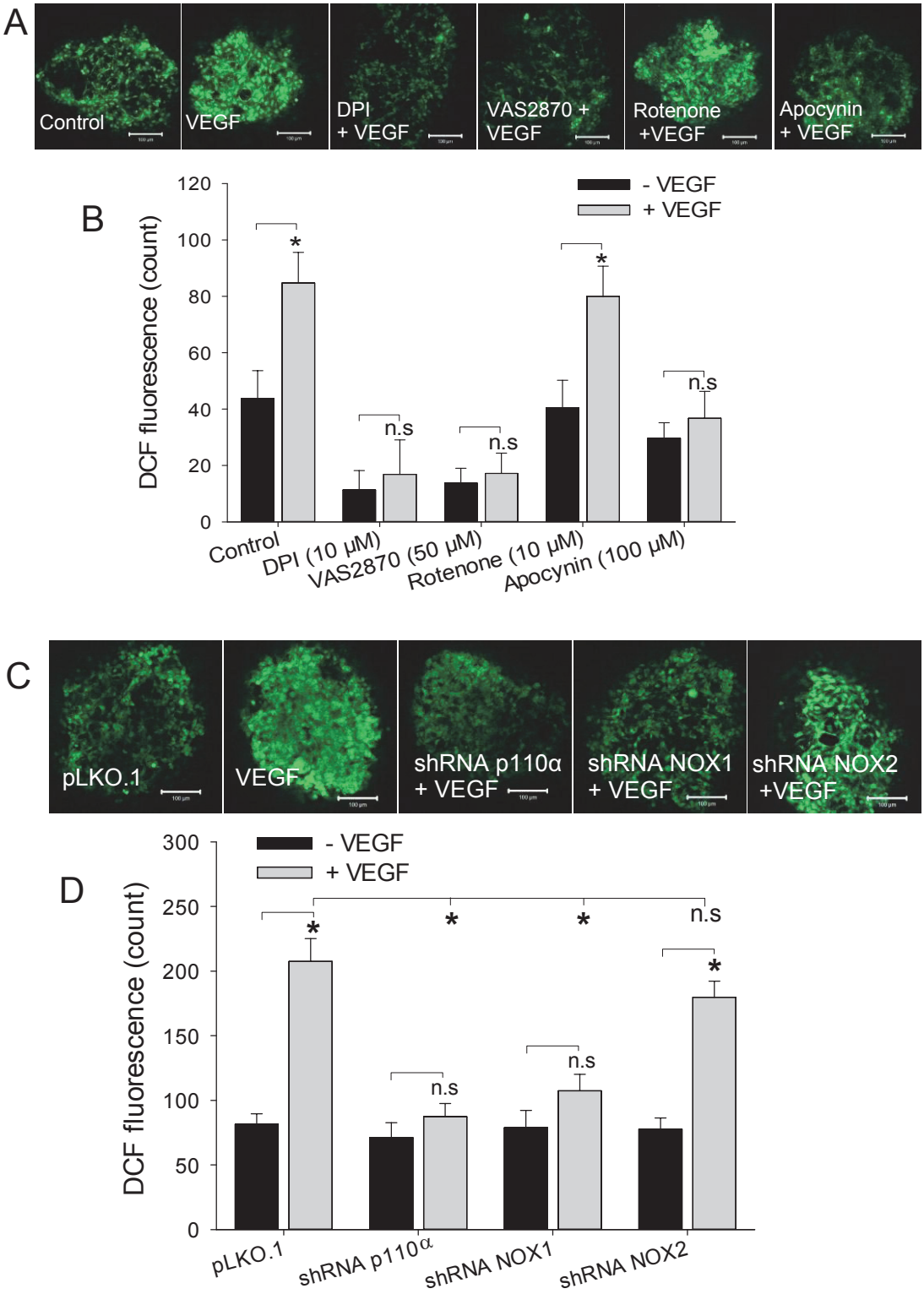

Figure 4.4: VEGF induced ROS production in embryoid bodies. 5-day-old embryoid bodies were stimulated by VEGF (500 pM) for 30 min. ROS production of cells was measured using the fluorescent dye 2`,7`- dichlorodihydrofluorescein diacetate (H_2DCF-DA). (A), images show DCF fluorescence of embryoid bodies treated with NADPH oxidase inhibitors DPI (10 µM), VAS2780 (50 µM) or apocynin (100 µM) or respiratory chain complex I inhibitor rotenone on VEGF-induced ROS generation as indicated. Bars represent 100 µm. (B), graph under the image shows mean values (+/- standard deviation) of ROS generation evaluated by determination of DCF fluorescence. NADPH oxidase inhibitors DPI, VAS2780

and apocynin completely inhibited ROS generation in embryoid bodies upon VEGF treatment, whereas rotenone did not affect the ROS generation. (C), images show DCF fluorescence of embryoid bodies depleted for p110α, NOX1, NOX2 or wild type (pLKO.1) treated with VEGF. Bars represent 100 μm. (D), VEGF failed to increase the ROS generation in p110α and NOX1 shRNA gene-inactivated embryoid bodies in comparison to pLKO.1 embryoid bodies. **P* < 0.05, statistically significant as indicated, n. s. not significant.

4.5 VEGF induced O_2^- production is dependent on PI3K-Rac1 activation in Flk-1$^+$ cells

To confirm experiments with the non-specific ROS indicator H_2DCF additional experiments were performed for measuring intracellular O_2^- (Carter et al. 1994). VEGF (500 pM) and DHE (10 μM) were added and 20 min after stimulation incubation at 37ºC, the cells were examined microscopically. As shown in Figure 4.5, VEGF treatment strongly elevated O_2^- generation in plated Flk-1$^+$ cells isolated from 4-day-old embryoid bodies whereas O_2^- remained at the control level when the Flk-1$^+$ cells were isolated from shRNA p110α or shRNA NOX1 embryoid bodies (Fig. 4.5A). Moreover, to determine whether the ROS production is dependent on Rac1, Rac1 inhibitor (50 μM) was used. The results shown in Figure 4.5A demonstrate that VEGF did not increase O_2^- production upon pharmacological inhibition of Rac1. Furthermore, we investigated whether NOX2 deficiency in Flk-1$^+$ cells has an impact on O_2^- production upon VEGF treatment. For this purpose, we quantified the DHE fluorescence in both untreated and VEGF-treated Flk-1$^+$ cells (Fig. 4.5B). As shown in Figure 4.5B, knockdown of NOX1 in Flk-1$^+$ cells abolished the effects of VEGF on O_2^- production. In contrast, knockdown NOX2 in Flk-1$^+$ cells showed no significant effects on O_2^- production (Fig. 4.5B). These findings point to an involvement of class IA PI3Kα-Rac1 in O_2^- production through NOX1 upon VEGF treatment.

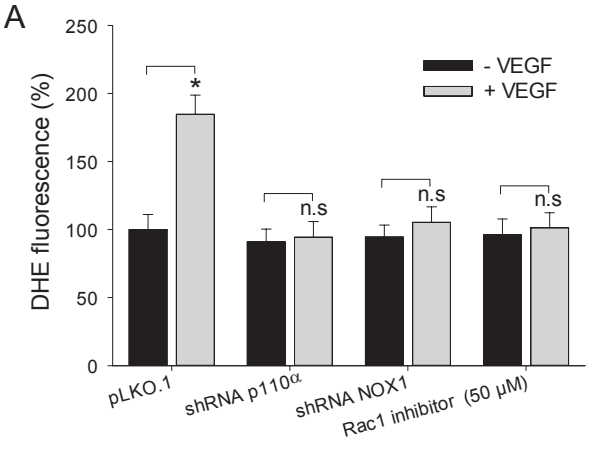

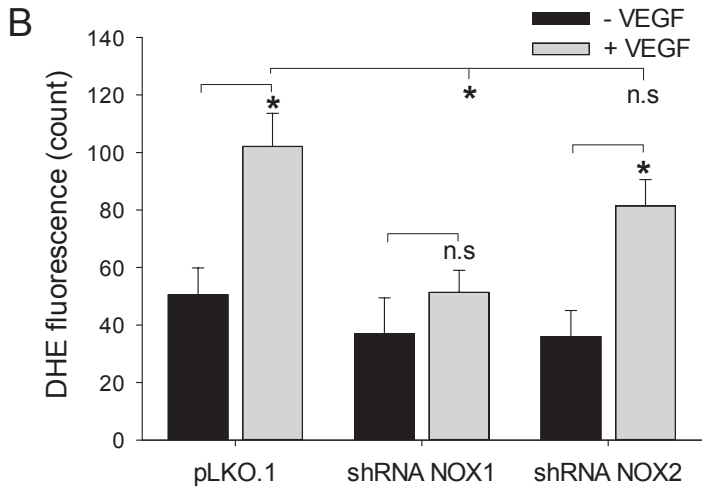

Figure 4.5: VEGF induced O_2^- production is dependent on PI3K-Rac1 activation in Flk-1$^+$ cells. (A), O_2^- generation of sorted Flk-1 positive cells isolated from 4-day-old embryoid bodies in response to VEGF stimulation was analysed by determination of DHE fluorescence. Cells depleted for p110α or NOX1 or wild type (pLKO.1) cells pre-treated for 30 min with Rac1 inhibitor (50 μM) were used. The graph shows percentage values (+/- standard deviation) *$P < 0.05$, statistically significant as indicated, n. s. not significant. Down regulation of NOX2 in Flk-1$^+$ cells inhibits O_2^- production upon VEGF treatment. (B), O_2^- generation of sorted Flk-1 positive cells depleted for NOX1 or NOX2 or wild type (pLKO.1) cells isolated from 4-day-old embryoid bodies in response to VEGF stimulation was analysed by determination of DHE fluorescence. The graph shows percentage values in relation to VEGF treated cells (+/- standard deviation) *$P < 0.05$, statistically significant as indicated, n. s. not significant.

4.6 PI3K catalytic subunit p110α is essential for vasculogenesis/angiogenesis

It is known that VEGF, and more precisely VEGF A, is a central regulator of blood vessel formation (Neufeld et al. 1999). Moreover, we previously showed that vascular differentiation starts at day 4 of embryoid bodies culture (Bartsch et al. 2011). To investigate whether class IA PI3Kα, NOX1 and Rac1 are essential for VEGF signaling pathways leading to vascular differentiation of the ES cells, p110α and NOX1 shRNA embryoid bodies were treated from day 4 to day 10 of cell culture with VEGF (500 pM). This treatment resulted in a significant increase in vascular differentiation in a non-targeting shRNA control (pLKO.1) as evaluated by quantification of endothelial marker PECAM-1 positive areas and branching points (Fig. 4.6A-C) as well as FCM (Fig. 4.6D,E) analysis for the percentage of Flk-1$^+$ cells in embryoid bodies. In contrast, stimulation of vascular differentiation upon treatment with VEGF was nearly absent in embryoid bodies co-incubated with the general PI3K inhibitor wortmannin (1μM) and embryoid bodies lacking p110α catalytic subunits (see Fig. 4.6A-C). Moreover, incubation the embryoid bodies with Rac1 inhibitor significantly

reduced the size of PECAM-1 positive vascular areas and nearly abolished the branching points (Fig. 4.6A-C) as well as the number of Flk-1^{+} cells (Fig. 4.6D,E). It was apparent that silencing the p110α catalytic subunit of PI3K resulted in significant inhibition of the PECAM-1 positive vascular area and branching points (Fig. 4.6A-C). In the absence of NOX1 or pharmacological inhibition of Rac1 a significant reduction of the VEGF-induced PECAM-1 positive vascular area and branching points in the embryoid bodies compared to untreated controls was observed, although still a significant enhancement of vascular differentiation occurred upon VEGF treatment (Fig. 4.6A-C). Taken together these experiments demonstrate that the PI3K catalytic subunit p110α as well as Rac1 and NOX1 regulate vascular differentiation of embryoid bodies.

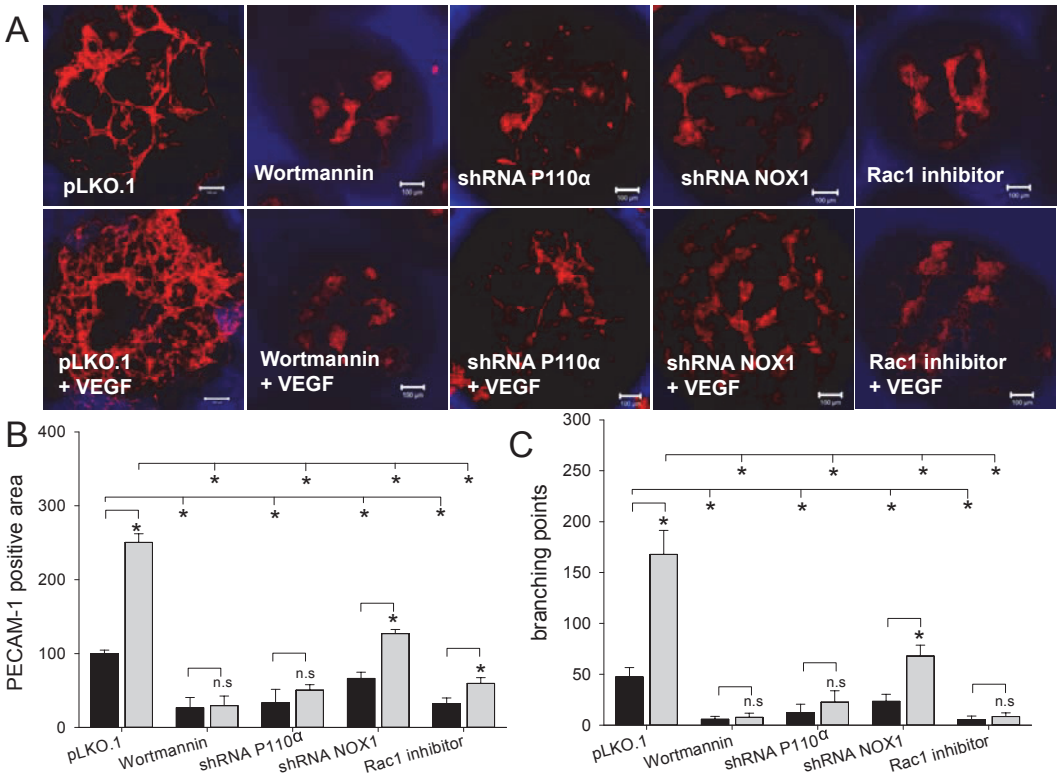

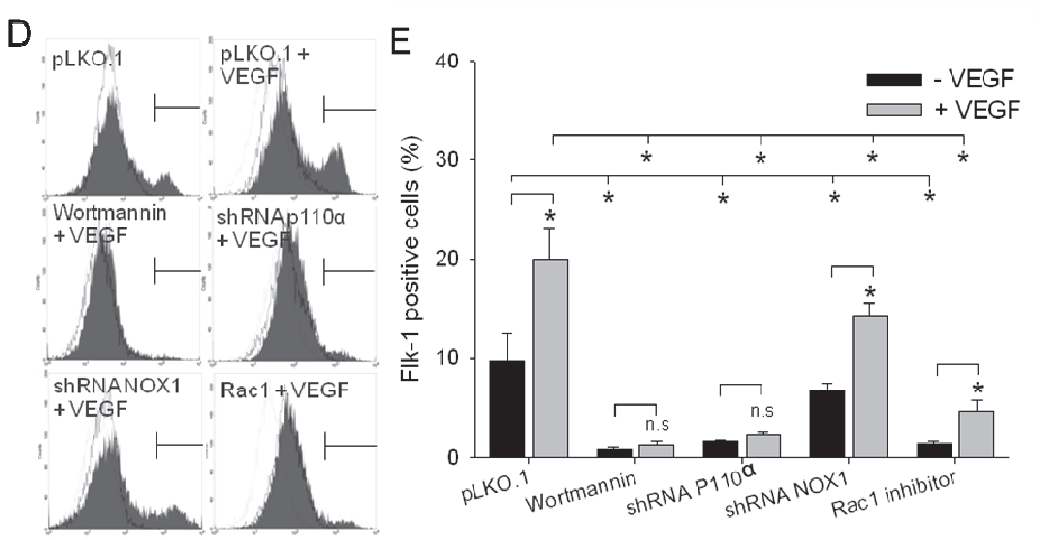

Figure 4.6: Class IA PI3Kα and Rac1 are essential for VEGF-induced vascular differentiation of ES cells. p110α or NOX1 knockdown and wild type (pLKO.1)ES cells were differentiated for 10 days. Inhibitors were applied from day 4 to day 10 of cell culture were stimulated with VEGF (500 pM) or left unstimulated. Cells were treated with wortmannin (1 μM) or Rac1 inhibitor (50 μM) as indicated. (A), representative immunefluorescence (IF) images showing the on vascular differentiation in embryoid bodies. The bars represent 100 μm. (B,C), vascular differentiation as indicated by PECAM-1 positive areas (B) and branching points (C). (D,E), FCM analysis of Flk-1 expression in cells of embryoid bodies as well as after application of inhibitors from day 4 to day 10 of cell culture either in the absence or presence of VEGF (500 pM). **P* < 0.05, statistically significant as indicated, n. s. not significant.

4.7 The catalytic subunit p110α is essential for angiogenesis

Based on our previous studies, we believe that vasculogenesis starts around day 4 and angiogenesis around day 6 during the differentiation of ES cells (Bartsch et al. 2011). To examine the effect of pan-PI3K inhibition and specific PI3K subunit inhibition targeting class 1A p110α catalytic subunits on angiogenesis, 6-day-old embryoid bodies were incubated with the inhibitors from day 6 to day 10 of cell culture. IF staining showed that incubation of embryoid bodies during the second phase of vascular development with either wortmannin (1μM), a pan-inhibitor of PI3K members, or compound 15e (0.5 μM), a specific p110α inhibitor, significantly reduced the PECAM-1positive vascular area and branching points (see Fig. 4.7A-C). Furthermore, 2-APT (0.5 μM) an inhibitor of NOX1, significantly decreased the vascular area and branching points of PECAM-1 positive cells compared to the VEGF treated control, although VEGF still significantly increased the vascular area and branching points under these experimental conditions (Fig. 4.7A-C). Since Rac1 is required for NOX activation additional experiments were performed by blocking Rac1 activity using Rac1 inhibitor (1 μM). It was apparent that Rac1 inhibitor completely abolished the

branching of endothelial cells and reduced the PECAM-1positive area compared to their respective control (Fig. 4.7A-C). However, VEGF treatment still significantly increased the CD31 positive area in the embryoid bodies co-incubated with Rac1 inhibitor compared to untreated embryoid bodies, although to a lesser extent as compared to the untreated control (Fig. 4.7A-C).

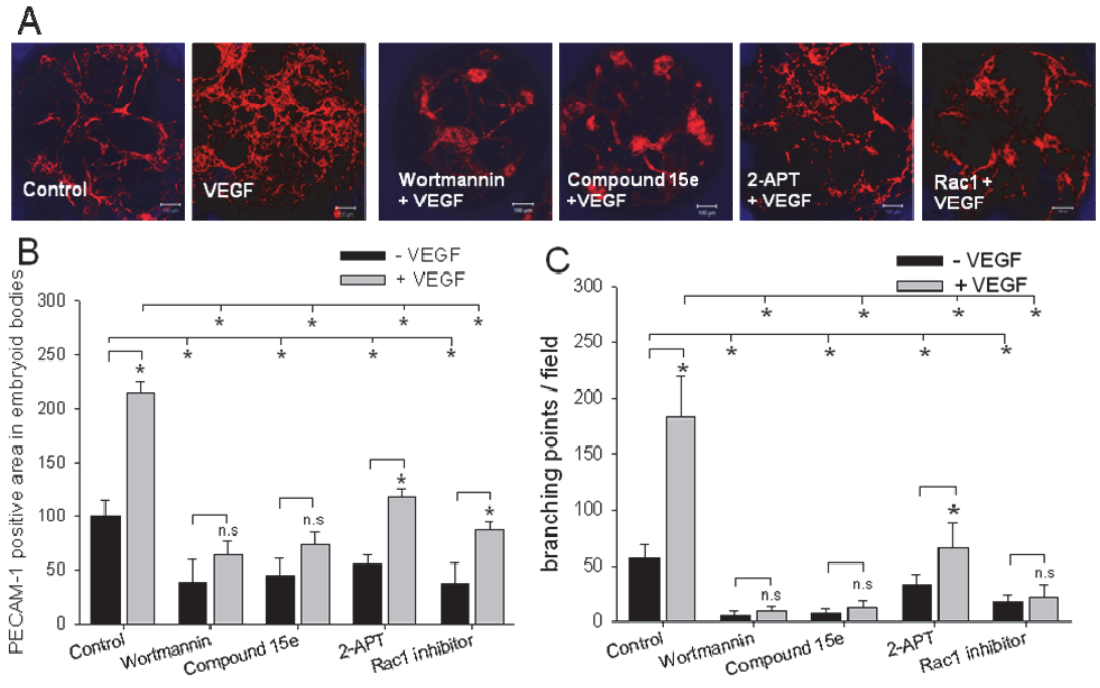

Figure 4.7: Effects of pan-PI3K inhibitor and specific inhibitor of p110α, NOX1 and Rac1 on angiogenesis. ES cells were differentiated for 10 days. Inhibitors were applied from day 6 to day 10 of cell culture were stimulated with VEGF (500 pM) as indicated. Compound 15e (0.5 µM) as well as the NOX1 inhibitor 2-acetylphenothiazine (2-APT, 0,5 µM), Rac1 inhibitor or left unstimulated. (A), representative IF images regarding vascular differentiation of embryoid bodies. The bars represent 100 µm. PECAM-1 positive areas (B) and branching points (C) $*P < 0.05$, statistically significant as indicated, n. s. not significant.

4.8 Vascular progenitor cells isolated from shRNA p110α and shRNA NOX1 embryoid bodies

As previously described VEGF acts mainly on Flk-1, which serves as an early vascular marker (Choi et al. 1998, Kabrun et al. 1997). To guarantee a specific and significant inhibition of the NOX1 isoform and the class IA PI3K catalytic subunit p110α, we screened the presence of mRNA and protein of NOX1 and p110α by RT-PCR and western blot in Flk-1^+ cells isolated from knockdown embryoid bodies. As shown in Figure 4.8, PI3K catalytic subunit p110α was decreased in Flk-1^+ isolated from shRNA p110α embryoid bodies within the time window of vascular differentiation at day 4, whereas no change in level of NOX1 production was noticed (Fig.

4.8A,B). Vice versa NOX1 mRNA production in Flk-1$^+$ cells isolated from 4-day-old shRNA NOX1 embryoid bodies was significantly decreased than compared pLKO.1 cells, whereas no change was noticed in level of p110α cells (Fig. 4.8A,B). These data indicate that NOX1 production is not affected by down regulation of p110α and p110α not by down regulation of NOX1 (Fig. 4.8A,B).

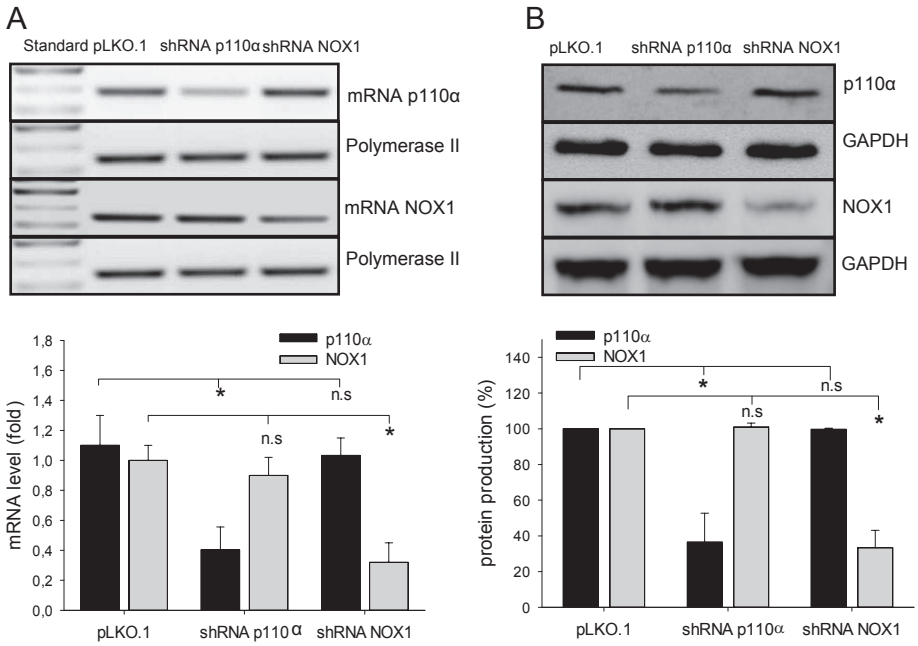

Figure 4.8: Level of p110α and NOX1 in Flk-1$^+$ cells isolated from knockdown embryoid bodies. Flk-1 positive cells were MACS sorted from 4-day-old wild type (pLKO.1), shRNA p110α or shRNA NOX1 embryoid bodies. (A), mRNA from Flk-1 positive cells was prepared and expression level of p110α, NOX1 or Polymerase II was detected using RT-PCR. Amplification was processed by DNA agarose gel electrophoresis. Representative gels for at least 3 repeated experiments are demonstrated. Graph beside the blot shows expression of p110α in relation to Polymerase II. (B), western blot analysis of p110α and NOX1. GAPDH was used as an internal standard. The blots shown are representative for at least 3 experiments with consistent results. Graphs under the blots shows mean values (+/- standard deviation). *$P < 0.05$, statistically significant as indicated, n. s. not significant.

4.9 p110α is essential for the formation of tube structures

To further examine key factors regulating the sprouting of vascular structures, we investigated tube-like structure formation of Flk-1$^+$ cells on matrigel, which recapitulates the process of sprouting and tube formation that occurs during angiogenesis. Flk-1$^+$ cells were plated on matrigel coated 96 multiwell plates. Images were taken after 16 h. The results showed that VEGF treatment significantly increased organization of Flk-1$^+$ cells into interconnected tubes and enhanced the formation of tube-like structures on matrigel (Fig. 4.9A). In contrast, pharmacologic inhibition of PI3K by

wortmannin completely inhibited VEGF-induced tube formation on matrigel. Quantitative analysis showed that both the total length of tubes and number of branching points were clearly decreased after knockdown of p110α and NOX1 (Fig. 4.9B,C). Furthermore, shRNA p110α cells failed to form interconnected tubes even when stimulated with VEGF (Fig. 4.9A-C). Moreover, VEGF loses the ability to increase tube length and branching points in shRNA NOX1 Flk-1^+ cells cultured on matrigel (Fig. 4.9A-C). Hence, our findings suggest that p110α as well as NOX1 are directly linked to VEGF-induced tube formation involved in the angiogenesis process.

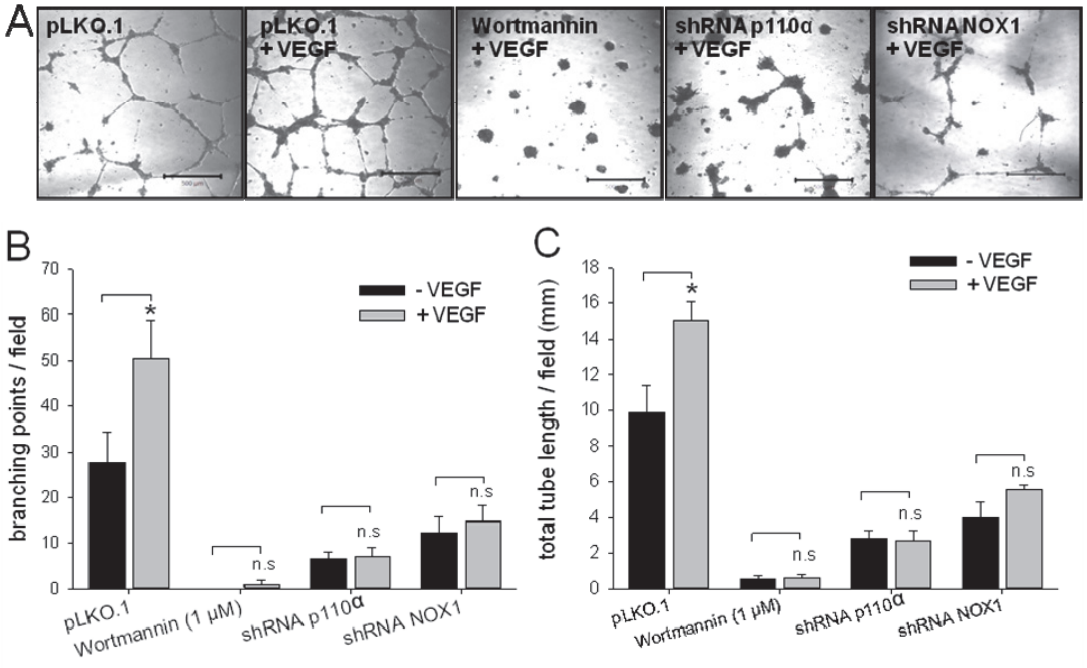

Figure 4.9: Angiogenesis assay for Flk-1^+ cells after depleted p110α or NOX1. Flk-1^+ cells were seeded on matrigel in 96-well plates. Tube structure was analyzed either in the presence or absence of VEGF (500 pM) after 16 h of cultivation. The ability to form tubes was expressed as total length of tubes and branching points per field. The bars represent 500 µm. (A), representative transmission images of tube formation of Flk-1^+ cells on matrigel upon treatment with wortmannin (1 µM) or knock down of p110α or NOX1 in the presence or absence of VEGF (500 pM). (B,C), VEGF-induced capillary-like tube formation and branching points are significant inhibited in the presence of the nonspecific PI3K inhibitor wortmannin or silencing p110α and NOX1 in Flk-1^+ cells. *$P < 0.05$, statistically significant as indicated, n. s. not significant.

4.10 p110α and Rac1 are essential for Flk-1^+ cell migration stimulated by VEGF

To address the effect of VEGF on cell migration which is an essential step for the angiogenesis process a scratch migration assay was performed. In this experiment cell migration into the scratch area was assessed, 6 h after stimulation of plated Flk-1^+ cells with VEGF (500 pM). Analysis results showed that VEGF treatment significantly increased cell migration (Fig. 4.10A,B). To examine whether PI3K is involved

in VEGF-induced migration, we treated the Flk-1$^+$ cells with wortmannin which totally inhibited the migration of Flk-1$^+$ cells (Fig. 4.10A,B). To determine whether silencing p110α or NOX1 could affect cell migration and hence the ability of the cell to form interconnected network structures, cells depleted for p110α or NOX1 were used in a scratch assay. A complete inhibition in migration of the p110α deficient Flk-1$^+$ cells was observed (Fig. 4.10A,B). Furthermore, knocking down NOX1 in Flk-1$^+$ cells caused a significantly reduction in cell migration and decrease in scratch closure compared to the VEGF treated pLKO.1 control (Fig. 4.10A,B). These data demonstrate that p110α is responsible for triggering cell migration stimulated by VEGF and may involve ROS generation by NOX1.

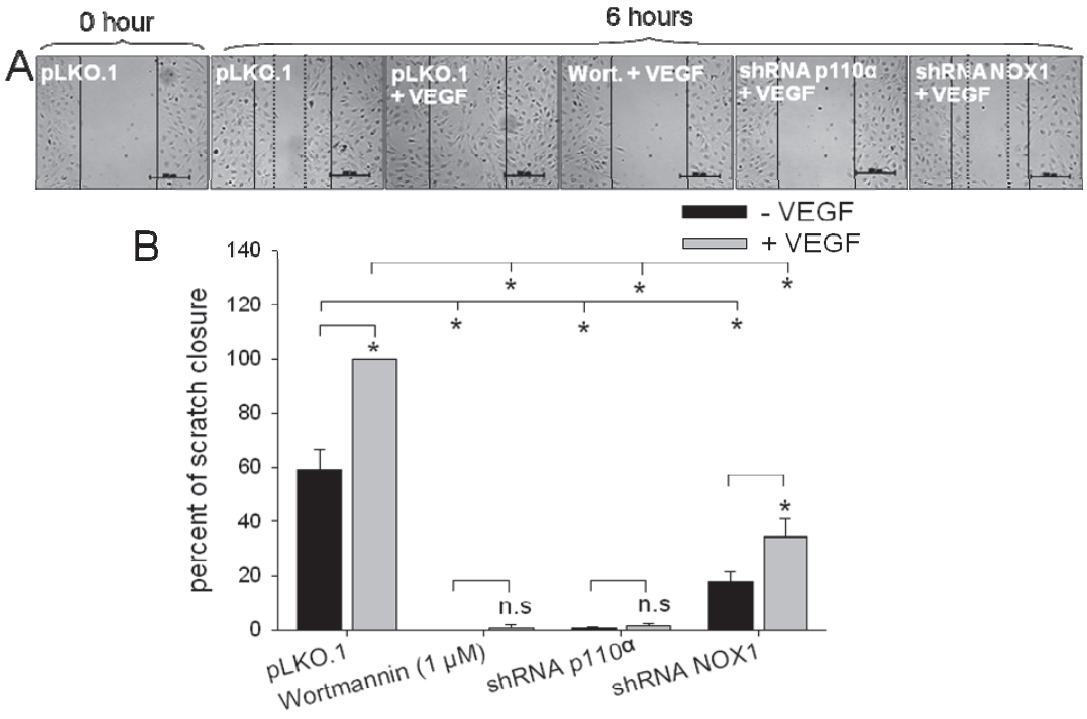

Figure 4.10: VEGF positively regulates cell migration via PI3K signaling *in vitro*. (A), representative images of Flk-1$^+$ cells isolated from 4-day-old embryoid bodies in the scratch assay for Flk-1$^+$ wild type (pLKO.1), p110α or NOX1 shRNA cells, either alone or in the presence of VEGF (500 pM). The bars represent 200 μm. (B), VEGF treated cells exhibited a highly induced migratory potential which was totally abolished by treatment of Flk-1$^+$ cells with wortmannin or knocking down the catalytic subunit p110α. *$P < 0.05$, statistically significant as indicated, n. s. not significant.

4.11 VEGF induces cytoskeletal changes via p110α to induce Flk-1$^+$ cell migration

Actin cytoskeleton reorganization is a fundamental process in the regulation of cell migration (Kaibuchi et al. 1999). To unravel the involvement of p110α and NOX1 in

this process we examined VEGF-induced actin cytoskeleton changes in Flk-1^+ cells. As shown in representative micrographs of phalloidin-stained Flk-1^+ cells, VEGF treated cells showed significant increase in lamellipodia structures and polarized cell shapes (Fig. 4.11A,B). Wortmannin treatment or knockdown p110α abrogated VEGF-induced lamellipodia structure and polarized shapes formation compared to the con trol group. In shRNA NOX1 cells still a significantly polarization after VEGF treatment compared with untreated cells was observed, although this effect was significantly less pronounced as compared to pLKO.1 cells (Fig. 4.11A,B).

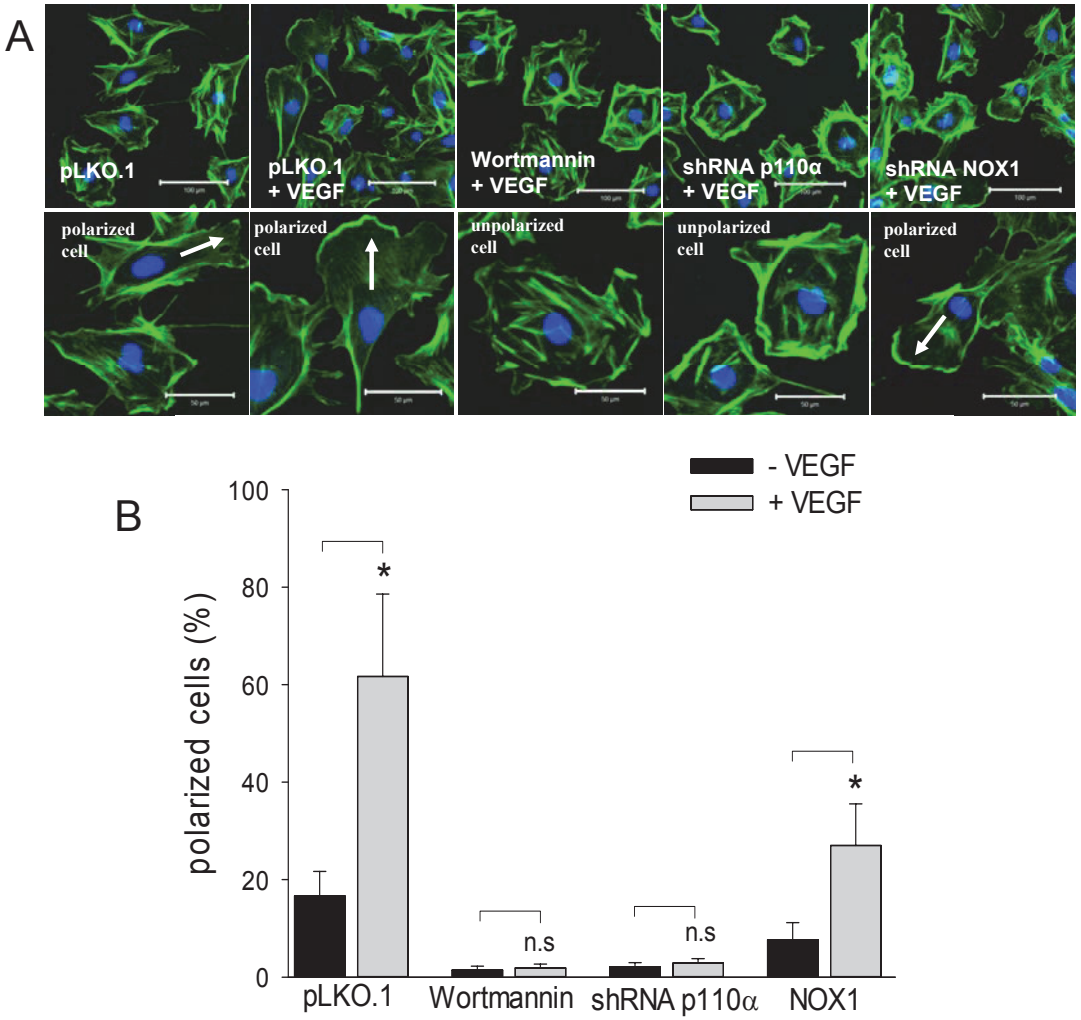

Figure 4.11: VEGF-induced changes in the Flk-1^+ cell cytoskeleton reorganization depending on PI3K. (A), representative images of Flk-1^+ cells stained with phalloidin (green) and DAPI (blue). The bar represents 100 µm (upper) and 50 µm (lower). Lamellipodia (indicated by arrow) were observed at the leading edge of VEGF-induced migrating cells. (B), VEGF induces actin cytoskeleton reorganization and showed significant increase in polarized shapes of VEGF-induced Flk-1^+ cells. Cell polarization was measured by formation the lamellipodium in the direction of migration. Wortmannin treatment and silencing p110α abrogated VEGF-induced lamellipodia formation and polarized shapes of Flk-1^+ cells. *P < 0.05, statistically significant as indicated, n. s. not significant.

4.12 VEGF induces Rac1 and RhoA activity in the ES cells

The primary requirement for lamellipodia formation is the activation Rac1 after extracellular stimuli (Disanza et al. 2005). In order to investigate the role of Rac1 in lamellipodia formation during cell migration, we performed western blot-based Rac1 phosphorylation assay from 5 day-old plated embryoid bodies stimulated with VEGF (500 pM). The results showed that the phosphorylation of Rac1 increased rapidly within 10 min after adding VEGF. Subsequently Rac1 activation decreased after 30 min but remained on a significantly elevated plateau as compared to 0 min (Fig. 4.12A). Moreover, there was significant change in RhoA activation from 30 min to 2 h after addition of VEGF (Fig. 4.12A). However, when the shRNA p110α embryoid bodies were stimulated with VEGF, Rac1 (Fig. 4.12B) and RhoA (Fig. 4.12C) activation was absent. In contrast, Rac1 (Fig. 4.12B) and RhoA (Fig. 4.12C) activation induced by VEGF was significantly increased in shRNA NOX1 embryoid bodies compared to the untreated control group. Pre-treatment of the shRNA NOX1 embryoid bodies with compound 15e (0.5 μM), completely inhibited the increase of Rac1 (Fig. 4.12D) and RhoA (Fig. 4.12E) activation induced by VEGF. Collectively, these results suggest that VEGF-induced activation of Rac1 and RhoA in the ES cells is mediated by class IA PI3Kα signalling but is not dependent on NOX1.

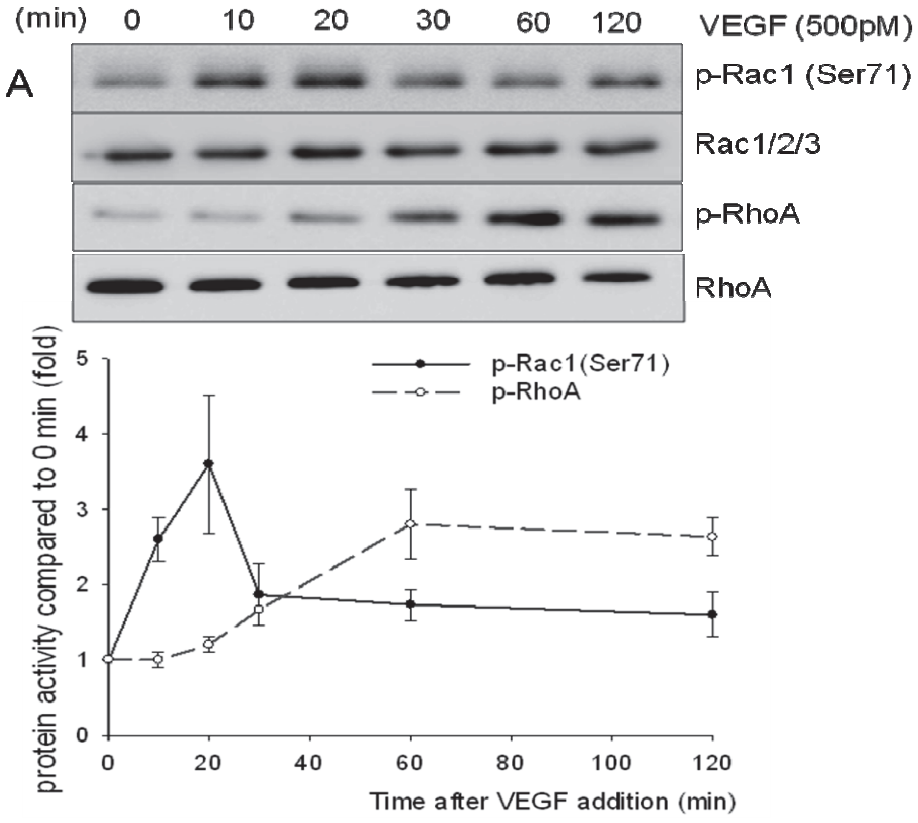

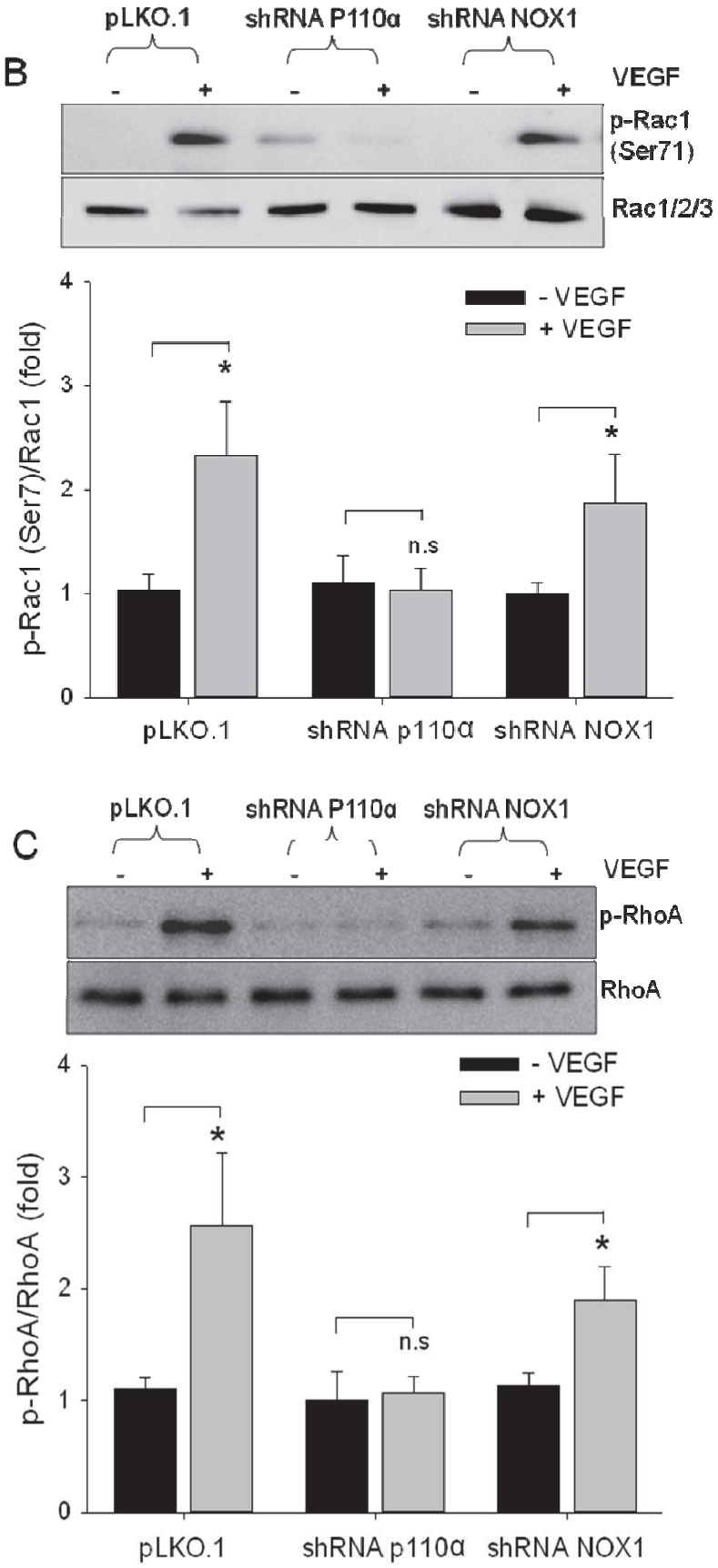
B
pLKO.1
shRNA P110α
shRNA NOX1
VEGF
- + - + - +
p-Rac1 (Ser71)
Rac1/2/3
- VEGF
+ VEGF
p-Rac1 (Ser7)/Rac1 (fold)
0
1
2
3
4
*
n.s
*
pLKO.1
shRNA p110α
shRNA NOX1
C
pLKO.1
shRNA P110α
shRNA NOX1
VEGF
- + - + - +
p-RhoA
RhoA
- VEGF
+ VEGF
p-RhoA/RhoA (fold)
0
1
2
3
4
*
n.s
*
pLKO.1
shRNA p110α
shRNA NOX1

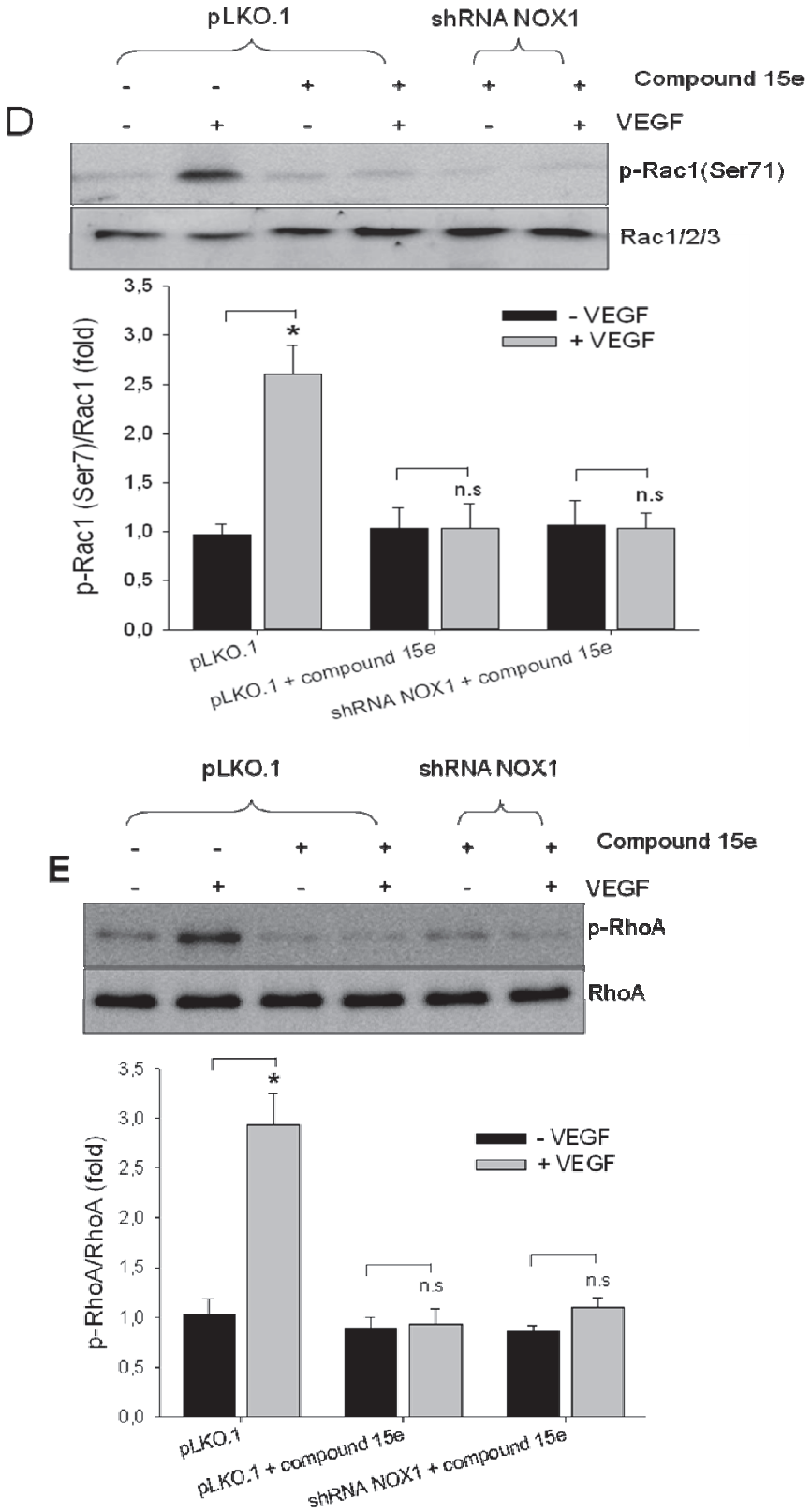

Figure 4.12: VEGF-mediated activation of RhoA and Rac1 in ES cells depends on PI3Kα. ES cells were stimulated with VEGF (500 pM). Whole cell lysates were blotted and subjected to immunoblotting. Activation of Rac1 (Ser71) and RhoA was analyzed using phospho-specific antibodies. Blots were subsequently reprobed with pan-specific antibodies recognizing Rac1/2/3 or RhoA, respectively. Specific activation was quantified as ratio of

phospho-specific to pan-specific signals. The blots shown are representative for at least 3 experiments with consistent results. Graphs under the blots shows mean values (+/- standard deviation) of 3 independent experiments. (A), kinetics of Rac1 and RhoA activation. Cells were subjected to immunoblotting at indicated time points after stimulation with VEGF. (B-E), ES cells stably producing shRNA targeting p110α, NOX1 or pLKO.1 shRNA control were stimulated with VEGF and pre-treated for 30 min with compound 15e (0.5 μM) as indicated. (D,E) $*P < 0.05$, statistically significant, n. s. not significant.

4.13 VEGF stimulates Akt activation dependent on p110α and independent of NOX1

Accumulating evidence has indicated that the PI3K-Akt pathway can be activated by growth factor and angiogenic stimuli such as VEGF and angiopoietins (Jiang and Liu 2009). We first investigated whether VEGF could regulate Akt activation in 5-day-old differentiating embryoid bodies. Our assays revealed that VEGF-induced Akt activation with an early peak at 10 min, which then returned to the basal levels after 30 min, while second peak of Akt activation appeared at 60 min (Fig. 4.13A). To determine whether VEGF-induced Akt activation is p110α dependent, we blocked p110α by compound 15e inhibitor, and examined Akt activation upon VEGF treatment. We found that pre-treatment the cells with 0.5 μM compound 15e totally abolished the effect of VEGF on Akt activation (Fig. 4.13B). To check whether NOX1 is involved in VEGF-induced Akt activation, we blocked NOX1 activity by using 2-APT and examined Akt activity after VEGF treatment (Fig. 4.13C). Interestingly, our results showed that pre-treatment with 0.5 μM 2-APT did not affect VEGF-induced Akt activity. To verify the results obtained from the specific inhibitor we used ES cells depleted p110α or NOX1. As expected, down regulation of p110α resulted in significant inhibition in Akt phosphorylation upon VEGF treatment (Fig. 4.13D). In contrast, non-significant decrease in Akt phosphorylation was observed after suppression of NOX1 (Fig. 4.13D). The second peak of Akt activity was also inhibited by 10 nM BIM-1 (PKC inhibitor) (Fig. 4.13E). Thus our data indicate a crosslink between PI3K and PKC pathway during VEGF-induced vasculogenesis in ES cell derived embryoid bodies. Taken together these results suggest that p110α but not NOX1 acts as upstream effector of Akt activation.

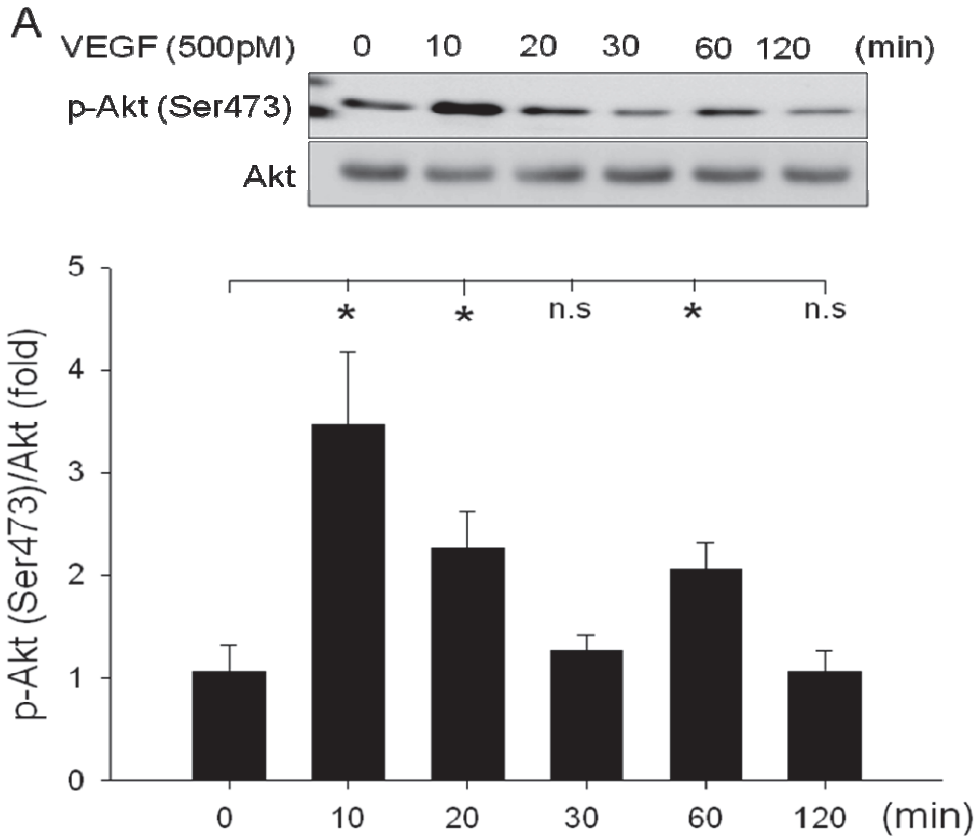
A
VEGF (500pM)
0
10
20
30
60
120
(min)
p-Akt (Ser473)
Akt
p-Akt (Ser473)/Akt (fold)
5
4
3
2
1
0
*
*
n.s
*
n.s
0
10
20
30
60
120
(min)

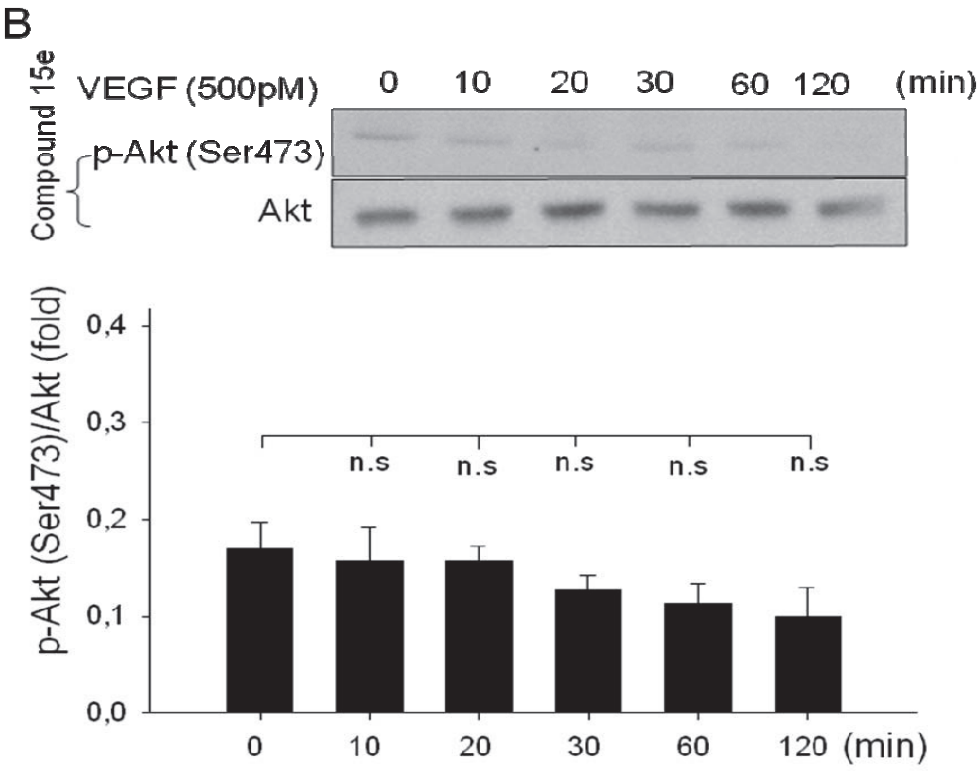
B
Compound 15e
VEGF (500pM)
0
10
20
30
60
120
(min)
p-Akt (Ser473)
Akt
p-Akt (Ser473)/Akt (fold)
0,4
0,3
0,2
0,1
0,0
n.s
n.s
n.s
n.s
n.s
0
10
20
30
60
120
(min)

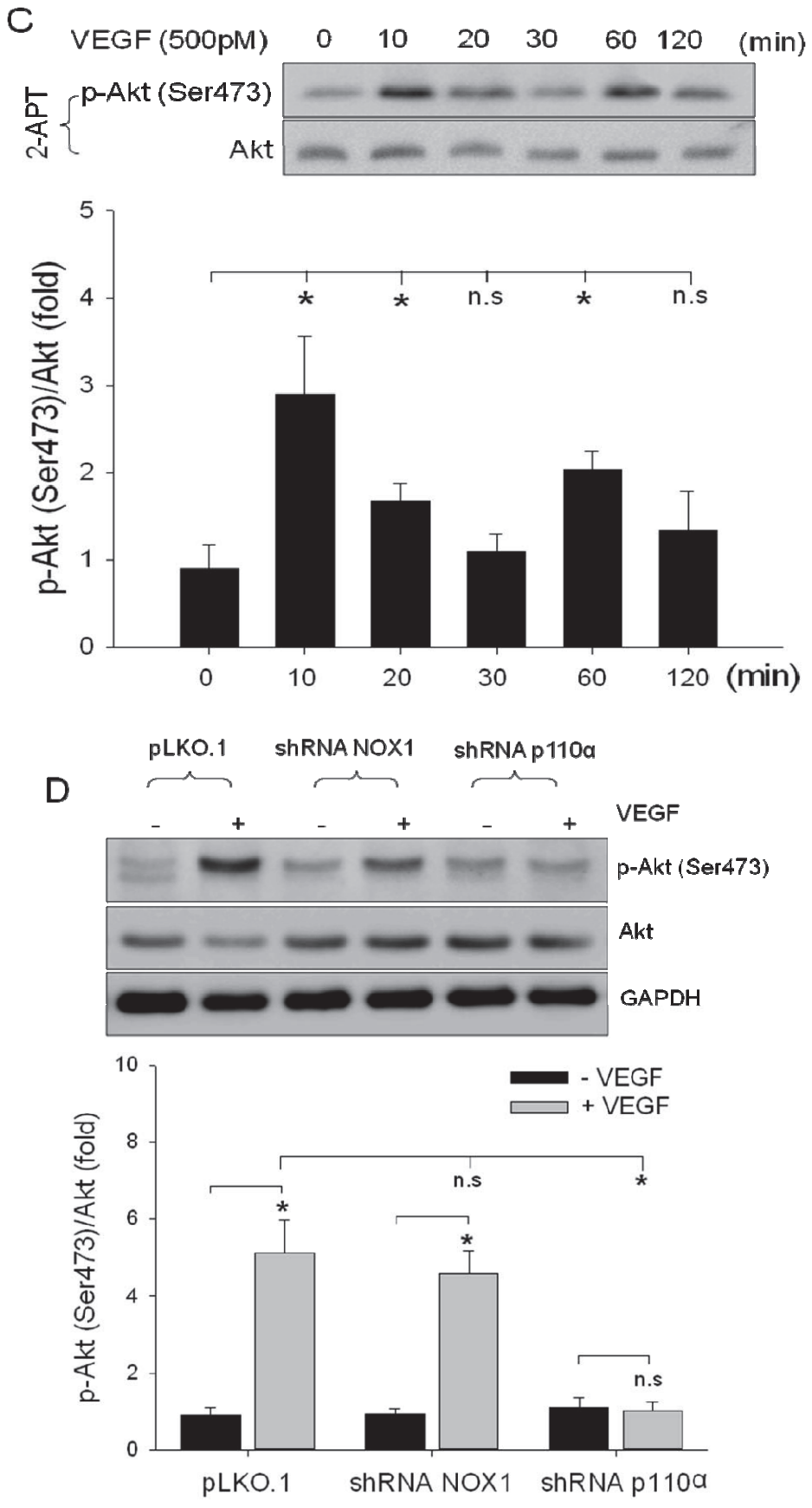
C
VEGF (500pM)
0
10
20
30
60
120
(min)
2-APT
p-Akt (Ser473)
Akt
p-Akt (Ser473)/Akt (fold)
*
*
n.s
*
n.s
0
10
20
30
60
120
(min)
D
pLKO.1
shRNA NOX1
shRNA p110α
VEGF
p-Akt (Ser473)
Akt
GAPDH
- VEGF
+ VEGF
p-Akt (Ser473)/Akt (fold)
n.s
*
n.s
pLKO.1
shRNA NOX1
shRNA p110α

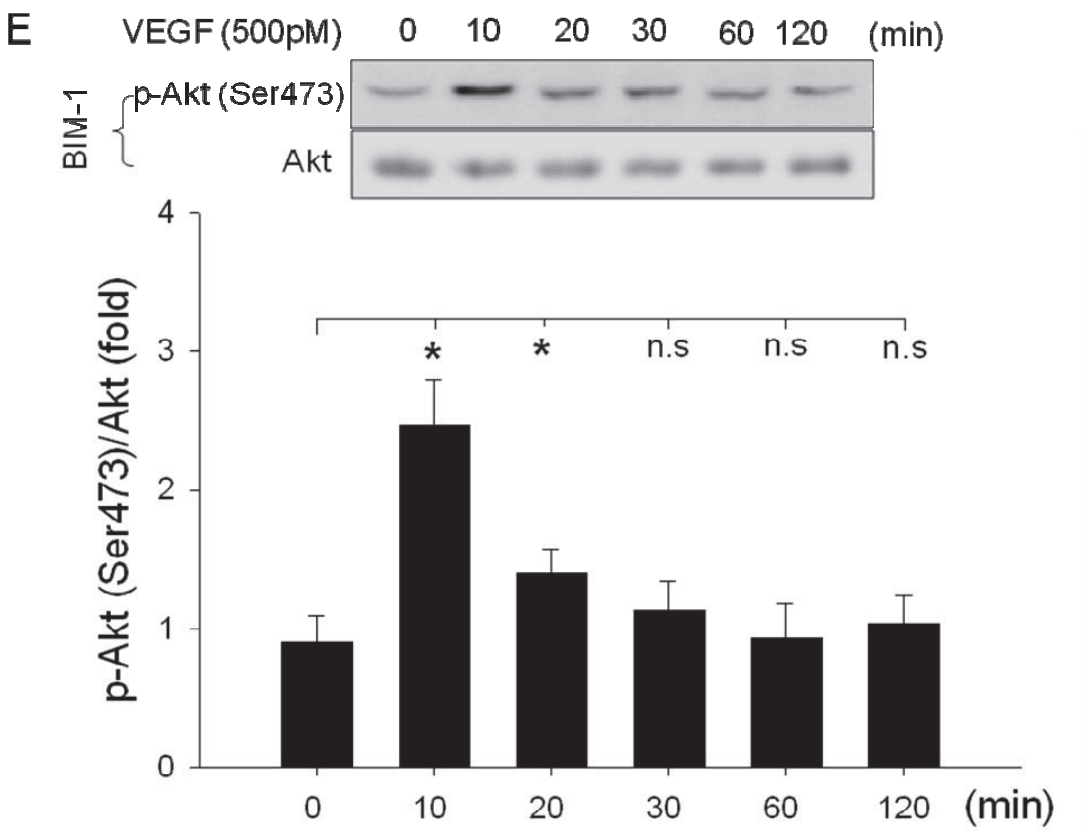

Figure 4.13: Activation of Akt by VEGF is dependent on class 1A PI3Kα but not NOX1. Whole cell lysates were blotted and subjected to immunoblotting. Activation of Akt (Ser473) was analyzed using phospho-specific antibodies. Blots were subsequently reprobed with specific antibodies recognizing Akt. Specific activation was quantified as ratio of phospho-specific to specific signals. The blots shown are representative for at least 3 experiments with consistent results. Graphs under the blots shows mean values (+/- standard deviation) of 3 independent experiments. (A), time course of Akt and phospho-Akt (Ser473) upon VEGF treatment. Note that VEGF stimulated Akt phosphorylation after 10 min. (B-D), after 30 min pre-treatment with inhibitor and VEGF for the indicated time, the level of total Akt and phospho-Akt (Ser473) in embryoid bodies was determined. (B), compound 15e (0.5 μM) inhibited the upregulation of phospho-Akt (Ser473) induced by VEGF (500 pM). (C), the NOX1 inhibitor 2-APT did not affect VEGF-induced Rac1 activity. (D), knock down of p110α resulted in significant inhibition in Akt phosphorylation upon VEGF treatment. In contrast, non-significant decrease in Akt phosphorylation was observed after silencing NOX1. (E), second peak of Akt activation at 60 min after VEGF treatment was blunted by pre-treatment with 10 nM BIM-1 (PKC inhibitor). **P* < 0.05, statistically significant as indicated, n. s. not significant.

4.14 Targeting p110α catalytic subunit inhibits VEGF-induced MAP kinase p44/42 activation

MAP kinase activation was measured using phosphor-specific antibodies to elucidate the signaling pathway involved in response to VEGF stimulation. After incubation with VEGF (500 pM) we could observe a high level of MAP kinase phosphor-p44/42 within 10 min in 5-day-old embryoid bodies (Fig. 4.14). It was apparent that the

PI3K inhibitor wortmannin completely prevented this activation (Fig. 4.14). Moreover, MAP kinase p44/42 activation upon VEGF treatment was absent in the presence of the p110α catalytic subunit inhibitor compound 15e (Fig. 4.14). In contrast, the NOX1 inhibitor (2-APT) did not affect p44/42 activation after VEGF treatment (Fig. 4.14). Furthermore, no significant involvement of JNK or p38 MAP kinase pathway could be observed in response to VEGF stimulation (Fig. 4.14). Thus our data indicate that MAP kinase p44/42 is mainly involved in VEGF mediated vascular differentiation processes.

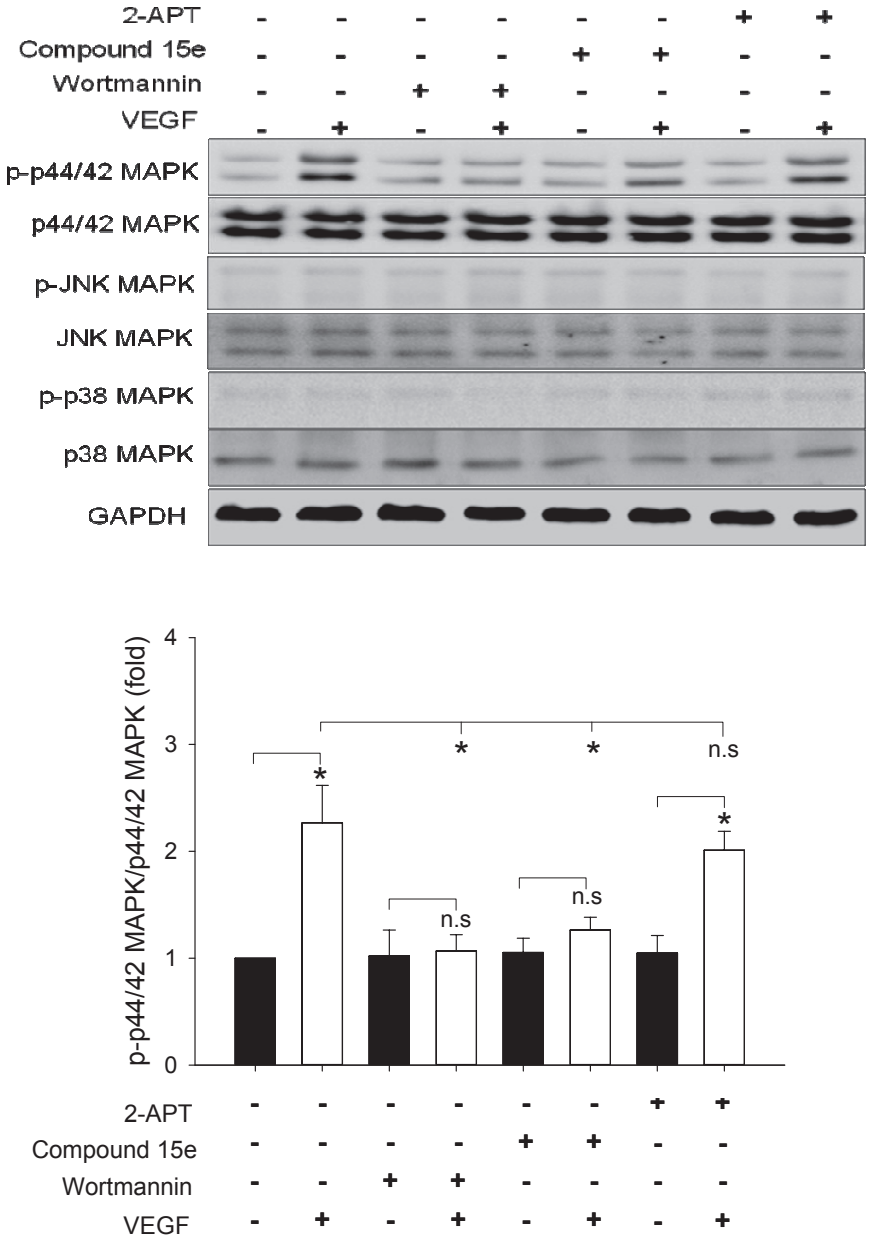

Figure 4.14: Targeting p110α catalytic subunit inhibits VEGF-induced MAP kinase p44/42 activation. Whole cell lysates were blotted and subjected to immunoblotting. Activation of protein was analyzed using phospho-specific antibodies. Blots were subsequently reprobed with specific antibodies recognizing total protein. Specific activation was quanti-

fied as ratio of phospho-specific to specific signals. The blots shown are representative for at least 3 experiments with consistent results. Graphs under the blots shows mean values (+/- standard deviation) of 3 independent experiments. MAP kinase p44/42 phosphorylation by VEGF is blocked by wortmannin and compound 15e in 5-day-old embryoid bodies. In contrast inhibition of NOX1 by 2-APT did not impair the activation of p44/42 observed upon VEGF treatment. No significant involvement of JNK or p38 MAPK pathway could be observed in response to VEGF stimulation. $*P < 0.05$, statistically significant as indicated, n. s. not significant.

4.15 Silencing the p110α inhibits tumor-induced angiogenesis in confrontation cultures of embryoid bodies and multicellular prostate cancer spheroids

Tumor vascularization of DU-145 prostate tumor spheroids was investigated in confrontation cultures with vascularized embryoid bodies to analyse further the role of PI3K and p110α as anti-angiogenic target. In the presents experiment we investigated the effects of wortmannin (1µM) on tumor-induced angiogenesis using co-culturing of embryonic stem cell-derived embryoid bodies and multicellular tumour spheroids, which were previously established by Wartenberg et al. (Wartenberg et al. 2001) as *in vitro* system to study tumor-angiogenesis. We found that wortmannin (1µM) strongly reduced the percentage of vascularized tumor (6.6 ± 5.5%) and the vascularization of multicellular tumor spheroids in confrontation cultures in comparison with untreated control (Fig. 4.15A-D). interestingly, silencing the p110α catalytic subunit of PI3K resulted in significantly reduced the tumor vascularisation and the percentage of vascularized tumor spheroids (20 ± 10%) as compared to the pLKO.1 control (Fig. 4.15A,B). Furthermore, the positive area in vascularized tumor spheroids was significantly abolished in the absence of p110α (Fig. 4.15E,F), which clearly underscores the meaning of this isoform as an anti-angiogenic target. Moreover, silencing the NOX1 significantly reduced the tumor vascularisation and the percentage of vascularized tumor spheroids (72,6 ± 8,2%) as compared to the pLKO.1 control (Fig. 4.15G,H). However, tumor vascularisation and the percentage of vascularized tumor spheroids in silencing the NOX1 still highly significant in compared with silencing the p110α catalytic subunit of PI3K. In contrast, confrontation cultures incubated with 1µM Rac1 inhibitor from day 6 to day 8 totally inhibited the tumor vascularisation (0.0%) and angiogenic sprouting into tumor spheroids (Fig. 4.15I,J)

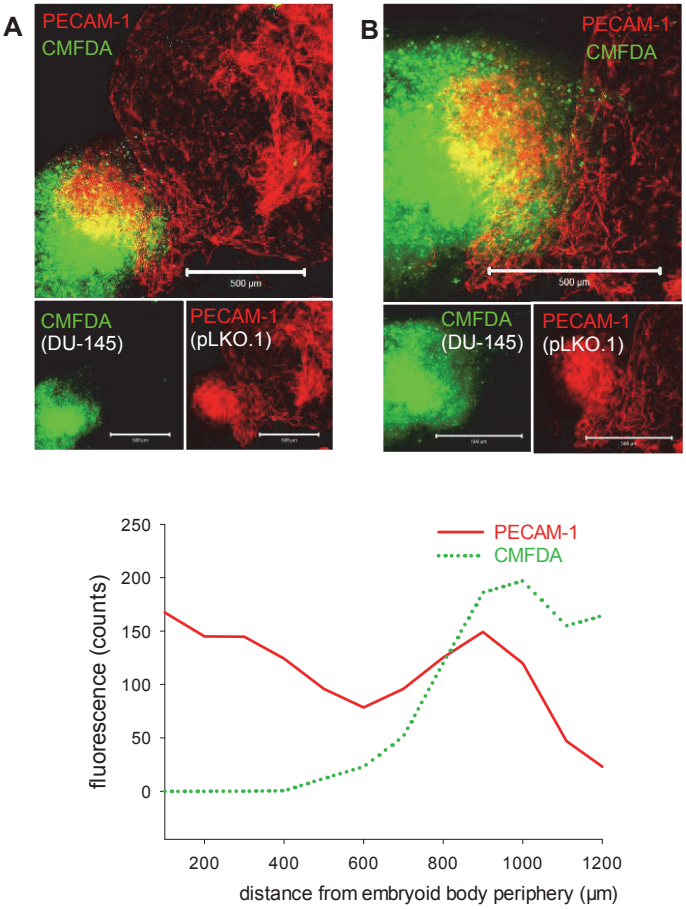
A
PECAM-1
CMFDA
500 µm
CMFDA
(DU-145)
PECAM-1
(pLKO.1)
B
PECAM-1
CMFDA
500 µm
CMFDA
(DU-145)
PECAM-1
(pLKO.1)
PECAM-1
CMFDA
fluorescence (counts)
250
200
150
100
50
0
200
400
600
800
1000
1200
distance from embryoid body periphery (µm)
C
PECAM-1
CMFDA
500 µm
CMFDA
(DU-145)
PECAM-1
(pLko.1 +
wortmannin)
D
PECAM-1
CMFDA
500 µm
CMFDA
(DU-145)
PECAM-1
(pLko.1 +
wortmannin)
PECAM-1
CMFDA
fluorescence (counts)
180
160
140
120
100
80
60
40
20
0
200
400
600
800
1000
1200
distance from embryoid body periphery (µm)

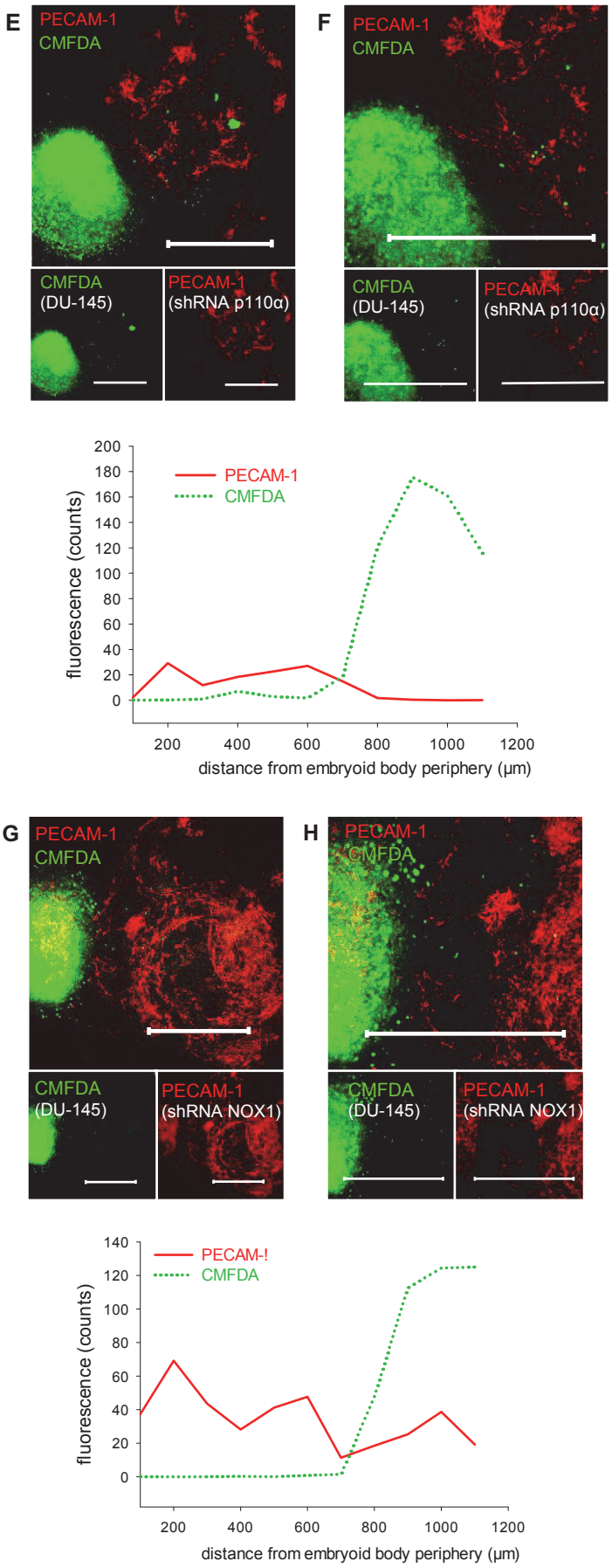
E
PECAM-1
CMFDA
CMFDA
(DU-145)
PECAM-1
(shRNA p110α)
F
PECAM-1
CMFDA
CMFDA
(DU-145)
PECAM-1
(shRNA p110α)
PECAM-1
CMFDA
fluorescence (counts)
distance from embryoid body periphery (μm)
G
PECAM-1
CMFDA
CMFDA
(DU-145)
PECAM-1
(shRNA NOX1)
H
PECAM-1
CMFDA
CMFDA
(DU-145)
PECAM-1
(shRNA NOX1)
PECAM-!
CMFDA
fluorescence (counts)
distance from embryoid body periphery (μm)

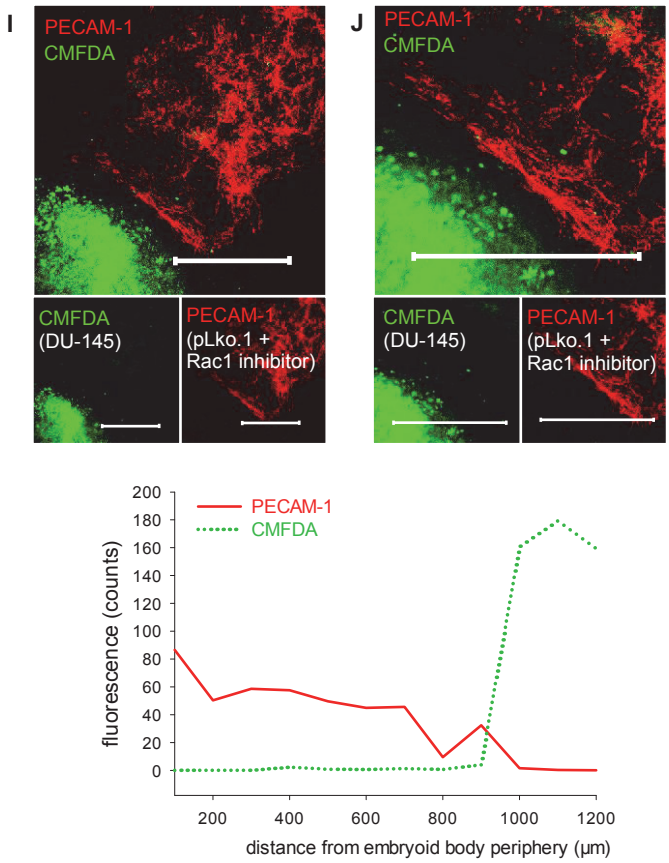

Figure 4.15: Inhibition of tumor-induced angiogenesis by silencing the p110α. The endothelial cells were visualized by anti-PECAM-1 (CD31, red color). The tissue of multicellular DU-145 prostate tumor spheroids was visualized by long-term cell tracker dye 5-chloromethylfluorescein diacetate (CMFDA) (green color). The bars represent 500 µm. Histograms of PECAM-1fluorescence (solid red line) and CMFDA fluorescence (dotted green line) are presented as fluorescence counts in relation to the distance from the embryoid body periphery. (A,B), representative immunefluorescence (IF) images showing the tumor-induced angiogenesis in confrontation cultures consisting of embryoid bodies pLKO.1 control and multicellular DU-145 prostate tumor spheroids. (C,D), confrontation cultures incubated with 1µM wortmannin from day 6 to day 8. (E,F), confrontation cultures with embryoid bodies stably producing shRNA targeting p110α catalytic subunit. (G.H), confrontation cultures with embryoid bodies stably producing shRNA targeting NOX1, (I,J) confrontation cultures incubated with 1µM Rac1 inhibitor from day 6 to day 8.

5. DISCUSSION

It has been established that VEGF signaling is crucial for both normal and disease-associated vascular development (Ferrara 2009). In fact, the mechanism of the VEGF stimulation on blood vessels formation has been the subject of intensive research over the last two decades (Connolly et al. 1989, Ferrara and Henzel 1989, Keck et al. 1989, Leung et al. 1989). There are a number of studies describing that VEGF could activate PI3K and stimulate vascular differentiation (Bekhite et al. 2011, Gerber et al. 1998, Jiang and Liu 2009). Moreover, inhibition PI3K activity by wortmannin or LY294002, which are first generation PI3K inhibitors, decreased VEGF-induced endothelial cell survival (Gerber et al. 1998). However, targeting vascular development by using wortmannin additionally inhibits PI3K-related kinases such as mTOR and PI4-kinase ß (Finan and Thomas 2004). Furthermore, these inhibitors do not discriminate between different PI3K isoforms, which are important for all organ systems (Marone et al. 2008). To overcome these disadvantages, many inhibitors targeting specific PI3K catalytic subunit were developed (Marone et al. 2008).

There is strong evidence in the literature to indicate that Akt is a major downstream target of PI3K for regulating angiogenesis. (Jiang and Liu 2009, Morello et al. 2009). However, selective involvement of specific class IA PI3K in vascular signalling pathways is not known (Cebe-Suarez et al. 2006, Gliki et al. 2002, Laramee et al. 2007). In addition, the contribution of VEGF to activate ROS production through PI3K and its involvement in vascular differentiation is still not fully understood (Chatterjee et al. 2012, Chen et al. 2006, Kennedy and DeLeo 2008). It has been previously demonstrated that the family of NADPH oxidases (NOX) plays an important role in ROS production in response to VEGF in non-phagocytic cells such as endothelial cells (Ushio-Fukai et al. 2002, Yamaoka-Tojo et al. 2004).

Embryonic stem (ES) cells are pluripotent cells derived from the early mouse embryo that can be propagated stably in the undifferentiated state *in vitro*. ES cells are maintained *in vitro* as totipotent stem cells by culture on a feeder layer of embryonic fibroblasts or in the presence of the cytokine leukemia inhibitory factor (LIF). When LIF is removed, they are able to spontaneously undergo *in vitro* differentiation, either in monolayer or form embryo-like aggregates, called embryoid bodies, into all the derivatives of the inner cell mass cells (ICM). The embryoid bodies can also give rise to highly differentiated cells when embryoid bodies formed in suspension are subsequently allowed to attach and to form outgrowths. It has been conclusively demon-

strated that ES cells differentiate *in vitro* to endothelial cells through successive maturation steps with sequential expression of cell lineage-specific markers: platelet endothelial cell adhesion molecule (PECAM,CD31), VEGF receptors, VEGFR1 (fms-related tyrosine kinase-1, Flt-1) and VEGFR2 (fetal liver kinase-1 Flk-1/KDR), tyrosine kinase with immunoglobulin-like and EGF-like domains 1 (tie-1), tie-2 and vascular endothelial cadherin (VE-cadherin), (Kabrun et al. 1997, Redick and Bautch 1999).

In this study, we for the first time studied the time course of class IA PI3K catalytic subunits p110α, Flk-1 and PECAM-production as well as intracellular ROS production in embryoid bodies. Our results indicated a striking synchronicity in the occurrence of endothelial cell markers with the appearance of class IA PI3K catalytic subunits p110α and ROS generation. Thus it was reasonable to speculate that p110α and ROS may be playing a role during the vascular differentiation. Moreover, Flk-1^{+} cells isolated from 4-day-old embryoid bodies mainly produced NOX1 and NOX4. Furthermore, class IA PI3K catalytic subunit p110α was produced in Flk-1^{+} cells, suggesting its involvement in vascular differentiation. This assumption is supported by studies showing that knock out of p110*α* in endothelial cells results in embryonic lethality at mid-gestation with defective development of the major vessels and lack of small branched vessels (Graupera et al. 2008).

The importance of NOX in ROS production was linked with PI3K pathway by several authors (Nakanishi et al. 2014, Seshiah et al. 2002, Xu et al. 2011), however, the precise signaling mechanisms of VEGF on NOX stimulation through PI3K are not yet completely understood (Chatterjee et al. 2012, Cheng et al. 2006, Kennedy and DeLeo 2008, Ushio-Fukai 2006). To elucidate a potential crosslink between PI3K and NADPH oxidase activation embryoid bodies were incubated during the time of VEGF treatment with PI3K inhibitors. This treatment significantly decreased ROS production in embryoid bodies. Moreover, we showed that VEGF stimulation of intracellular ROS formation was completely inhibited by the NADPH oxidase inhibitors DPI, VAS2870 and apocynin but not by rotenone. Previous data have shown that apocynin is able to prevent $p47^{phox}$ and $p47^{phox}$ homolog translocation to the plasma membrane, thereby inhibiting the NADPH oxidases to be active and functional (Banfi et al. 2003, Touyz et al. 2002). ROS formed by VEGF stimulation in might be derived from NOX1 and NOX2 (Bedard and Krause 2007). To further test the role of NOX1 and NOX2 as well was the p110α in intracellular ROS formation, we treated

the shRNA p110α and shRNA NOX1 embryoid bodies with VEGF and observed that VEGF failed to increase the ROS level. In contrast, treatment of shRNA NOX2 embryoid bodies with VEGF did not affect the ROS production, indicating that NOX2 is not involved in ROS production during. These data were confirmed in Flk-1^+ cells where VEGF treatment strongly elevated O_2^- generation which was significantly inhibited by wortmannin. Furthermore, knockdown p110α or NOX1 in Flk-1^+ cells abolished the effects of VEGF on O_2^- production. In contrast, knockdown of NOX2 in the Flk-1^+ cells did not show significant effects on O_2^- production. It is well known that the GTPase Rac1 plays a critical role in VEGF-induced O_2^- formation via NADPH oxidase activation in different cell types (Abid et al. 2001, Ushio-Fukai et al. 2002). Therefore, we investigated the role of Rac1 in O_2^- generation of differentiating ES cells. As expected Rac1 inhibitor abolished the VEGF mediated increase in O_2^- production, thus pointing to an involvement of Rac1 in VEGF-induced O_2^- production through activation of NOX1. This result is consistent with a previous report which suggested a direct link between Rac1 activity and ROS production in non-phagocytic cells (Sundaresan et al. 1996).

It is generally accepted that the PI3K pathway is important in mediating VEGF stimulation of endothelial cell proliferation, migration and tube formation (Gingras et al. 2000, van Nieuw Amerongen et al. 2003, Yuan et al. 2008). However, the precise signaling mechanism of VEGF-PI3K in vascular development is not yet completely understood. In this study, we have shown that treatment the embryoid with VEGF resulted in a significant increase in vascular differentiation in the pLKO.1 ES cells. This effect was still obvious in NOX1 depleted embryoid bodies but to a significantly lesser degree. Treatment of embryoid bodies with PI3K inhibitors reduced not only the area of PECAM-1 positive cells but also the vessel-like structures in embryoid bodies. These results are consistent with the previously demonstrated link between PI3K and vascular differentiation (Hamada et al. 2005, Jiang et al. 2000). PI3K probably stimulates vascular differentiation through one or several isoforms (Yuan et al. 2008). Thus, we targeted single isoforms to avoid side effects of pan-PI3K inhibitor on the immune system, which is largely dependent on p110δ and p110γ (Banham-Hall et al. 2012). Our results demonstrated that the increase in the vascular differentiation upon treatment with VEGF was nearly absent in the presence of p110α inhibitor or silencing p110α subunits. Similar findings were observed in other studies which showed that endothelial cell-specific-p110α knock out led to

embryonic lethality at mid-gestation due to severe defects in angiogenic sprouting and vascular remodelling (Graupera et al. 2008). Furthermore, Rac1 inhibitor significantly reduced the size of PECAM-1 positive area and nearly abolished branching points in embryoid bodies. These results are consistent with data from other groups which demonstrated that PI3K and Rac1 are required for vascular function (Fiedler 2009, Soga et al. 2001) as well as for VEGF-dependent angiogenesis in endothelial cells (Colavitti et al. 2002, Zhang et al. 2012). In addition, an essential role for Rac1 in mediating the effect of VEGF on endothelial cell proliferation and migration *in vitro* and in inducing angiogenesis in a mouse sponge implant model has been reported (Ushio-Fukai et al. 2002).

In the present study, using shRNA knockdown embryoid bodies enabled us to examine the contribution of p110*α* and NOX1 in the vascular development. Previous reports have shown that the most relevant NOX isoforms in vascular cells are presumably NOX1 and NOX2, which can both be regulated through Rac1 (Chatterjee et al. 2012). Our results showed that NOX1 is produced at significant higher levels compared to NOX2, which was scarcely present in Flk-1^+ cells. Results from tube-like structure formation and scratch migration assay using Flk-1^+ cells indicted that shRNA p110α Flk-1^+ cells failed to migrate and to form interconnected tubes even when stimulated with VEGF. Likewise, silencing NOX1 in Flk-1^+ cells caused a significantly reduction in cell migration and tubes length as well as the branching points upon VEGF treatment. Hence, our findings suggest that p110α as well as NOX1 are important for VEGF-induced tube formation. Since VEGF still increased the number of Flk-1^+ cells in NOX1 shRNA embryoid bodies it may be concluded that NOX1 is not required for the initial stages of vasculogenesis but is playing a role in the migration and sprouting of the endothelial cells to promote the establishment of capillary-like networks upon VEGF treatment. It may be further speculated that other NOX isoforms, e.g. NOX4 may overtake the function of NOX1 in NOX1 shRNA embryoid bodies. Consistent with our data others have suggested a role for Nox1 in stimulating branching morphogenesis of sinusoidal endothelial cells (Kobayashi et al. 2004). Moreover it has been shown that mice deficient in NOX1, but not NOX2 or NOX4, exhibit significant reduction in angiogenesis (Garrido-Urbani et al. 2011).

It is well known that remodelling of the actin cytoskeleton is essential for cell migration (Lamalice et al. 2007). In the present study we demonstrated that VEGF treated

Flk-1$^+$ cells displayed polarized shapes due to formation of lamellipodia during cell migration. Pre-treatment with wortmannin or silencing p110α in Flk-1$^+$ cells abrogated VEGF-induced lamellipodia structure formation. Moreover the absence of NOX1 in Flk-1$^+$ cells resulted in significant inhibition in polarized cell numbers, although this effect was less pronounced as compared to conditions of PI3K inhibition. These observations may suggest that class IA PI3Kα signaling is required for cytoskeletal changes during cell migration, whereas, silencing NOX1 in Flk-1$^+$ cells is affecting lamellipodia structure formation. Cell migration is a fundamental aspect of cancer cell growth (Jimenez et al. 2000) and is a complex process that requires the high coordination of actin polymerization, formation, release of focal adhesions and myosin motor activity (Lauffenburger and Horwitz 1996). An important finding in this study is that the inhibition of p110α by shRNA significantly decreased the rate of cell migration. This demonstrates that the p110α subunit affects multiple cell functions and also reveals the expected functions of the PI3K isoforms on cancer cells.

Several lines of investigation have indicated that Rac1 plays a crucial role in transducing the signals from cell surface receptors to downstream effectors and is involved in cell migration and gene expression (Burridge and Wennerberg 2004, Etienne-Manneville and Hall 2002). In addition, Rac1is involved in cytoskeleton organization and is defining cell shape and morphology (Colley 2000, Etienne-Manneville and Hall 2002). A previous study has demonstrated that Rac1 is involved in the control of angiogenesis by inducing ROS production (Diebold et al. 2009, Li et al. 2010, Tobar et al. 2008). In our study, suppression of p110α using shRNA significantly inhibited the activation of Rac1 and RhoA in ES cells upon VEGF treatment. This is in line with previous studies which showed that the activation of Rac1 is selectively dependent on the p110α isoform of PI3K (Graupera et al. 2008). Since NOX1 was produced in the Flk-1$^+$ cells and shRNA-mediated dwonregulation of NOX1 suppressed ROS generation, our findings are in line with the observation that VEGF stimulates ROS production via activation of Rac1-dependent NADPH oxidase (Ushio-Fukai 2007) or Rac1-regulated NOX1 enzyme (Cheng et al. 2006, Miyano et al. 2006). Collectively, these data suggest that PI3K functions as an upstream activator of Rac1 and RhoA and subsequently affects the cytoskeleton and induces endothelial cell migration. Moreover, NOX1 may take part in VEGF-induced cell migration, since silencing NOX1 strongly reduced these responses.

Akt is known to be involved in the regulation of angiogenesis (Fujio et al. 2000, Shiojima and Walsh 2006). Moreover, we and other groups provided direct evidence that the PI3K-Akt pathway is required for VEGF to induce vascular development (Abid et al. 2004, Bekhite et al. 2011, Karar and Maity 2011). In this study, we showed that VEGF induced Akt activation with an early peak at 10 min while asecond peak of Akt activation appeared at 60 min. Given that the activation of Akt has been shown to play an essential role in VEGF-PI3K stimulation (Madeddu et al. 2008), we thought that it was possible that NOX1 may regulate Akt in embryoid bodies. However, our data demonstrated that inhibition of NOX1 did not impair VEGF-induced Rac1 as well as Akt phosphorylation. Therefore our results indicate that p110α but not NOX1 act as the upstream effector of Rac1 and Akt activation.

In an effort to elucidate further the pathway by which MAP kinase VEGF stimulates the vascular differentiation. MAP kinase activation was measured to elucidate whether the class IA PI3Kα and NOX1 are essential for VEGF-MAP kinases signalling pathways leading to vascular differentiation. As seen in the results, stimulation the embryoid bodies with VEGF showed a high level of phosphor-p44/42 in 5-day-old embryoid bodies within 10 minutes. We also observed that MAP kinase p44/42 phosphorylation was blocked by wortmannin the PI3K inhibitor and the p110α inhibitor compouned15e. While 2-APT the NOX1 inhibitor was not able to prevent the VEGF-induced MAP kinase p44/42 phosphorylation. Furthermore, no significant involvement of JNK or p38 MAP kinase pathway could be observed in response to VEGF stimulation. Based on currently evidence, PI3K as well as PI3K catalytic subunit p110α are involved in VEGF mediated vascular differentiation processes. These findings indicated a regulatory role of the PI3K pathway through the activation of MAP kinase p44/42. Qiang et al. (Qiang et al. 2002) also reported this crosstalk between the PI3K and MAP kinase p42/44 in human myeloma cells. The phosphorylation status of the other MAP kinases e.g. p38 and JNK did not change after stimulation embryoid bodies with VEGF, suggesting that effects of VEGF on vascular differentiation of ES cells are mediated by MAP kinase p44/42. Our hypothesis is consistent with previous findings demonstrating that activation of MAP kinase p44/42 is essential for cell differentiation induced by VEGF (Ferrara et al. 1996, Pimentel et al. 2002).

Similar to embryos, growing any tumor more than 2mm needs functional blood vessels (Ferrara 2002). In order to achieve this, tumor cells have to undergo a so-called

angiogenic switch (Leite de Oliveira et al. 2011). This will supply the tumor with oxygen. Experimental and clinical evidence suggests that the process of metastasis is also angiogenesis dependent. For a tumor cell to metastasize successfully, it must breach several barriers and respond to specific growth factors (Fidler et al. 1978, Nicolson 1988a, Nicolson 1988b). Thus, tumor cells must gain access to the vasculature in the primary tumor, survive the circulation, arrest in the microvasculature of the target organ exit from this vasculature, grow in the target organ and induce angiogenesis (Weidner et al. 1991, Weinstat-Saslow and Steeg 1994, Zetter 1998). Therefore, angiogenesis appears to be necessary at the beginning as well as at the completion of the metastatic cascade. Hence, if it were possible to prevent tumors from being vascularized cancer could probably be cured (Folkman 1971). Antiangiogenic therapy is currently one of the most promising and efficient therapies against cancer. This has initiated intensive research for novel antiangiogenic agents that exert specific effects on endothelial cell migration and/or proliferation as well as for innovative *in vitro* models to study the efficacy of antiangiogenic compounds (Sounni and Noel 2013).

In addition to normal physiological angiogenesis, the ES derived embryoid bodies system used in confrontation cultures with multicellular tumor spheroids is also suitable for studying tumor-induced angiogenesis. Invasion of endothelial cells into the tumor tissue can be observed in tumor spheroids cultivated in confrontation cultures with embryoid bodies which became efficiently vascularised within a few days (Wartenberg et al. 2001). This angiogenesis resulted in the growth stimulation of the tumor spheroid, the disappearance of the central necrosis, the improvement of oxygen supply and the downregulation of the expression of both HIF-1αand VEGF, features normally observed during the vascularization of a tumor tissue (Wartenberg et al. 2001).

To examine the role of PI3K/p110α and NOX1 pathway in tumor-induced angiogenesis, we used confrontation culture consists of embryoied bodies derived from ES cells and multicellular tumor spheroids from human prostate carcinoma cell line (DU-145). Interestingly, we found PI3K inhibitor wortmannin and silencing p110α can strongly inhibited the vascularization of multicellular tumor spheroids in confrontation cultures, NOX1 knockdown has no strong effect as p110α knockdown on tumor-induced angiogenesis.

5.1 Conclusion

Taken together, our data demonstrated that the VEGF-VEGFR-PI3K-Akt/Rac1 signaling pathway plays a vital role in VEGF-induced blood vessels differentiation. Further analysis of this signaling cascade demonstrates that p110α is critical for vascular development because silence p110α causes defective vasculogenesis and angiogenesis, while VEGF-PI3K-NOX1 is involved in angiogenesis through O_2^- generation. Interestingly, silencing p110α can strongly inhibited the vascularization of multicellular tumor spheroids in confrontation cultures. Importantly, these findings provide direct evidence that the activity of p110*α* in endothelial cells is essential for vascular development and suggest that p110*α* and their downstream signalling cascade may represent promising therapeutic targets for the treatment of numerous human diseases that involve aberrant neovascularization.

6. LITERATURE

Abid MR, Guo S, Minami T, Spokes KC, Ueki K, Skurk C, Walsh K, and Aird WC. 2004. Vascular endothelial growth factor activates PI3K/Akt/forkhead signaling in endothelial cells. Arterioscler Thromb Vasc Biol 24(2):294-300.

Abid MR, Tsai JC, Spokes KC, Deshpande SS, Irani K, and Aird WC. 2001. Vascular endothelial growth factor induces manganese-superoxide dismutase expression in endothelial cells by a Rac1-regulated NADPH oxidase-dependent mechanism. Faseb J 15(13):2548-2550.

Adams RH, and Alitalo K. 2007. Molecular regulation of angiogenesis and lymphangiogenesis. Nat Rev Mol Cell Biol 8(6):464-478.

Awwad HK, el Naggar M, Mocktar N, and Barsoum M. 1986. Intercapillary distance measurement as an indicator of hypoxia in carcinoma of the cervix uteri. Int J Radiat Oncol Biol Phys 12(8):1329-1333.

Banfi B, Clark RA, Steger K, and Krause KH. 2003. Two novel proteins activate superoxide generation by the NADPH oxidase NOX1. J Biol Chem 278(6):3510-3513.

Banham-Hall E, Clatworthy MR, and Okkenhaug K. 2012. The Therapeutic Potential for PI3K Inhibitors in Autoimmune Rheumatic Diseases. Open Rheumatol J 6:245-258.

Bartsch C, Bekhite MM, Wolheim A, Richter M, Ruhe C, Wissuwa B, Marciniak A, Muller J, Heller R, Figulla HR et al. . 2011. NADPH oxidase and eNOS control cardiomyogenesis in mouse embryonic stem cells on ascorbic acid treatment. Free Radic Biol Med 51(2):432-443.

Becker LB. 2004. New concepts in reactive oxygen species and cardiovascular reperfusion physiology. Cardiovasc Res 61(3):461-470.

Bedard K, and Krause KH. 2007. The NOX family of ROS-generating NADPH oxidases: physiology and pathophysiology. Physiol Rev 87(1):245-313.

Bednarz J, Teifel M, Friedl P, and Engelmann K. 2000. Immortalization of human corneal endothelial cells using electroporation protocol optimized for human corneal endothelial and human retinal pigment epithelial cells. Acta Ophthalmol Scand 78(2):130-136.

Bekhite MM, Finkensieper A, Abou-Zaid FA, El-Shourbagy IK, Omar KM, Figulla HR, Sauer H, and Wartenberg M. 2010. Static electromagnetic fields induce vasculogenesis and chondro-osteogenesis of mouse embryonic stem cells by reactive oxygen species-mediated up-regulation of vascular endothelial growth factor. Stem Cells Dev 19(5):731-743.

Bekhite MM, Finkensieper A, Binas S, Muller J, Wetzker R, Figulla HR, Sauer H, and Wartenberg M. 2011. VEGF-mediated PI3K class IA and PKC signaling in cardiomyogenesis and vasculogenesis of mouse embryonic stem cells. J Cell Sci 124(Pt 11):1819-1830.

Bhattacharya R, Kwon J, Li X, Wang E, Patra S, Bida JP, Bajzer Z, Claesson-Welsh L, and Mukhopadhyay D. 2009. Distinct role of PLCbeta3 in VEGF-mediated directional migration and vascular sprouting. J Cell Sci 122(Pt 7):1025-1034.

Bi L, Okabe I, Bernard DJ, Wynshaw-Boris A, and Nussbaum RL. 1999. Proliferative defect and embryonic lethality in mice homozygous for a deletion in the p110alpha subunit of phosphoinositide 3-kinase. J Biol Chem 274(16):10963-10968.

Boheler KR, Czyz J, Tweedie D, Yang HT, Anisimov SV, and Wobus AM. 2002. Differentiation of pluripotent embryonic stem cells into cardiomyocytes. Circ Res 91(3):189-201.

Bos JL. 1995. A target for phosphoinositide 3-kinase: Akt/PKB. Trends Biochem Sci 20(11):441-442.

Brindle NP, Saharinen P, and Alitalo K. 2006. Signaling and functions of angiopoietin-1 in vascular protection. Circ Res 98(8):1014-1023.

Burridge K, and Wennerberg K. 2004. Rho and Rac take center stage. Cell 116(2):167-179.

Caliceti C, Nigro P, Rizzo P, and Ferrari R. 2014. ROS, Notch, and Wnt signaling pathways: crosstalk between three major regulators of cardiovascular biology. Biomed Res Int 2014:318714.

Carmeliet P, Ferreira V, Breier G, Pollefeyt S, Kieckens L, Gertsenstein M, Fahrig M, Vandenhoeck A, Harpal K, Eberhardt C et al. . 1996. Abnormal blood vessel development and lethality in embryos lacking a single VEGF allele. Nature 380(6573):435-439.

Carter WO, Narayanan PK, and Robinson JP. 1994. Intracellular hydrogen peroxide and superoxide anion detection in endothelial cells. J Leukoc Biol 55(2):253-258.

Cebe-Suarez S, Zehnder-Fjallman A, and Ballmer-Hofer K. 2006. The role of VEGF receptors in angiogenesis; complex partnerships. Cell Mol Life Sci 63(5):601-615.

Chatterjee S, Browning EA, Hong N, DeBolt K, Sorokina EM, Liu W, Birnbaum MJ, and Fisher AB. 2012. Membrane depolarization is the trigger for PI3K/Akt activation and leads to the generation of ROS. Am J Physiol Heart Circ Physiol 302(1):H105-114.

Chen YW, Huang CF, Tsai KS, Yang RS, Yen CC, Yang CY, Lin-Shiau SY, and Liu SH. 2006. The role of phosphoinositide 3-kinase/Akt signaling in low-dose mercury-induced mouse pancreatic beta-cell dysfunction in vitro and in vivo. Diabetes 55(6):1614-1624.

Cheng G, Diebold BA, Hughes Y, and Lambeth JD. 2006. Nox1-dependent reactive oxygen generation is regulated by Rac1. J Biol Chem 281(26):17718-17726.

Choi K, Kennedy M, Kazarov A, Papadimitriou JC, and Keller G. 1998. A common precursor for hematopoietic and endothelial cells. Development 125(4):725-732.

Clayton E, Bardi G, Bell SE, Chantry D, Downes CP, Gray A, Humphries LA, Rawlings D, Reynolds H, Vigorito E et al. . 2002. A crucial role for the p110delta subunit of phosphatidylinositol 3-kinase in B cell development and activation. The Journal of experimental medicine 196(6):753-763.

Colavitti R, Pani G, Bedogni B, Anzevino R, Borrello S, Waltenberger J, and Galeotti T. 2002. Reactive oxygen species as downstream mediators of angiogenic signaling by vascular endothelial growth factor receptor-2/KDR. J Biol Chem 277(5):3101-3108.

Colley NJ. 2000. Cell biology. Actin' up with Rac1. Science 290(5498):1902-1903.

Connolly DT, Heuvelman DM, Nelson R, Olander JV, Eppley BL, Delfino JJ, Siegel NR, Leimgruber RM, and Feder J. 1989. Tumor vascular permeability factor stimulates endothelial cell growth and angiogenesis. J Clin Invest 84(5):1470-1478.

Davies SP, Reddy H, Caivano M, and Cohen P. 2000. Specificity and mechanism of action of some commonly used protein kinase inhibitors. The Biochemical journal 351(Pt 1):95-105.

de Bruijn MF, Ma X, Robin C, Ottersbach K, Sanchez MJ, and Dzierzak E. 2002. Hematopoietic stem cells localize to the endothelial cell layer in the midgestation mouse aorta. Immunity 16(5):673-683.

Diebold I, Djordjevic T, Petry A, Hatzelmann A, Tenor H, Hess J, and Gorlach A. 2009. Phosphodiesterase 2 mediates redox-sensitive endothelial cell proliferation and angiogenesis by thrombin via Rac1 and NADPH oxidase 2. Circ Res 104(10):1169-1177.

Disanza A, Steffen A, Hertzog M, Frittoli E, Rottner K, and Scita G. 2005. Actin polymerization machinery: the finish line of signaling networks, the starting point of cellular movement. Cell Mol Life Sci 62(9):955-970.

Etienne-Manneville S, and Hall A. 2002. Rho GTPases in cell biology. Nature 420(6916):629-635.

Evans MJ, and Kaufman MH. 1981. Establishment in culture of pluripotential cells from mouse embryos. Nature 292(5819):154-156.

Feraud O, Cao Y, and Vittet D. 2001. Embryonic stem cell-derived embryoid bodies development in collagen gels recapitulates sprouting angiogenesis. Lab Invest 81(12):1669-1681.

Ferrara N. 2002. VEGF and the quest for tumour angiogenesis factors. Nat Rev Cancer 2(10):795-803.

Ferrara N. 2009. Vascular endothelial growth factor. Arterioscler Thromb Vasc Biol 29(6):789-791.

Ferrara N, Carver-Moore K, Chen H, Dowd M, Lu L, O'Shea KS, Powell-Braxton L, Hillan KJ, and Moore MW. 1996. Heterozygous embryonic lethality induced by targeted inactivation of the VEGF gene. Nature 380(6573):439-442.

Ferrara N, and Henzel WJ. 1989. Pituitary follicular cells secrete a novel heparin-binding growth factor specific for vascular endothelial cells. Biochem Biophys Res Commun 161(2):851-858.

Ferrara N, and Kerbel RS. 2005. Angiogenesis as a therapeutic target. Nature 438(7070):967-974.

Fidler IJ, Gersten DM, and Hart IR. 1978. The biology of cancer invasion and metastasis. Adv Cancer Res 28:149-250.

Fiedler LR. 2009. Rac1 regulates cardiovascular development and postnatal function of endothelium. Cell Adh Migr 3(2):143-145.

Finan PM, and Thomas MJ. 2004. PI 3-kinase inhibition: a therapeutic target for respiratory disease. Biochem Soc Trans 32(Pt 2):378-382.

Fischer C, Schneider M, and Carmeliet P. 2006. Principles and therapeutic implications of angiogenesis, vasculogenesis and arteriogenesis. Handb Exp Pharmacol(176 Pt 2):157-212.

Folkman J. 1971. Tumor angiogenesis: therapeutic implications. N Engl J Med 285(21):1182-1186.

Folkman J, Merler E, Abernathy C, and Williams G. 1971. Isolation of a tumor factor responsible for angiogenesis. J Exp Med 133(2):275-288.

Fong GH, Rossant J, Gertsenstein M, and Breitman ML. 1995. Role of the Flt-1 receptor tyrosine kinase in regulating the assembly of vascular endothelium. Nature 376(6535):66-70.

Fujio Y, Nguyen T, Wencker D, Kitsis RN, and Walsh K. 2000. Akt promotes survival of cardiomyocytes in vitro and protects against ischemia-reperfusion injury in mouse heart. Circulation 101(6):660-667.

Garrido-Urbani S, Jemelin S, Deffert C, Carnesecchi S, Basset O, Szyndralewiez C, Heitz F, Page P, Montet X, Michalik L et al. . 2011. Targeting vascular NADPH oxidase 1 blocks tumor angiogenesis through a PPARalpha mediated mechanism. PLoS One 6(2):e14665.

Gerber HP, McMurtrey A, Kowalski J, Yan M, Keyt BA, Dixit V, and Ferrara N. 1998. Vascular endothelial growth factor regulates endothelial cell survival through the phosphatidylinositol 3'-kinase/Akt signal transduction pathway. Requirement for Flk-1/KDR activation. J Biol Chem 273(46):30336-30343.

Gingras D, Lamy S, and Beliveau R. 2000. Tyrosine phosphorylation of the vascular endothelial-growth-factor receptor-2 (VEGFR-2) is modulated by Rho proteins. Biochem J 348 Pt 2:273-280.

Gliki G, Wheeler-Jones C, and Zachary I. 2002. Vascular endothelial growth factor induces protein kinase C (PKC)-dependent Akt/PKB activation and phosphatidylinositol 3'-kinase-mediates PKC delta phosphorylation: role of PKC in angiogenesis. Cell Biol Int 26(9):751-759.

Graham FL, Smiley J, Russell WC, and Nairn R. 1977. Characteristics of a human cell line transformed by DNA from human adenovirus type 5. J Gen Virol 36(1):59-74.

Graham FL, and van der Eb AJ. 1973. A new technique for the assay of infectivity of human adenovirus 5 DNA. Virology 52(2):456-467.

Graupera M, Guillermet-Guibert J, Foukas LC, Phng LK, Cain RJ, Salpekar A, Pearce W, Meek S, Millan J, Cutillas PR et al. . 2008. Angiogenesis selectively requires the p110alpha isoform of PI3K to control endothelial cell migration. Nature 453(7195):662-666.

Guan K, Rohwedel J, and Wobus AM. 1999. Embryonic stem cell differentiation models: cardiogenesis, myogenesis, neurogenesis, epithelial and vascular smooth muscle cell differentiation in vitro. Cytotechnology 30(1-3):211-226.

Guo D, Jia Q, Song HY, Warren RS, and Donner DB. 1995. Vascular endothelial cell growth factor promotes tyrosine phosphorylation of mediators of signal transduction that contain SH2 domains. Association with endothelial cell proliferation. J Biol Chem 270(12):6729-6733.

Hamada K, Sasaki T, Koni PA, Natsui M, Kishimoto H, Sasaki J, Yajima N, Horie Y, Hasegawa G, Naito M et al. . 2005. The PTEN/PI3K pathway governs normal vascular development and tumor angiogenesis. Genes Dev 19(17):2054-2065.

Hanahan D. 1983. Studies on transformation of Escherichia coli with plasmids. J Mol Biol 166(4):557-580.

Hayakawa M, Kaizawa H, Moritomo H, Koizumi T, Ohishi T, Okada M, Ohta M, Tsukamoto S, Parker P, Workman P et al. . 2006. Synthesis and biological evaluation of 4-morpholino-2-phenylquinazolines and related derivatives as novel PI3 kinase p110alpha inhibitors. Bioorg Med Chem 14(20):6847-6858.

Heistad DD. 2006. Oxidative stress and vascular disease: 2005 Duff lecture. Arterioscler Thromb Vasc Biol 26(4):689-695.

Ide A, Baker N, and Warren S. 1939. Vascularization of the Brown Pearce rabbit epithelioma transplant as seen in the transparent ear chamber. Am J Roentgenol 42:891-899

Igarashi J, and Michel T. 2001. Sphingosine 1-phosphate and isoform-specific activation of phosphoinositide 3-kinase beta. Evidence for divergence and convergence of receptor-regulated endothelial nitric-oxide synthase signaling pathways. J Biol Chem 276(39):36281-36288.

Jiang BH, and Liu LZ. 2009. PI3K/PTEN signaling in angiogenesis and tumorigenesis. Adv Cancer Res 102:19-65.

Jiang BH, Zheng JZ, Aoki M, and Vogt PK. 2000. Phosphatidylinositol 3-kinase signaling mediates angiogenesis and expression of vascular endothelial growth factor in endothelial cells. Proc Natl Acad Sci U S A 97(4):1749-1753.

Jimenez C, Portela RA, Mellado M, Rodriguez-Frade JM, Collard J, Serrano A, Martinez AC, Avila J, and Carrera AC. 2000. Role of the PI3K regulatory subunit in the control of actin organization and cell migration. J Cell Biol 151(2):249-262.

Kabrun N, Buhring HJ, Choi K, Ullrich A, Risau W, and Keller G. 1997. Flk-1 expression defines a population of early embryonic hematopoietic precursors. Development 124(10):2039-2048.

Kaibuchi K, Kuroda S, and Amano M. 1999. Regulation of the cytoskeleton and cell adhesion by the Rho family GTPases in mammalian cells. Annu Rev Biochem 68:459-486.

Karar J, and Maity A. 2011. PI3K/AKT/mTOR Pathway in Angiogenesis. Front Mol Neurosci 4:51.

Keck PJ, Hauser SD, Krivi G, Sanzo K, Warren T, Feder J, and Connolly DT. 1989. Vascular permeability factor, an endothelial cell mitogen related to PDGF. Science 246(4935):1309-1312.

Keller G. 2005. Embryonic stem cell differentiation: emergence of a new era in biology and medicine. Genes Dev 19(10):1129-1155.

Kennedy AD, and DeLeo FR. 2008. PI3K and NADPH oxidase: a class act. Blood 112(13):4788-4789.

Keyhani A, Jendiroba DB, and Freireich EJ. 2001. Angiogenesis and leukemia. Leuk Res 25(8):639-645.

Kim KJ, Li B, Winer J, Armanini M, Gillett N, Phillips HS, and Ferrara N. 1993. Inhibition of vascular endothelial growth factor-induced angiogenesis suppresses tumour growth in vivo. Nature 362(6423):841-844.

Knight ZA, Chiang GG, Alaimo PJ, Kenski DM, Ho CB, Coan K, Abraham RT, and Shokat KM. 2004. Isoform-specific phosphoinositide 3-kinase inhibitors from an arylmorpholine scaffold. Bioorganic & medicinal chemistry 12(17):4749-4759.

Kobayashi S, Nojima Y, Shibuya M, and Maru Y. 2004. Nox1 regulates apoptosis and potentially stimulates branching morphogenesis in sinusoidal endothelial cells. Exp Cell Res 300(2):455-462.

Koyasu S. 2003. The role of PI3K in immune cells. Nature immunology 4(4):313-319.

Kroll J, and Waltenberger J. 1997. The vascular endothelial growth factor receptor KDR activates multiple signal transduction pathways in porcine aortic endothelial cells. J Biol Chem 272(51):32521-32527.

Lamalice L, Le Boeuf F, and Huot J. 2007. Endothelial cell migration during angiogenesis. Circ Res 100(6):782-794.

Lambeth JD. 2007. Nox enzymes, ROS, and chronic disease: an example of antagonistic pleiotropy. Free Radic Biol Med 43(3):332-347.

Lambeth JD, Kawahara T, and Diebold B. 2007. Regulation of Nox and Duox enzymatic activity and expression. Free Radic Biol Med 43(3):319-331.

Laramee M, Chabot C, Cloutier M, Stenne R, Holgado-Madruga M, Wong AJ, and Royal I. 2007. The scaffolding adapter Gab1 mediates vascular endothelial growth factor signaling and is required for endothelial cell migration and capillary formation. J Biol Chem 282(11):7758-7769.

Lassegue B, and Clempus RE. 2003. Vascular NAD(P)H oxidases: specific features, expression, and regulation. Am J Physiol Regul Integr Comp Physiol 285(2):R277-297.

Lassegue B, San Martin A, and Griendling KK. 2012. Biochemistry, physiology, and pathophysiology of NADPH oxidases in the cardiovascular system. Circ Res 110(10):1364-1390.

Lauffenburger DA, and Horwitz AF. 1996. Cell migration: a physically integrated molecular process. Cell 84(3):359-369.

Lee TK, Poon RT, Yuen AP, Man K, Yang ZF, Guan XY, and Fan ST. 2006. Rac activation is associated with hepatocellular carcinoma metastasis by up-regulation of vascular endothelial growth factor expression. Clin Cancer Res 12(17):5082-5089.

Leite de Oliveira R, Hamm A, and Mazzone M. 2011. Growing tumor vessels: more than one way to skin a cat - implications for angiogenesis targeted cancer therapies. Mol Aspects Med 32(2):71-87.

Leung DW, Cachianes G, Kuang WJ, Goeddel DV, and Ferrara N. 1989. Vascular endothelial growth factor is a secreted angiogenic mitogen. Science 246(4935):1306-1309.

Li SM, Zeng LW, Feng L, and Chen DB. 2010. Rac1-dependent intracellular superoxide formation mediates vascular endothelial growth factor-induced placental angiogenesis in vitro. Endocrinology 151(11):5315-5325.

Liu Y, Shreder KR, Gai W, Corral S, Ferris DK, and Rosenblum JS. 2005. Wortmannin, a widely used phosphoinositide 3-kinase inhibitor, also potently inhibits mammalian polo-like kinase. Chemistry & biology 12(1):99-107.

Madamanchi NR, Vendrov A, and Runge MS. 2005. Oxidative stress and vascular disease. Arterioscler Thromb Vasc Biol 25(1):29-38.

Madeddu P, Kraenkel N, Barcelos LS, Siragusa M, Campagnolo P, Oikawa A, Caporali A, Herman A, Azzolino O, Barberis L et al. . 2008. Phosphoinositide 3-kinase gamma gene knockout impairs postischemic neovascularization and endothelial progenitor cell functions. Arterioscler Thromb Vasc Biol 28(1):68-76.

Manjila SB, Baby JN, Bijin EN, Constantine I, Pramod K, and Valsalakumari J. 2013. Novel gene delivery systems. Int J Pharm Investig 3(1):1-7.

Marone R, Cmiljanovic V, Giese B, and Wymann MP. 2008. Targeting phosphoinositide 3-kinase: moving towards therapy. Biochim Biophys Acta 1784(1):159-185.

Maulik N. 2002. Redox regulation of vascular angiogenesis. Antioxid Redox Signal 4(5):783-784.

McAuslan BR, and Gole GA. 1980. Cellular and molecular mechanisms in angiogenesis. Trans Ophthalmol Soc U K 100(3):354-358.

Michell BJ, Griffiths JE, Mitchelhill KI, Rodriguez-Crespo I, Tiganis T, Bozinovski S, de Montellano PR, Kemp BE, and Pearson RB. 1999. The Akt kinase signals directly to endothelial nitric oxide synthase. Curr Biol 9(15):845-848.

Millauer B, Wizigmann-Voos S, Schnurch H, Martinez R, Moller NP, Risau W, and Ullrich A. 1993. High affinity VEGF binding and developmental expression suggest Flk-1 as a major regulator of vasculogenesis and angiogenesis. Cell 72(6):835-846.

Milosevic N, Bekhite MM, Sharifpanah F, Ruhe C, Wartenberg M, and Sauer H. 2010. Redox stimulation of cardiomyogenesis versus inhibition of vasculogenesis upon treatment of mouse embryonic stem cells with thalidomide. Antioxid Redox Signal 13(12):1813-1827.

Miyano K, Ueno N, Takeya R, and Sumimoto H. 2006. Direct involvement of the small GTPase Rac in activation of the superoxide-producing NADPH oxidase Nox1. J Biol Chem 281(31):21857-21868.

Morales-Ruiz M, Lee MJ, Zollner S, Gratton JP, Scotland R, Shiojima I, Walsh K, Hla T, and Sessa WC. 2001. Sphingosine 1-phosphate activates Akt, nitric oxide production, and chemotaxis through a Gi protein/phosphoinositide 3-kinase pathway in endothelial cells. J Biol Chem 276(22):19672-19677.

Morello F, Perino A, and Hirsch E. 2009. Phosphoinositide 3-kinase signalling in the vascular system. Cardiovasc Res 82(2):261-271.

Mueller-Klieser W. 1997. Three-dimensional cell cultures: from molecular mechanisms to clinical applications. Am J Physiol 273(4 Pt 1):C1109-1123.

Muramatsu F, Kidoya H, Naito H, Sakimoto S, and Takakura N. 2013. microRNA-125b inhibits tube formation of blood vessels through translational suppression of VE-cadherin. Oncogene 32(4):414-421.

Nakagami H, Morishita R, Yamamoto K, Taniyama Y, Aoki M, Matsumoto K, Nakamura T, Kaneda Y, Horiuchi M, and Ogihara T. 2001. Mitogenic and antiapoptotic actions of hepatocyte growth factor through ERK, STAT3, and AKT in endothelial cells. Hypertension 37(2 Pt 2):581-586.

Nakanishi A, Wada Y, Kitagishi Y, and Matsuda S. 2014. Link between PI3K/AKT/PTEN Pathway and NOX Proteinin Diseases. Aging Dis 5(3):203-211.

Naldini L, Blomer U, Gage FH, Trono D, and Verma IM. 1996. Efficient transfer, integration, and sustained long-term expression of the transgene in adult rat brains injected with a lentiviral vector. Proc Natl Acad Sci U S A 93(21):11382-11388.

Neufeld G, Cohen T, Gengrinovitch S, and Poltorak Z. 1999. Vascular endothelial growth factor (VEGF) and its receptors. Faseb J 13(1):9-22.

Nichols J, Evans EP, and Smith AG. 1990. Establishment of germ-line-competent embryonic stem (ES) cells using differentiation inhibiting activity. Development 110(4):1341-1348.

Nicolson GL. 1988a. Cancer metastasis: tumor cell and host organ properties important in metastasis to specific secondary sites. Biochim Biophys Acta 948(2):175-224.

Nicolson GL. 1988b. Organ specificity of tumor metastasis: role of preferential adhesion, invasion and growth of malignant cells at specific secondary sites. Cancer Metastasis Rev 7(2):143-188.

Okkenhaug K, Bilancio A, Farjot G, Priddle H, Sancho S, Peskett E, Pearce W, Meek SE, Salpekar A, Waterfield MD et al. . 2002. Impaired B and T cell antigen receptor signaling in p110delta PI 3-kinase mutant mice. Science (New York, NY 297(5583):1031-1034.

Opitz N, Drummond GR, Selemidis S, Meurer S, and Schmidt HH. 2007. The 'A's and 'O's of NADPH oxidase regulation: a commentary on "Subcellular localization and function of alternatively spliced Noxo1 isoforms". Free Radic Biol Med 42(2):175-179.

Oshikawa J, Kim SJ, Furuta E, Caliceti C, Chen GF, McKinney RD, Kuhr F, Levitan I, Fukai T, and Ushio-Fukai M. 2012. Novel role of p66Shc in ROS-dependent VEGF signaling and angiogenesis in endothelial cells. Am J Physiol Heart Circ Physiol 302(3):H724-732.

Papapetropoulos A, Fulton D, Mahboubi K, Kalb RG, O'Connor DS, Li F, Altieri DC, and Sessa WC. 2000. Angiopoietin-1 inhibits endothelial cell apoptosis via the Akt/survivin pathway. J Biol Chem 275(13):9102-9105.

Pardanaud L, and Dieterlen-Lievre F. 1999. Manipulation of the angiopoietic/hemangiopoietic commitment in the avian embryo. Development 126(4):617-627.

Patan S. 2000. Vasculogenesis and angiogenesis as mechanisms of vascular network formation, growth and remodeling. J Neurooncol 50(1-2):1-15.

Pimentel RC, Yamada KA, Kleber AG, and Saffitz JE. 2002. Autocrine regulation of myocyte Cx43 expression by VEGF. Circ Res 90(6):671-677.

Qiang YW, Kopantzev E, and Rudikoff S. 2002. Insulinlike growth factor-I signaling in multiple myeloma: downstream elements, functional correlates, and pathway cross-talk. Blood 99(11):4138-4146.

Rathjen PD, Lake J, Whyatt LM, Bettess MD, and Rathjen J. 1998. Properties and uses of embryonic stem cells: prospects for application to human biology and gene therapy. Reprod Fertil Dev 10(1):31-47.

Ratner M. 2004. Genentech discloses safety concerns over Avastin. Nat Biotechnol 22(10):1198.

Redick SD, and Bautch VL. 1999. Developmental platelet endothelial cell adhesion molecule expression suggests multiple roles for a vascular adhesion molecule. Am J Pathol 154(4):1137-1147.

Ribatti D. 2006. Genetic and epigenetic mechanisms in the early development of the vascular system. J Anat 208(2):139-152.

Risau W. 1995. Differentiation of endothelium. Faseb J 9(10):926-933.

Risau W. 1997. Mechanisms of angiogenesis. Nature 386(6626):671-674.

Robertson M, Chambers I, Rathjen P, Nichols J, and Smith A. 1993. Expression of alternative forms of differentiation inhibiting activity (DIA/LIF) during murine embryogenesis and in neonatal and adult tissues. Dev Genet 14(3):165-173.

Roskoski R, Jr. 2007. Vascular endothelial growth factor (VEGF) signaling in tumor progression. Crit Rev Oncol Hematol 62(3):179-213.

Sauer H, Bekhite MM, Hescheler J, and Wartenberg M. 2005. Redox control of angiogenic factors and CD31-positive vessel-like structures in mouse embryonic stem cells after direct current electrical field stimulation. Exp Cell Res 304(2):380-390.

Sauer H, and Wartenberg M. 2005. Reactive oxygen species as signaling molecules in cardiovascular differentiation of embryonic stem cells and tumor-induced angiogenesis. Antioxid Redox Signal 7(11-12):1423-1434.

Schambach A, Galla M, Modlich U, Will E, Chandra S, Reeves L, Colbert M, Williams DA, von Kalle C, and Baum C. 2006. Lentiviral vectors pseudotyped with murine ecotropic envelope: increased biosafety and convenience in preclinical research. Exp Hematol 34(5):588-592.

Seshiah PN, Weber DS, Rocic P, Valppu L, Taniyama Y, and Griendling KK. 2002. Angiotensin II stimulation of NAD(P)H oxidase activity: upstream mediators. Circ Res 91(5):406-413.

Shiojima I, and Walsh K. 2006. Regulation of cardiac growth and coronary angiogenesis by the Akt/PKB signaling pathway. Genes & development 20(24):3347-3365.

Soga N, Connolly JO, Chellaiah M, Kawamura J, and Hruska KA. 2001. Rac regulates vascular endothelial growth factor stimulated motility. Cell Commun Adhes 8(1):1-13.

Sounni NE, and Noel A. 2013. Targeting the tumor microenvironment for cancer therapy. Clin Chem 59(1):85-93.

Steelman LS, Chappell WH, Abrams SL, Kempf RC, Long J, Laidler P, Mijatovic S, Maksimovic-Ivanic D, Stivala F, Mazzarino MC et al. . 2011. Roles of the Raf/MEK/ERK and PI3K/PTEN/Akt/mTOR pathways in controlling growth and sensitivity to therapy-implications for cancer and aging. Aging (Albany NY) 3(3):192-222.

Stephens L, Smrcka A, Cooke FT, Jackson TR, Sternweis PC, and Hawkins PT. 1994. A novel phosphoinositide 3 kinase activity in myeloid-derived cells is activated by G protein beta gamma subunits. Cell 77(1):83-93.

Stephens LR, Hughes KT, and Irvine RF. 1991. Pathway of phosphatidylinositol(3,4,5)-trisphosphate synthesis in activated neutrophils. Nature 351(6321):33-39.

Stewart SA, Dykxhoorn DM, Palliser D, Mizuno H, Yu EY, An DS, Sabatini DM, Chen IS, Hahn WC, Sharp PA et al. . 2003. Lentivirus-delivered stable gene silencing by RNAi in primary cells. Rna 9(4):493-501.

Stone KR, Mickey DD, Wunderli H, Mickey GH, and Paulson DF. 1978. Isolation of a human prostate carcinoma cell line (DU 145). Int J Cancer 21(3):274-281.

Sui L, Wang J, and Li BM. 2008. Role of the phosphoinositide 3-kinase-Akt-mammalian target of the rapamycin signaling pathway in long-term potentiation and trace fear conditioning memory in rat medial prefrontal cortex. Learn Mem 15(10):762-776.

Sundaresan M, Yu ZX, Ferrans VJ, Sulciner DJ, Gutkind JS, Irani K, Goldschmidt-Clermont PJ, and Finkel T. 1996. Regulation of reactive-oxygen-species generation in fibroblasts by Rac1. Biochem J 318 (Pt 2):379-382.

Tammela T, Zarkada G, Wallgard E, Murtomaki A, Suchting S, Wirzenius M, Waltari M, Hellstrom M, Schomber T, Peltonen R et al. . 2008. Blocking VEGFR-3 suppresses angiogenic sprouting and vascular network formation. Nature 454(7204):656-660.

Tobar N, Caceres M, Santibanez JF, Smith PC, and Martinez J. 2008. RAC1 activity and intracellular ROS modulate the migratory potential of MCF-7 cells through a NADPH oxidase and NFkappaB-dependent mechanism. Cancer Lett 267(1):125-132.

Touyz RM, Chen X, Tabet F, Yao G, He G, Quinn MT, Pagano PJ, and Schiffrin EL. 2002. Expression of a functionally active gp91phox-containing neutrophil-type NAD(P)H oxidase in smooth muscle cells from human resistance arteries: regulation by angiotensin II. Circ Res 90(11):1205-1213.

Ushio-Fukai M. 2006. Redox signaling in angiogenesis: role of NADPH oxidase. Cardiovasc Res 71(2):226-235.

Ushio-Fukai M. 2007. VEGF signaling through NADPH oxidase-derived ROS. Antioxid Redox Signal 9(6):731-739.

Ushio-Fukai M, Tang Y, Fukai T, Dikalov SI, Ma Y, Fujimoto M, Quinn MT, Pagano PJ, Johnson C, and Alexander RW. 2002. Novel role of gp91(phox)-containing NAD(P)H oxidase in vascular endothelial growth factor-induced signaling and angiogenesis. Circ Res 91(12):1160-1167.

Ushio-Fukai M, and Urao N. 2009. Novel role of NADPH oxidase in angiogenesis and stem/progenitor cell function. Antioxid Redox Signal 11(10):2517-2533.

van Nieuw Amerongen GP, Koolwijk P, Versteilen A, and van Hinsbergh VW. 2003. Involvement of RhoA/Rho kinase signaling in VEGF-induced endothelial cell migration and angiogenesis in vitro. Arterioscler Thromb Vasc Biol 23(2):211-217.

Vanhaesebroeck B, Leevers SJ, Panayotou G, and Waterfield MD. 1997. Phosphoinositide 3-kinases: a conserved family of signal transducers. Trends in biochemical sciences 22(7):267-272.

Verheul HM, and Pinedo HM. 2007. Possible molecular mechanisms involved in the toxicity of angiogenesis inhibition. Nat Rev Cancer 7(6):475-485.

Violi F, Cangemi R, and Brunelli A. 2005. Oxidative stress, antioxidants, and cardiovascular disease. Arterioscler Thromb Vasc Biol 25(4):e37; author reply e37.

Vittet D, Prandini MH, Berthier R, Schweitzer A, Martin-Sisteron H, Uzan G, and Dejana E. 1996. Embryonic stem cells differentiate in vitro to endothelial cells through successive maturation steps. Blood 88(9):3424-3431.

Vlahos CJ, Matter WF, Hui KY, and Brown RF. 1994. A specific inhibitor of phosphatidylinositol 3-kinase, 2-(4-morpholinyl)-8-phenyl-4H-1-benzopyran-4-one (LY294002). The Journal of biological chemistry 269(7):5241-5248.

Wartenberg M, Budde P, De Marees M, Grunheck F, Tsang SY, Huang Y, Chen ZY, Hescheler J, and Sauer H. 2003. Inhibition of tumor-induced angiogenesis and matrix-metalloproteinase expression in confrontation cultures of embryoid bodies and tumor spheroids by plant ingredients used in traditional chinese medicine. Lab Invest 83(1):87-98.

Wartenberg M, Donmez F, Ling FC, Acker H, Hescheler J, and Sauer H. 2001. Tumor-induced angiogenesis studied in confrontation cultures of multicellular tumor spheroids and embryoid bodies grown from pluripotent embryonic stem cells. Faseb J 15(6):995-1005.

Wartenberg M, Gunther J, Hescheler J, and Sauer H. 1998a. The embryoid body as a novel in vitro assay system for antiangiogenic agents. Lab Invest 78(10):1301-1314.

Wartenberg M, Hescheler J, Acker H, Diedershagen H, and Sauer H. 1998b. Doxorubicin distribution in multicellular prostate cancer spheroids evaluated by confocal laser scanning microscopy and the "optical probe technique". Cytometry 31(2):137-145.

Weidner N, Semple JP, Welch WR, and Folkman J. 1991. Tumor angiogenesis and metastasis--correlation in invasive breast carcinoma. N Engl J Med 324(1):1-8.

Weinstat-Saslow D, and Steeg PS. 1994. Angiogenesis and colonization in the tumor metastatic process: basic and applied advances. Faseb J 8(6):401-407.

Welti J, Loges S, Dimmeler S, and Carmeliet P. 2013. Recent molecular discoveries in angiogenesis and antiangiogenic therapies in cancer. J Clin Invest 123(8):3190-3200.

Whitman M, Downes CP, Keeler M, Keller T, and Cantley L. 1988. Type I phosphatidylinositol kinase makes a novel inositol phospholipid, phosphatidylinositol-3-phosphate. Nature 332(6165):644-646.

Williams MR, Arthur JS, Balendran A, van der Kaay J, Poli V, Cohen P, and Alessi DR. 2000. The role of 3-phosphoinositide-dependent protein kinase 1 in activating AGC kinases defined in embryonic stem cells. Curr Biol 10(8):439-448.

Wobus AM, and Boheler KR. 2005. Embryonic stem cells: prospects for developmental biology and cell therapy. Physiol Rev 85(2):635-678.

Wymann MP, Bulgarelli-Leva G, Zvelebil MJ, Pirola L, Vanhaesebroeck B, Waterfield MD, and Panayotou G. 1996. Wortmannin inactivates phosphoinositide 3-kinase by covalent modification of Lys-802, a residue involved in the phosphate transfer reaction. Molecular and cellular biology 16(4):1722-1733.

Wymann MP, Zvelebil M, and Laffargue M. 2003. Phosphoinositide 3-kinase signalling--which way to target? Trends Pharmacol Sci 24(7):366-376.

Xia P, Aiello LP, Ishii H, Jiang ZY, Park DJ, Robinson GS, Takagi H, Newsome WP, Jirousek MR, and King GL. 1996. Characterization of vascular endothelial growth factor's effect on the activation of protein kinase C, its isoforms, and endothelial cell growth. J Clin Invest 98(9):2018-2026.

Xu FH, Xiong D, Xu YF, Cao SM, Xue WQ, Qin HD, Liu WS, Cao JY, Zhang Y, Feng QS et al. . 2012. An epidemiological and molecular study of the relationship between smoking, risk of nasopharyngeal carcinoma, and Epstein-Barr virus activation. J Natl Cancer Inst 104(18):1396-1410.

Xu J, Tian W, Ma X, Guo J, Shi Q, Jin Y, Xi J, and Xu Z. 2011. The molecular mechanism underlying morphine-induced Akt activation: roles of protein phosphatases and reactive oxygen species. Cell Biochem Biophys 61(2):303-311.

Yamaoka-Tojo M, Ushio-Fukai M, Hilenski L, Dikalov SI, Chen YE, Tojo T, Fukai T, Fujimoto M, Patrushev NA, Wang N et al. . 2004. IQGAP1, a novel vascular endothelial growth factor receptor binding protein, is involved in reactive oxygen species--dependent endothelial migration and proliferation. Circ Res 95(3):276-283.

Yamashita J, Itoh H, Hirashima M, Ogawa M, Nishikawa S, Yurugi T, Naito M, and Nakao K. 2000. Flk1-positive cells derived from embryonic stem cells serve as vascular progenitors. Nature 408(6808):92-96.

Yuan TL, Choi HS, Matsui A, Benes C, Lifshits E, Luo J, Frangioni JV, and Cantley LC. 2008. Class 1A PI3K regulates vessel integrity during development and tumorigenesis. Proc Natl Acad Sci U S A 105(28):9739-9744.

Zetter BR. 1998. Angiogenesis and tumor metastasis. Annu Rev Med 49:407-424.

Zhang LJ, Tao BB, Wang MJ, Jin HM, and Zhu YC. 2012. PI3K p110alpha isoform-dependent Rho GTPase Rac1 activation mediates H2S-promoted endothelial cell migration via actin cytoskeleton reorganization. PLoS One 7(9):e44590.

Zufferey R, Dull T, Mandel RJ, Bukovsky A, Quiroz D, Naldini L, and Trono D. 1998. Self-inactivating lentivirus vector for safe and efficient in vivo gene delivery. J Virol 72(12):9873-9880.

Zufferey R, Nagy D, Mandel RJ, Naldini L, and Trono D. 1997. Multiply attenuated lentiviral vector achieves efficient gene delivery in vivo. Nat Biotechnol 15(9):871-875.

7. APPENDIX

7.1 List of own publications

7.1.1 Articles in journals

1. El-Sourbagy I K, Abo-Zaid F A, **Bakhite M M.** (**2000**): *Effect of anticoagulant coumadin on certain physiological and haematological parameters in albino mice*. **Proc. I.C.S.** 1(2): 45-52.
2. Wartenberg M, Gronczynska S, **Bekhite M M,** Saric T, Hescheler J, Sauer H. **(2004)**: *Regulation of the multidrug resistance transporter P-glycoprotein in multicellular prostate tumour spheroids by hyperthermia and reactive oxygen species*. **Int J Cancer**. 113(2): 229-240. (impact factor, **5.444**)
3. Sauer H, **Bekhite M M,** Hescheler J, Wartenberg M. **(2005)**: *Redox control of angiogenic factors and CD31-positive vessel-like structures in mouse embryonic stem cells after direct current electrical field stimulation.* **Exp Cell Res.** 304, 380-90. (impact factor, **3.580**)
4. Feldhahan N, Klein F, Mooster J L, Hadweh P, Sprangers M, Wernet P, **Bekhite M M**, Wartenberg M, Hofmann W K, Herzog S, Jumaa H, Müschen M. **(2005)**: *Uncoupling BTK from the pre-Bcell receptor: a mechanism for leukemic transformation of human pre-Bcells by BCR-ABL1*. **J Exp Med**. 201(11):1837-52. (impact factor**, 13.853**)
5. Abou-Zaid F A, Sauer H, EL-Shourbagy I K, Omar Kh M, **Bekhite M M. (2005)**: *Differentiation of embryonic stem cells towards the chondrogenic and osteogenic linage can be enhanced by magnetic field.* **Egypt J Exp Biol. (Zool.)**. 1: 187-194. http://www.egyseb.org
6. Ten Freyhaus H, Huntgeburth M, Wingler K., Schnitker J, Bäumer A T, Vantler M, **Bekhite M M,** Wartenberg M, Sauer H, Rosenkranz, S. **(2006)**: *Novel Nox inhibitor VAS2870 attenuates PDGF-dependent smooth muscle cell chemotaxis, but not proliferation*. **Cardiovasc Res.** 71, 331-41. (impact factor, **6.064**)
7. Abou-Zaid F A, Omar KM, Salem E I, Alm-Eldeen A A, **Bekhite M M. (2006)**: *Can man-made visible light radiation affect the reproductive capacity of male mice?* **Egypt J Exp Biol (Zool.)**. 2: 81-89.
8. **Mohamed M Bekhite. (2007)**: *Effect of 10 mT magnetic fields exposure on testicular germ cells, the role of VEGF, and the amelorative effect of vitamin C supplement*. **Egypt J Exp Biol (Zool.)**. 3: 271-281.
9. **Bekhite M M,** Finkensieper A, Abou–Zaid F A, EL-Shourbagy I K, Omar Kh M, Figulla HR, Sauer H, Wartenberg M. **(2010)**: *Static Electromagnetic Fields Induce Vasculogenesis And Chondroosteogenesis Of Mouse Embryonic Stem Cells By Reactive Oxygen Species-Mediated Upregulation Of Vascular Endothelial Growth Factor*. **Stem Cells Dev**. 19:731-743. (impact factor, **4.459**)
10. Finkensieper A, Kieser S, **Bekhite M M,** Richter M, Mueller J P, Graebner R, Figulla HR, Sauer H, Wartenberg M. **(2010)**: *The 5-lipoxygenase pathway regulates vasculogenesis in differentiating mouse embryonic stem cells.* **Cardiovasc Res**. 86, 37-44. (impact factor, **6.064**)
11. Wartenberg M, Richter M, Datchev A, Günther S, Milosevic N, **Bekhite M M**, Figulla HR, Aran J M, Pétriz J, Sauer H. **(2010):** *Glycolytic pyruvate regulates P-glycoprotein expression in multicellular tumour spheroids via modulation of the intracellular redox state*. **J Cell Biochem.** 109: 434-446. (impact factor, **2.686**)

12. **Mohamed M Bekhite**. **(2010)**: The role of Ca^{2+} during early stage of heart development: an *in vitro* model utilizing mouse embryonic stem cell. **Egypt J Exp Biol (Zool.)**. 6(2): 285-296.

13. Milosevic N, **Bekhite M M**, Sharifpanah F, Ruhe C, Wartenberg M, Sauer, H. **(2010):** Redox Stimulation of Cardiomyogenesis Versus Inhibition of Vasculogenesis Upon Treatment of Mouse Embryonic Stem Cells with Thalidomid. **Antioxid Redox Signal**. 13(12): 1813-1827. (impact factor, **8.456**)

14. **Bekhite M M,** Finkensieper A, Binas S, Müller J, Wetzker R, Figulla HR, Sauer H, Wartenberg M. (2011): *VEGF-mediated PI3K class IA and PKC signaling in cardiomyogenesis and vasculogenesis of mouse embryonic stem cells.* **Journal of cell science. 124** (11). 1819-30. (impact factor, **6.111**)

15. Bartsch C, **Bekhite M M,** Ruhe C, Wissuwa B, Marciniak A, Müller J, Heller R, Figulla HR, Sauer H, Wartenberg M. **(2011):** *NADPH-oxidase and eNOS controling cardiomyogenesis of mouse embryonic stem cells upon ascorbic acid treatment.* **Submitted** to the **Free Radical Biology & Medicine**. 51(2): 432-443. (impact factor, **5.423**)

16. **Bekhite M M,** Figulla HR, Sauer H, Wartenberg M. **(2013):** Static magnetic fields increase cardiomyocyte differentiation of Flk-1^{+} cells derived from mouse embryonic stem cells via Ca(2+) influx and ROS production. **Int J Cardiol**. 10;167(3):798-808. (impact factor, **4.125**)

17. Finkensieper A, **Bekhite M M,** Fischer H, Nitza S, Figulla HR, Sauer H, Wartenberg M. **(2013)**: *Antibacterial Capacity of Differentiated Mice Embryonic Stem Cells During Defined in vitro Inflammatory Conditions"*; **Stem Cells Dev.** 15;22(14):1977-90. (impact factor, **4.670**)

18. **Bekhite** MM, Finkensieper A, Rebhan J, Huse S, Schultze-Mosgau S, **Figulla HR,** Sauer H, Wartenberg M. **(2014):** *Hypoxia, leptin, and vascular endothelial growth factor stimulate vascular endothelial cell differentiation of human adipose tissue-derived stem cells.* **Stem Cells Dev.** 15;23(4):333-51. (impact factor, **4.670**)

19. Falk J, Rohde M, **Bekhite MM,** Sophie Neugebauer, Hemmerich P, Kiehntopf M, Deufel T, Hübner CA, Beetz C. **(2014):** *Functional Mutation Analysis Provides Evidence for a Role of REEP1 in Lipid Droplet Biology*. **Hum Mutat.** 35(4):497-504. (impact factor, **5.213**)

20. Sharifpanah F, Saliu F, **Bekhite MM,** Wartenberg M, Sauer H. **(2014):** *β-adrenergic receptor antagonists inhibit vasculogenesis of embryonic stem cells by downregulation of nitric oxide generation and interference with VEGF signalling.* **Cell Tissue Res.** Aug 19. [Epub ahead of print] (impact factor, **3.33**)

21. **Bekhite M M,** Finkensieper A, Abou–Zaid F A, EL-Shourbagy I K, Omar Kh M, Figulla HR, Sauer H, Wartenberg, M. **(2014):** *Effects of static and 50 Hz magnetic fields on mouse embryonic development and vasculogenesis of embryonic stem cells.* **Journal of Applied Toxicology** (2nd revision) (impact factor, **2.597**)

22. **Bekhite M M,** Müller J, Figulla HR, Sauer H, Wartenberg M. **(2013):** *Class IA PI3Kα and NOX1 regulate vascular differentiation induced by VEGF in mouse embryonic stem cells*. **Stem Cells International** (under review) (impact factor, **2.809**)

7.2.2 Published contributions to academic conferences (abstracts)

1. Sauer, H., **Bekhite, M. M.**, Rahimi, G., Hescheler, J. and Wartenberg, M. **(2003)**: *Effects of DC electrical fields on vasculogenesis and cardiomyogenesis of embryonic stem cells.* **European Journal of Physiology**, Vol.445, Suppl.1 p: 22**.**
2. **Bekhite, M. M.**, Abou – Zaid, F., EL-Shourbagy, I., Omer, Kh., Hescheler, J., Wartenberg, M. and Sauer, H. **(2004)**: *Effects of magnetic field on embryonic development of BALBIc Mouse*. **European Journal of Physiology**, Vol.447, Suppl.1 p: 154.
3. Wartenberg, M., Gronczynska, S., **Bekhite, M.M.**, Saric, T., Hescheler, J. and Sauer, H. **(2004)**: *Regulation of P-glycoprotein in prostate tumor spheroids by hyperthermia and reactive oxygen species***. European Journal of Physiology**, Vol.447, Suppl.1 p: 40.
4. Finkensieper, A., Schwindt, H., **Bekhite, M. M.**, Gruenheck, F., Hescheler, J., Sauer, H. and Wartenberg, M. **(2005)**: *Leukotriene Receptor mRNA Expression in the Mouse Embryonic Stem Cell Line*. **European Journal of Physiology**, Vol.449, Suppl.1 p: 121,
5. Sauer, H., **Bekhite, M. M.**, Hescheler, J. and Wartenberg, M**. (2005)**: *Redox-control of angiogenic factors and capillary sprouting in mouse embryonic stem cells after direct current electrical field stimulation.* **European Journal of Physiology**, Vol.449, Suppl.1 p: 69,
6. Sauer, H., **Bekhite, M. M.**, Wartenberg, M., Abou-Zaid, F., ELShourbagy, I, Omer, KH. and Hescheler, J. **(2005)**: *Differentiation of ES cells towards the chondrogenic and osteogenic lineage can be enhanced by magnetic fields*. **European Journal of Physiology**, Vol.449, Suppl.1 p: 122,
7. Ten Freyhaus, H., Huntgeburth, M., Wingler, K., Schnitker, J., Bäumer, A T., Vantler, M., **Bekhite, M. M.,** Wartenberg, M., Sauer, H., Rosenkranz, S. **(2006)**: *Inhibation of ROS liberatiom attenuates PDGF-dependent chemotaxis, but not proliferation vascular smooth muscle cell- critical role of Src Kinase.* Vol. 114, Issue 18 Supplement; Scientific Sessions 2006. Chicago. **USA**
8. **Bekhite, M. M.,** Sauer, H., Abou-Zaid, F A., EL-Shourbagy, I K., Omar, Kh. M., Figulla, H R. and Wartenberg, M. **(2008)**: *The Role of Ros In The Chondro-Osteogenic Differentiation From Embryonic Stem Cells Under The Magnetic Field Exposure***. Acta Physiologica**, Vol.192, Suppl.663 p: 160,
9. **Bekhite, M. M.,** Finkensieper, A., Sauer, H., Figulla, HR and Wartenberg, M. **(2009)**: *Phosphoinositide 3-kinases (PI3Ks) and Protein Kinase C (PKC) Control Early Steps of Cardiovascular Differentiation of Mouse Embryonic Stem Cells*. **Acta Physiologica**, Vol.195, Suppl. 669, p: 74.
10. Kieser S, Finkensieper, A., **Bekhite M M.**, Hannig, M., Sauer, H., Figulla, H. R. and Wartenberg, M. **(2009)**: *Characterisation of the 5-Lipoxygenase pathway and Leukotriene Receptors in Differentiating Mouse Embryonic Stem Cell Derived Embryoid Bodies*. **Acta Physiologica**, Vol.195, Suppl.669 p: 45.
11. Wartenberg, M., Richter, M., Datchev, A., Günther, S., Milosevic, N., **Bekhite, M.M.**, Figulla, HR., Aran, J., Pétriz, J. and Sauer, H. **(2010)**: *Glycolytic pyruvate regulates P-glycoprotein expression in multicellular tumour spheroids via modulation of the intracellular redox state.* **Acta Physiologica**; Vol. 198, Suppl. 677.
12. **Bekhite M.**, Finkensieper A., Binas S., Figulla H.-R., Sauer H. and Wartenberg M. **(2011):** *PI3K and PKC regulate cardiac and vascular differentiation of Flk-1+ cells derived from mouse embryonic stem cells upon VEGF treatment.* **Acta Physiologica**; Vol. 201, Suppl. 682, p: 185.
13. **Bekhite El Saied M.**, Bienas S., Finkensieper A., Figulla H.-R., Sauer H. and Wartenberg M. **(2012):** *Differentiation of $CD45^+$, $CD31^+$ and alpha $actinin^+$ cells from $Flk\text{-}1^+$*

and Flk-1$^-$ cell subpopulations derived from murine embryonic stem cells. **Acta Physiologica**; Vol. 204, Suppl. 689, p: 204.

14. Bekhite M.M., Finkensieper A., Figulla H.-R., Sauer H. and Wartenberg M. **(2012):** *Enhanced Cardiomyocyte Differentiation of Flk-1$^+$ Cells Derived from Mouse Embryonic Stem Cells by Application of Static Magnetic Fields.* **Acta Physiologica**; Vol. 204, Suppl. 689, p: 201.

15. Mohner D., Latz S., **Bekhite M.**, Kleger A., Figulla H.-R., Sauer H. and Wartenberg M. **(2012):** *Characterization the Influence of Zoxazolamine on Cardiomyocyte Differentiation of Embryonic Stem Cells*. **Acta Physiologica**; Vol. 204, Suppl. 689, p: 202.

16. Finkensieper A., **Bekhite M. M.,** Figulla H.-R., Sauer H. and Wartenberg M. **(2012):** *Antibacterial Capacity of Differentiated Embryoid Bodies Derived from Murine Embryonic Stem Cells During Defined in vitro Inflammatory Conditions.* **Acta Physiologica**; Vol. 204, Suppl. 689, p: 201.

17. Fischer, H., Finkensieper, A., **Bekhite, M. M.,** Nitza, S., Figulla, H.R., Sauer, H., Wartenberg M. **(2013):** *Potential signaling pathway activating matrix metalloproteinase isoforms during septic myocardial dysfunction.* **Acta Physiologica**; Vol. 207, Suppl. 694, p: 213-214

18. Bekhite, EL Saied M. M., Finkensieper, A., Rebhan, J., Huse, S., Figulla, HR., Sauer, H. and Wartenberg, M. **(2013):** *Human adipose–derived stems cells as an attractive cell source for endothelial cells by culturing the cells in hypoxic conditions in combination with leptin and VEGF*. **Acta Physiologica**; Vol. 207, Suppl. 694, p: 159

19. Danzer, C., **Bekhite, EL Saied M. M.,** Finkensieper, A., pörner, T., Figulla, HR., Sauer, H. and Wartenberg, M. **(2013):** *PPAR-gamma controls the cardiovascular differentiation in embryonic stem cells in vitro.* **Acta Physiologica**; Vol. 207, Suppl. 694, p: 159

Jena, 01. 10. 2014

Mohamed M. Bekhite ELsaied

7.2 Curriculum Vitae

Biographical

Name:	**Mohamed Mohamed Bekhite ELsaied**
Date of birth:	04/10/1970
Nationality:	Egyptian
Marital Status:	Married with two children
Address:	Molecular Cardiology and Stem Cells, University Heart Center, Clinic of Internal Medicine I, University Hospital Jena, Germany Erlanger Allee 101 07743 Jena Tel.: 03641-9325813
e-mail:	mbekhite@yahoo.com Mohamed.el_Saied@med.uni-jena.de
Private address:	Felix Auerbach str. 4, 07747 Jena, Germany Tel.: 03641 771340

Education and academic qualifications

1986-1989	**Secondary School,** ALraml school**,** Alexandria, **Egypt**.
1989-1993	**B.Sc. Zoology,** (*very good with Honours*) Tanta University, **Egypt**.
1994-1998	**Master of Science** [**M.Sc**] **(experimental embryology)** Tanta University. **Egypt**. **Title of M.Sc. Thesis**: *Experimental and physiological studies on the effect of an anticoagulant Drug "Warfarin" on the development of mice.*
1999-2005	**Ph.D of Science**: Experimental Embryology, Tanta University. **Egypt** **Title of Ph.D. Thesis**: *The induced magnetic field effects on the embryonic development of mice.*

Academic positions

1993-1998	**Demonstrator** in Zoology Department, Faculty of Science, Tanta Univ. **Egypt**.
1998-2002	**Assistant Lecturer** in Zoology Department, Faculty of Science, Tanta Univ. **Egypt**.
2003-2004	**Visiting researcher** in Institute for Neurophysiology, Köln Univ. **Germany**.
2004-2006	**Lecturer** in Zoology Department, Faculty of Science, Tanta Univ. **Egypt**
9/2006-2007	**Lecturer** in Faculty of Arts and Sciences, Al-Mergeb Univ**. Libya**.
2008-2014	**Research scientist** in Clinic of Internal Medicine, Division of Molecular Cardiology and Stem Cells, Friedrich Schiller Univ. Jena, **Germany**.

Award

2012	**The 1st poster prize of *Deutsche Physiologische Gesellschaft, the*** 91th Annual Meeting of the German Physiological Society in Dresden, 2012, **Germany**

Memberships

Egyptian Society of Experimental Biology
Egyptian Society of Zoology
Egyptian German Society of Zoology

Reviwing activities

. Antioxid Redox Signal.
. Cardiovasc Res.
. Egypt J Exp Biol.
. Stem Cells Dev.

Contributions in the international conferences

83th Annual Meeting of the German Physiological Society in Leipzig, 2004, **Germany. (Poster Presentation)**
1st Egyptian Society of Experimental Biology Congress in Kaffer El-Sheikh, 2005, **Egypt. (Oral Presentation)**
2nd Egyptian Society of Experimental Biology Congress in Alexandria, 2006, **Egypt. (Oral Presentation)**
3rd Egyptian Society of Experimental Biology Congress in Minoufiya, 2007, Egypt. **(Oral Presentation)**
4th Egyptian Society of Experimental Biology Congress in Cairo, 2008, Egypt. **(Oral Presentation)**
87th Annual Meeting of the German Physiological Society in Cologne, 02/03/2008-05/03/2008, Germany. **(Poster Presentation)**
5th Egyptian Society of Experimental Biology Congress in Tanta, 2008, Egypt. **(Oral Presentation)**
88th Annual Meeting of the German Physiological Society in Giessen, 22/03/09-25/03/09, Germany. **(Poster Presentation)**
75th Annual Meeting of the German Cardiac Society in Mannheim 2009, Germany. **(Poster Presentation)**
6th Egyptian Society of Experimental Biology Congress in Minoufiya, 2010, Egypt. **(Oral Presentation)**
3rd International Congress on Stem Cells and Tissue Formation in Dresden 2010, Germany. **(Oral Presentation)**
6th International Conference on Biological Science in Tanta 2010, Egypt. **(Oral Presentation)**
90th Annual Meeting of the German Physiological Society in Regensburg, 26/03/2011-29/03/2011, Germany. **(Oral Presentation)**
91th Annual Meeting of the German Physiological Society in Dresden 22/03/2012-25/03/2012, Germany. **(Poster Presentation)**
92nd Annual Meeting of the German Physiological Society in Heidelberg, 02/03/2013-05/03/2013, Germany. **(Poster Presentation)**

Workshops/Training courses attended

Training course: *Preparing the University Teacher.* **1999**, Faculty of Education. Tanta university. Egypt.
Training course: *2nd level of computer***. 2005**, faculty of commerce. Tanta university. **Egypt.**
Training course: *The Effective Teaching.* Faculty and Leadership Development Project. **2005**, Tanta university. Egypt.
Training course: *Evaluate the Teaching.* Faculty and Leadership Development Project. **2006**, Tanta university. Egypt.
Training course: *The Quality Assurance and Credit.* Faculty and Leadership Development Project. **2006**, Tanta university. Egypt.
Training course: *Credit Hour System*, Faculty and Leadership Development Project. **2006**, Tanta university. Egypt.
Training course: *Teaching for a Large Numbers.* Faculty and Leadership Development Project. **2006**, Tanta university. Egypt.
Workshop: *The Viruses.* **2010**, Egyptian Society of Experimental Biology. Hurgada, Egypt.
Workshop: *Effectively Presenting Research Findings With Presentations and Posters*. **2010**, Graduate Academy. Friedrich Schiller University Jena, Germany.
Training course: *International Publishing of Scientific Research.* Faculty and Leadership Development Project. **09-11.11. 2010**, Tanta university. Egypt.

Jena, 01. 10. 2014

Mohamed M. Bekhite ELsaied

7.3 Acknowledgments

I deeply thank God for giving me the will, patience and perseverance to carry on and finish this work.

I am glad to have this opportunity to express my appreciation and gratitude to **Prof. Dr. Maria Wartenberg** for giving me the opportunity and the necessary materials to bring this study to fruition. Working with her has given me insights into the field of molecular and stem cell research.

I also thank **PD Dr. Jörg P. Müller** for his kind guidance and help to establish the knockdown cell lines. His advice is essential to the completion of this dissertation.

Special thanks to **Prof. Dr. Heinrich Sauer** (Department of Physiology, Faculty of Medicine, Justus Liebig University, Giessen) for his advices and hours of discussion during the progress of this work.

Words are not adequate to express my thanks to **Dr. Andreas Finkensieper** for his help in translating the summary of my dissertation in German. His friendship helped me through tough times and made Jena town my second home town.

I also owe my gratitude to **Prof. Dr. Hans-Reiner Figulla** for his financial support of my project.

I thank **PD Dr. Martin Förster** for providing me his support during FCM and cell sorting procedures. I also thank **Dr. Joachim Clement** for kindly providing the phalloidin-Alexa Fluor® 488 dye.

I would also like to thank **Martina Voigt** and **Heike Kersten** for their excellent technical assistance.

I would like to acknowledge all the present and past member of the molecular cardiology and stem cells Laboratory in Clinic of internal medicine I.

Most of all, I want to thank my beloved wife **Manar**, the mother of our two sweet children **Mohanad** and **Mazen**. Her love made this journey completely different.

7.4 Ehrenwörtliche Erklärung

Hiermit erkläre ich, dass mir die Promotionsordnung der Medizinischen Fakultät der Friedrich-Schiller-Universität bekannt ist,

ich die Dissertation selbst angefertigt habe und alle von mir benutzten Hilfsmittel, persönlichen Mitteilungen und Quellen in meiner Arbeit angegeben sind,

mich folgende Personen bei der Auswahl und Auswertung des Materials sowie bei der Herstellung des Manuskripts unterstützt haben: Prof. Dr. Maria Wartenberg.

die Hilfe eines Promotionsberaters nicht in Anspruch genommen wurde und dass Dritte weder unmittelbar noch mittelbar geldwerte Leistungen von mir für Arbeiten erhalten haben, die im Zusammenhang mit dem Inhalt der vorgelegten Dissertation stehen,

dass ich die Dissertation noch nicht als Prüfungsarbeit für eine staatliche oder andere wissenschaftliche Prüfung eingereicht habe und

dass ich die gleiche, eine in wesentlichen Teilen ähnliche oder eine andere Abhandlung nicht bei einer anderen Hochschule als Dissertation eingereicht habe.

Jena, 01. 10. 2014

Mohamed M. Bekhite ELsaied